

Materials for Advanced Ultrasupercritical Steam Turbines

**Topical Report:
Task 4: Cast Superalloy
Development
Oct. 1, 2009 – Sept. 30, 2015**

Submitted To:
Energy Industries of Ohio

Author:
Mani Thangirala

Submitted By:
GE Power & Water
Schenectady, NY 12345

September 2015

DOE Cooperative Agreement No. DE-FE0000234

DISCLAIMER

This report was prepared as an account of work sponsored by an agency of the United States Government. Neither the United States Government nor any agency thereof, nor any of their employees, makes any warranty, express or implied, or assumes any legal liability or responsibility for the accuracy, completeness, or usefulness of any information, apparatus, product, or process disclosed, or represents that its use would not infringe privately owned rights. Reference herein to any specific commercial product, process, or service by trade name, trademark, manufacturer, or otherwise does not necessarily constitute or imply its endorsement, recommendation, or favoring by the United States Government or any agency thereof. The views and opinions of authors expressed herein do not necessarily state or reflect those of the United States Government or any agency thereof.

ABSTRACT

The Steam Turbine critical stationary structural components are high integrity Large Shell and Valve Casing heavy section Castings, containing high temperature steam under high pressures. Hence to support the development of advanced materials technology for use in an AUSC steam turbine capable of operating with steam conditions of 760°C (1400°F) and 35 Mpa (5000 psia), Casting alloy selection and evaluation of mechanical, metallurgical properties and castability with robust manufacturing methods are mandated.

Alloy down select from Phase 1 based on producability criteria and creep rupture properties tested by NETL-Albany and ORNL directed the consortium to investigate cast properties of Haynes 282 and Haynes 263. The goals of Task 4 in Phase 2 are to understand a broader range of mechanical properties, the impact of manufacturing variables on those properties. Scale up the size of heats to production levels to facilitate the understanding of the impact of heat and component weight, on metallurgical and mechanical behavior.

GE Power & Water Materials and Processes Engineering for the Phase 2, Task 4.0 Castings work, systematically designed and executed casting material property evaluation, multiple test programs. Starting from 15 lbs. cylinder castings to world's first 17,000 lbs. poured weight, heavy section large steam turbine partial valve Haynes 282 super alloy casting. This has demonstrated scalability of the material for steam Turbine applications.

Activities under Task 4.0, Investigated and characterized various mechanical properties of Cast Haynes 282 and Cast Nimonic 263. The development stages involved were:

- 1) Small Cast Evaluation: 4 inch diam. Haynes 282 and Nimonic 263 Cylinders. This provided effects of liquidus super heat range and first baseline mechanical data on cast versions of conventional vacuum re-melted and forged Ni based super alloys.
- 2) Step block castings of 300 lbs. and 600 lbs. Haynes 282 from 2 foundry heats were evaluated which demonstrated the importance of proper heat treat cycles for Homogenization, and Solutionizing parameters selection and implementation.
- 3) Step blocks casting of Nimonic 263: Carried out casting solidification simulation analysis, NDT inspection methods evaluation, detailed test matrix for Chemical, Tensile, LCF, stress rupture, CVN impact, hardness and J1C Fracture toughness section sensitivity data and were reported.
- 4) Centrifugal Casting of Haynes 282, weighing 1400 lbs. with hybrid mold (half Graphite and half Chromite sand) mold assembly was cast using compressor casing production tooling. This test provided Mold cooling rates influence on centrifugally cast microstructure and mechanical properties. Graphite mold section out performs sand mold across all temperatures for 0.2% YS; %Elongation, %RA, UTS at 1400°F. Both Stress-LMP and conditional Fracture toughness plots data were in the scatter band of the wrought alloy.
- 5) Fundamental Studies on Cooling rates and SDAS test program. Evaluated the influence of 6 mold materials Silica, Chromite, Alumina, Silica with Indirect Chills, Zircon and Graphite on casting solidification cooling rates. Actual Casting cooling rates through Liquidus to Solidus phase transition were measured with 3 different locations based

thermocouples placed in each mold. Compared with solidification simulation cooling rates and measurement of SDAS, microstructure features were reported. The test results provided engineered casting potential methods, applicable for heavy section Haynes 282 castings for optimal properties, with foundry process methods and tools.

- 6) Large casting of Haynes 282 Drawings and Engineering FEM models and supplemental requirements with applicable specifications were provided to suppliers for the steam turbine proto type feature valve casing casting. Molding, melting and casting pouring completed per approved Manufacturing Process Plan during 2014 Q4.

The partial valve casing was successfully cast after casting methods were validated with solidification simulation analysis and the casting met NDT inspection and acceptance criteria. Heat treated and sectioned to extract trepan samples at different locations comparing with cast on coupons test data. Material properties requisite for design, such as tensile, creep/rupture, LCF, Fracture Toughness, Charpy V-notch chemical analysis testing were carried out. The test results will be presented in the final report.

The typical Haynes 282 large size Steam Turbine production casting from Order to Delivery foundry schedule with the activity break up is shown in Figures 107 and 108.

- **From Purchase Order placement to Casting pouring ~ 26 weeks.**

1. Sales and commercial review	3
2. Engineering Drawings/models review	4
3. Pattern and core box manufacturing	6
4. Casting process engineering review	4
5. FEM and solidification simulation analysis	4
6. Gating & Feeder Attachments, Ceramic tiling	2
7. Molding and coremaking production scheduling	6
8. Melting planning and schedule	3
9. Pouring, cooling and shake out	2

- **From Pouring to casting Delivery ~ 29 weeks**

10. Shot blast and riser cutting, gates removal	3
11. Homogenizing , solutionizing HT furnace prep	4
12. Grinding, Fettling	2
13. Aging HT Cycle, cooling	2
14. VT and LPT NDT inspections	2
15. Radiographic inspection	4
16. Mechanical testing, Chemical analysis test certs	4
17. Casting weld repair upgrades and Aging PWHT	4
18. NDT after weld repairs and casting upgrades	3
19. Casting Final Inspection and test certifications	3
20. Package and delivery	2

Hence the Total Lead time from P.O to Casting delivery is approximately 55 weeks. The Task 4.2 and Task 4.3 activities and reporting completed.

TABLE OF CONTENTS

<i>Topical Report:</i>	1
DISCLAIMER.....	2
ABSTRACT	3
FIGURES	6
TABLES.....	10
LIST OF ACRONYMS AND ABBREVIATIONS.....	11
SMALL CAST EVALUATION.....	12
STEP BLOCK CASTING OF HAYNES 282.....	21
STEP CASTING OF NIMONIC 263	24
CENTRIFUGAL CASTING OF HAYNES 282	55
FUNDAMENTAL STUDIES ON COOLING RATES AND SDAS	73
LARGE CASTING OF HAYNES 282	85
CONCLUSIONS.....	103

FIGURES

Figure 1: Schematic of the six 4 inch diameter, 4 inch high NETL-Albany cast Nimonic 263 and Haynes 282 cylinder castings	12
Figure 2: Super heat influence on N263 Tensile strength at RT and 1400°F	13
Figure 3: Super heat influence on N263- 0.2% YS at RT and 1400°F	13
Figure 4: Cast structure influence on N263 Tensile strength at RT and 1400°F	14
Figure 5: Cast structure influence on N263 0.2% YS at RT and 1400°F	14
Figure 6: Super heat influence on H 282 Tensile strength at RT and 1400°F	15
Figure 7: Super heat influence on H 282- 0.2% YS at RT and 1400°F	15
Figure 8: Cast structure influence on H 282 Tensile strength at RT and 1400°F	16
Figure 9: Cast structure influence on H 282 0.2% YS at RT and 1400°F	16
Figure 10: Super heat influence on N263 LCF at RT. Higher super heat temperatures of 150°C provides improved LCF properties	17
Figure 11: Cast structure influence on N263 LCF at RT. Columnar as cast structures tend to provide better LCF properties.	17
Figure 12: Super heat influence on H282 LCF at RT. Higher super heat pour temperatures of 100°C-150°C shows improved LCF properties	18
Figure 13: Cast Structure influence on H 282 LCF at RT. Columnar as cast structures shows improved LCF properties at RT.....	18
Figure 14: Super heat influence on N263 LCF at 1400F compared with Forged 263. 100°C- 150°C super heat pour temperatures shows improved LCF properties at 1400°F	19
Figure 15: Cast structure influence on N263 LCF at 1400F compared with Forged 263	19
Figure 16: Super heat influence on H 282 LCF at 1400F compared with Forged H282 data. 100°C super heat pours indicate comparable LCF to forged 282 data at 1400°F	20
Figure 17: Cast structure influence on H282 LCF at 1400F compared with Forged H282. Columnar as cast structure provides improved LCF at 1400°F compared with equiaxed cast structure.....	20
Figure 18: Schematic of the MetalTek 300 lbs. Haynes 282 step block casting with dimensions	21
Figure 19: MetalTek 300 lbs. Haynes 282 step block casting after mold shake out and shot blast cleaning operations. Bottom gated with casting top feeder arrangement shown.	22
Figure 20: Schematic of Flowserv Step block. Top feeder with section modulus controlled feeding.	23
Figure 21: Nimonic 263 step block test casting, weighing 605 lbs. Completed optimized Homogenizing and Age hardening heat treatments	24
Figure 22: Picture showing the N263 casting and the associated shrink cavity below the rise/feeder section.....	26
Figure 23: Casting solidification simulation analysis showing the hot spot location and the associated casting shrinkage defect.	27
Figure 24: Nimonic 263 test casting,CAD layout of specimen extraction isometric views from step block cast sections	28
Figure 25: Orientation and specimen layout of various test specimens from N263 test block 29	
Figure 26: Test matrix for Tensile, Charpy impact energy and LCF properties with specimen identification	30
Figure 27: Test matrix for Stress rupture, Fracture toughness and Chemical analysis with specimen identification.....	31

Figure 28: Step block casting thermal center trepanned section chemical analysis. No significant variation in chemistry when compared with casting section Thermal center analysis	32
Figure 29: Homogenizing and Aging Heat treatment cycles Optimized to within +/- 5% of nominal chemistry variation (NETL)	33
Figure 30: UT immersion scans of N263 step block casting 6 inch and 4 inch sections showing the inherent issue of achieving a superior back wall reflection in thick walled super alloy castings	34
Figure 31: Radiographic Scan Plan	35
Figure 32: Radiographic Test Report confirming no other casting defect in other cast sections, except the surface cavity defect in 10 inch section under the casting feeder	36
Figure 33: UTS plot with temperature and trepanned casting section thickness variation	37
Figure 34: UTS vs temperature plot for 10 inch section CL and DL location trepans	38
Figure 35 UTS vs temperature plot for 6 inch section CL and DL location trepans	38
Figure 36: 0.2 % YS vs. Temperature for all N263 step block cast section trepans. The 0.2% YS vs. temperature trend plot shows tighter band trepan CL values at elevated temperatures for all section thicknesses	39
Figure 37: 0.02 % YS vs. Temperature for all N263 step block cast section trepans. The 0.02% YS vs. temperature trend plot shows tighter band at elevated temperatures for all section thicknesses	40
Figure 38: N263 step block cast section trepan samples % Elongation vs. Temperature	41
Figure 39: N263 %RA Vs Temperature plots for all section trepans	42
Figure 40: Nimonic 263 step block casting SDAS measurements with section size	43
Figure 41: N263 Step block 10 inch and 6 inch sections cycles to failure compared at RT, A-ratio 1. The 10 inch section shows a debit in comparison with 6 inch section	45
Figure 42: N263 Step block 10 inch and 6 inch sections cycles to failure compared at 1400°F , A-Ratio 1. The 10 inch section shows increased debit in comparison with 6 inch section, while 6 inch section shows degradation	45
Figure 43: N263 Stress rupture strength vs, LMP (C=20) with section thickness. No significant changes in stress rupture data with section thickness variation	46
Figure 44: Plot showing Kq Fracture toughness value Vs. Temperature for various section sizes. Note that the conditional fracture toughness Kq values are minimum influenced with temperature raise up to 6 inch cast wall thickness	48
Figure 45: 10-J1C-01, J vs. a graph for 10 inch section tested at RT	49
Figure 46: 10-J1C-01, Force vs. COD graph for 10 inch section tested at RT	49
Figure 47: 10-J1C-03, J vs. a graph for 10 inch section tested at 1400°F	50
Figure 48: 10-J1C-03, Force vs. COD graph for 10 inch section tested at 1400°F	50
Figure 49: 4-J1C-02, J vs. a graph for 4 inch section tested at 1400°F	51
Figure 50: 4-J1C-02, Force vs. COD graph for 4 inch section tested at 1400°F	51
Figure 51: 4-J1C-01, J vs. a graph for 4 inch section tested at RT	52
Figure 52: 4-J1C-01, Force vs. COD graph for 4 inch section tested at RT	52
Figure 53: Charpy V notch Impact energy vs. section size combined data plot	53
Figure 54: N263 Cast hardness values are not section thickness dependent	54
Figure 55: Haynes 282 Test program Centrifugal casting	55
Figure 56: Sectional view drawing of 282 Centrifugal Casting	57
Figure 57: Haynes282 Centrifugal casting mold assembly comprising half mold Graphite and half mold Chromite sand	58
Figure 58: Casting simulation predicted cooling rates for Graphite and Chromite sand side molds	58

Figure 59: Picture showing the location of the casting utilized for micro-structural analysis and mechanical testing	59
Figure 60: Picture showing the extraction of the slice for heat treatment and micro-structural analysis	59
Figure 61: SDAS along the wall thickness for the two respective mold material.....	60
Figure 62 As cast microstructural evolution across the wall thickness for the two mold material	61
Figure 63 SEM image of grain boundary in as cast specimens. Most precipitates consists of Ti, Mo and Cr rich.....	62
Figure 64: Complete map of specimen extraction from the centrifugally cast Haynes 282. The specimens include tensile, LCF and fracture toughness	63
Figure 65: Color code of specimen type are as shown. All mini specimens are for the thinner wall thickness	63
Figure 66: Plots of UTS as a function of temperature [Sand and Graphite mold]. In general, the variation between the thick and thin sections on the sand side has less variability, when compared to the graphite side. Graphite side has better RT properties when compared to the sand. However at 1400°F, all data falls within a very tight band.....	64
Figure 67: Plots of 0.2% YS as a function of temperature for various mold material. Unlike the variation in UTS, the 0.2% YS has a very tight range across all temperatures tested..	65
Figure 68: Plots of % Elongation as a function of temperature for various mold material. The plots clearly show a wide variation in % Elongation, with the graphite mold being better than the sand mold across all temperatures	66
Figure 69: Plots of % RA as a function of temperature for various mold material. The plots clearly show a wide variation in % RA, and in general, graphite mold out performs sand mold across all temperatures	67
Figure 70: Plots of Cycles to Failure and Total Strain Range (%) for the Sand and Graphite molds at RT and 1400 F. The Graphite side shows a debit at 1400 F, while the sand side does degrade with the same severity.....	68
Figure 71: Plots of Cycles to Failure and Total Strain Range (%) for the Sand and Graphite molds at RT and 1400 F. The debit in the graphite compared to sand at high strains and 1400 F will need some further investigation.....	69
Figure 72: Plot of cycles to failure and total strain range from Table 4B-1. The graph clearly shows the better performance of faster cooling rates [finer SDAS in the graphite side] due to higher UTS at 75 F (+10 to15 KSI increase in UTS on Graphite side].....	70
Figure 73: Plot of cycles to failure and total strain range from Table 4B-2. The graph clearly shows no performance difference at 1400 F as the tensile properties of both sand and graphite are similar at 1400 F	70
Figure 74: Conditional Fracture toughness (K_Q) of centrifugally cast Haynes 282. The cast data [Sand & Graphite] falls in the scatter of wrought alloy. The wrought data in the figure above consists of PA, and exposed for 1 & 2 years at 1425 F	71
Figure 75: Stress-LMP plot of Centrifugal Cast H282 compared to wrought H282 data. The data scatter is in line with the wrought alloy.....	72
Figure 76: Enhancing SDAS prediction with casting solidification mold cooling rate studies. Six molds with different mold materials [to simulate different cooling rates] were poured with thermocouples located as shown to measure casting cooling rates	73
Figure 77: Detailed plan of casting solidification cooling rates measurement mold layout assembly	74
Figure 78: Sand molds from 5 different mold materials [left] coated with refractory paint and dried [right]. Six mold materials were evaluated: 1. Silica, 2. Chromite, 3. Graphite, 4. Alumina, 5. Zircon, 6. Silica with indirect chills placement	75

Figure 79: Photograph of chills location in mold pattern prior to molding	75
Figure 80: Thermocouples and extension wire were wrapped with Kaowool thermal insulation.	76
Figure 81: Photograph of thermocouple compensating cables routing within the drag mold.....	77
Figure 82: Type B Thermocouples, insulators and connectors assembly components	77
Figure 83: Photograph of completed mold ready for pour	78
Figure 84: Photograph showing castings after mold shake out, gating and feeders removal....	79
Figure 85: Haynes 282 cylinder castings thermocouple arrangements schematic view. Photograph showing Quartz sheathed Type-B thermocouples located within the molds ..	80
Figure 86: Casting cooling rates measured and simulated compared for different mold materials during liquidus to solidus transition temperature range	80
Figure 87: Casting Solidification Simulation Analysis cooling rates plot from pour to post solidification elevated temperature range for all the mold materials. Data from the 3 thermocouples T1, T2 and T3 vs. casting cooling time are plotted for different molds.	81
Figure 88: Haynes 282 Casting cooling rates during Liquidus to Solidus temperature range for different mold materials.....	82
Figure 89: Mold cooling rates influence on SDAS values.....	83
Figure 90: Steam turbine half valve casing selected for the large casting trial	86
Figure 91: Foundry Casting Pattern and feeder design	87
Figure 92: Picture showing Cope, drag molds and the valve body core after refractory coating and drying.	87
Figure 93: Solidification simulation indicates bottom to top filling (left) and temperature variation during liquidus to solidus transition temperature range (right)	88
Figure 94: Solidification fraction solid cut off indicates no trail of shrinkage	88
Figure 95: Assembled mold, hot air dried and purged with Argon prior to pouring [Courtesy- MetalTek MO].....	89
Figure 96: Induction melted, composition controlled with argon cover during melting and tapping melt quality controlled [Courtesy-MetalTek MO]	89
Figure 97: Pouring the mold after deslagging with covered ladles ensuring targeted pouring temperature and pour times	90
Figure 98: Casting after in mold cooling and shake out [Courtesy-MetalTek MO].....	90
Figure 99: Homogenization HT cycle with insert HT step detailed view	92
Figure 100: Two step Aging heat treat cycles thermocouple plot	93
Figure 101: Thermocouples attached, coated for double Age heat treat cycle.....	94
Figure 102: RT Scan sheet for the partial valve casing	95
Figure 103: RT Inspection report for the H282 valve casing.....	96
Figure 104: Haynes 282 Valve casing Liquid penetrant testing 100% surface area.....	97
Figure 105: LPT inspection pictures on 100 % Cast surface areas	98
Figure 106: Niyama criteria per solidification simulation analysis. Niyama indicates potential feeding difficulty zones in the casting with lower (N_y) values. This plot is primarily used to avoid sectioning through potential zones for micro shrinkage	99
Figure 107: Schedule from Purchase Order Placement to Casting Pouring ~ 26 weeks	101
Figure 108: Schedule from Pouring to Delivery 30 weeks~.....	101

TABLES

Table 1: N263 Step block trepan cast sections tensile strength (UTS) vs temperature data.....	37
Table 2: N263 Step block trepan cast sections 0.2% Yield strength vs temperature data.....	39
Table 3: N263 Step block trepan cast sections 0.02% Yield strength vs temperature data.....	40
Table 4: N263 step block trepan section samples % Elongation values.....	41
Table 5: N263 Step Block section Trepan sample % RA values data	42
Table 6: Nimonic 263 Step block cast sections SDAS Measurements. Consistently in the range of 0.35 to 0.40 mm for 100 to 250 mm cast sections	43
Table 7: Nimonic 263 Step block cast section thermal center trepanned samples SDAS values show independent of casting section thickness and orientation	44
Table 8: Stress rupture test results raw data	46
Table 9: Nimonic 263 Step block sections J-Integral Test results at RT; 1000°F and 1400°F summarized.....	47
Table 10: Kq Fracture toughness @ RT, `1000°F and 1400°F temperatures vs. section size data	48
Table 11: Charpy V-Notch Impact energy data for 10 inch,8 inch and 6 inch trepan samples ...	53
Table 12: N263 Casting section hardness values raw data	54
Table 13: Casting cooling rates, both measured and simulated compared for different mold materials at 3 different locations within each mold	82
Table 14: Mold materials influence on microstructure SDAS values for Graphite, Zircon and Silica sand with indirect chills.....	83
Table 15: Mold materials influence on SDAS values through casting liquidus to solidus range cooling rates variation	84
Table 16: H282 casting sections and cast on coupons test matrix and specimens identification	100

LIST OF ACRONYMS AND ABBREVIATIONS

UTS.....	Ultimate Tensile Strength
0.2YS.....	0.2% Yield Strength
% Elongation.....	% Elongation to failure
%RA.....	% Reduction in Area
KQ.....	Conditional Fracture Toughness
RT.....	Room Temperature
HT.....	Heat Treatment
UT.....	Ultrasonic Testing
LPT.....	Liquid Penetrant Testing
LCF.....	Low Cycle Fatigue
CL.....	Center Line
DL.....	Drag Line [1 inch above drag mold surface]
CAD.....	Computer Aided Design
COD.....	Crack Opening Displacement
LMP.....	Larsen Miller Parameter
NDT.....	Non Destructive Testing
SDAS.....	Secondary Dendritic Arm Spacing

SMALL CAST EVALUATION

Haynes 282 and Nimonic 263 alloy down select from Phase 1 based on producibility criteria and creep rupture properties, a series of small heats were poured at NETL-Albany. These initial heats showed the effect of liquidus superheat (50°, 100° and 150°C over the liquidus) immediately prior to pouring and also provided the first baseline mechanical data on cast versions of these traditionally vacuum remelted and forged nickel-based alloys.

These six small heats out of NETL-Albany were each 13-15 lb, 4 inch diameter cylinders 4 inches tall. The process used poured the alloy into a graphite mold embedded in sand under argon shrouding per the schematic in Figure 1. The chemical analyses of the 6 castings are provided in Table-1. The cylinder castings were subjected to following heat treat cycles:

Nimonic 263HT Cycle: (1) Homogenize for 3 hours at 1100°C followed directly by 9 hours at 1200°C, fast cool; (2) Age 8 hours at 800°C.

Haynes 282 HT Cycle: (1) Homogenize for 3 hours at 1100°C followed directly by 9 hours at 1200°C, fast cool; (2) Solutionize for 2 hours at 1010°C, fast cool, and (3) Age for 8 hours at 788°C

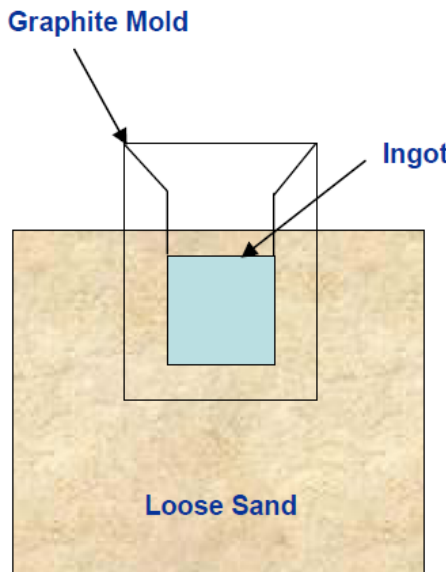


Figure 1: Schematic of the six 4 inch diameter, 4 inch high NETL-Albany cast Nimonic 263 and Haynes 282 cylinder castings

The six small cylinder castings were tested for tensile and low cycle fatigue (LCF) to capture the effects of both superheat as well as any impact of grain structure (equiaxed/dendritic and columnar). The castings were radiographed to identify valid test sample areas. Specimens extracted near outer surface, solidified in contact with graphite mold are marked columnar microstructure and specimens from interior are marked equiaxed grain structure.

The test results showed a few ksi increase in ultimate tensile strength (UTS) with super heat and no discernable pattern in LCF with super heat. Grain orientation did not appear to impact either of these properties.

Figures 2 and 3 plots show the influence of melt super heat temperatures on Nimonic 263 Tensile (UTS) and 0.2% yield strength (YS). Differences in Tensile properties at 1400°F (760°C) are minimal for 100° to 150°C super heat temperatures which are typical foundry casting pouring temperature practices.

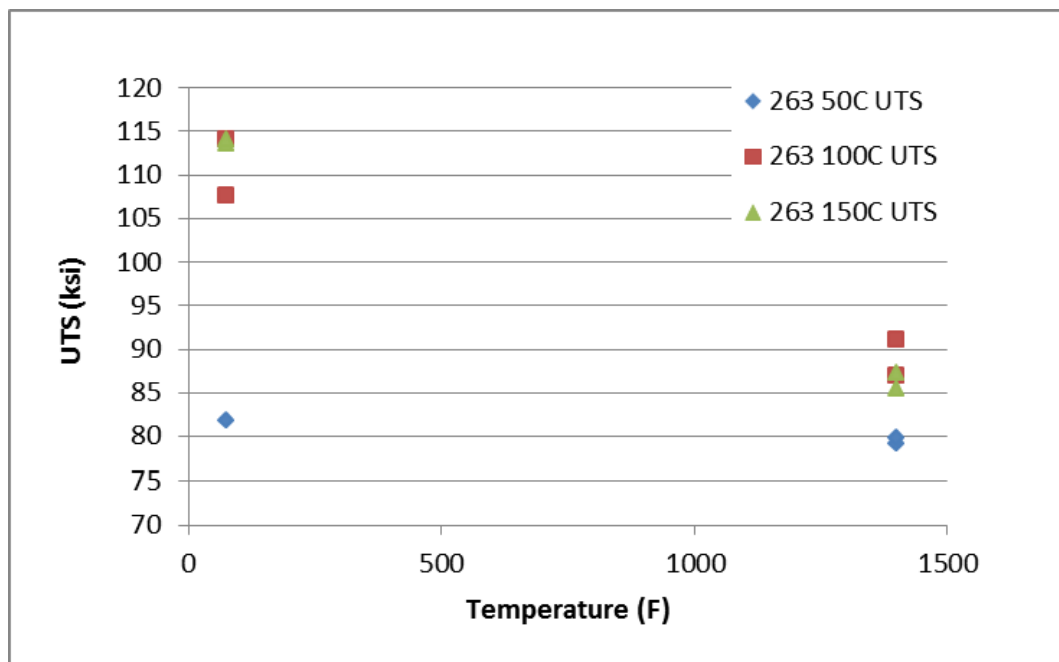


Figure 2: Super heat influence on N263 Tensile strength at RT and 1400°F (760°)

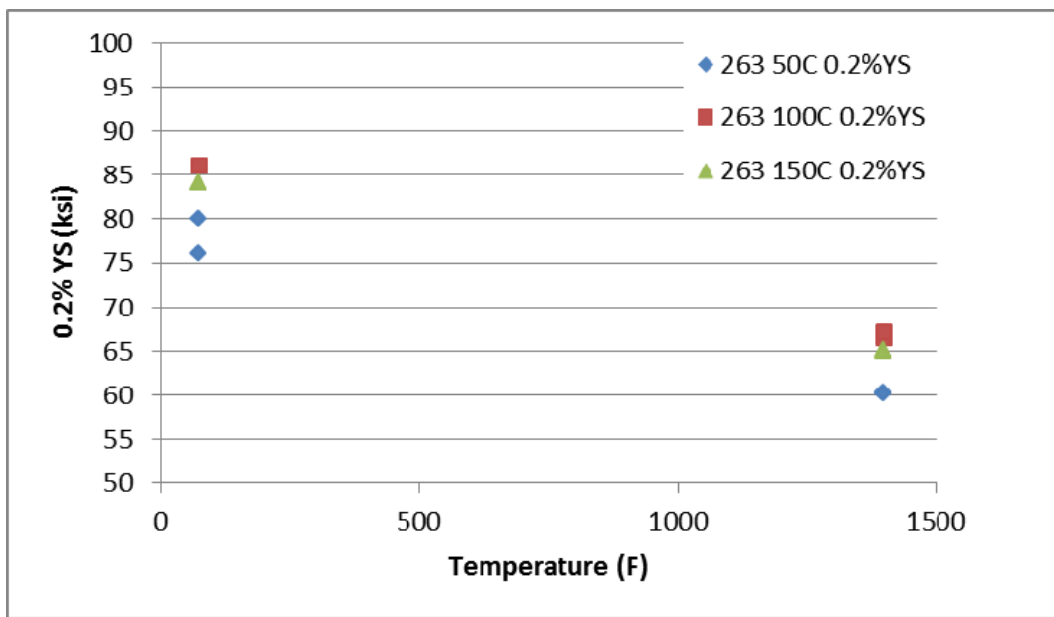


Figure 3: Super heat influence on N263- 0.2% YS at RT and 1400°F (760°C)

Figures 4 and 5 plots, show the influence of cast structure on Nimonic 263 Tensile (UTS) and 0.2% YS. Differences in Tensile and 0.2% YS values at elevated temperature (1400°F or 760°C) are minimal

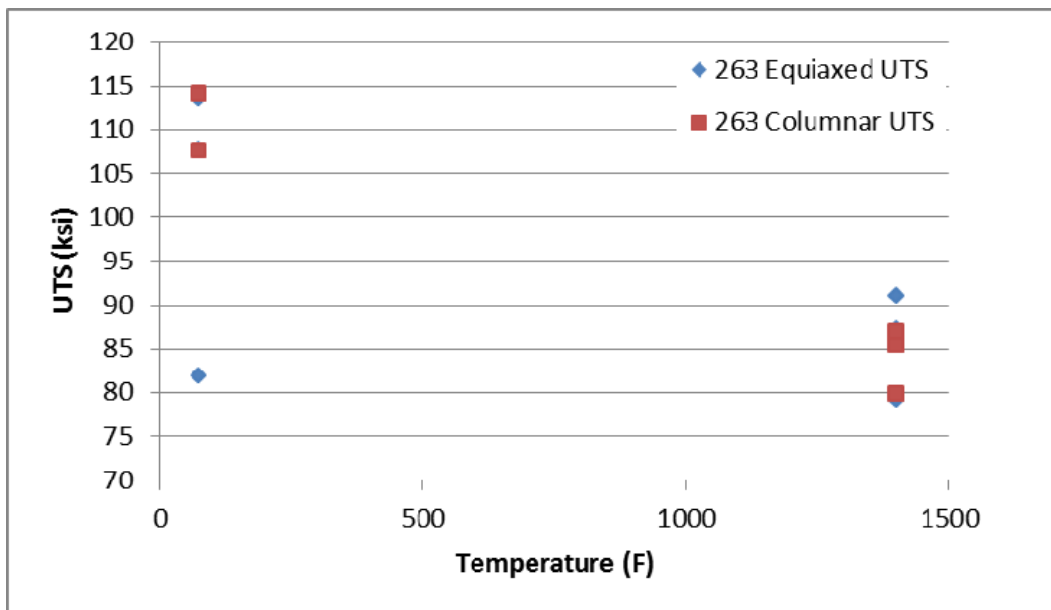


Figure 4: Cast structure influence on N263 Tensile strength at RT and 1400°F (760°C)

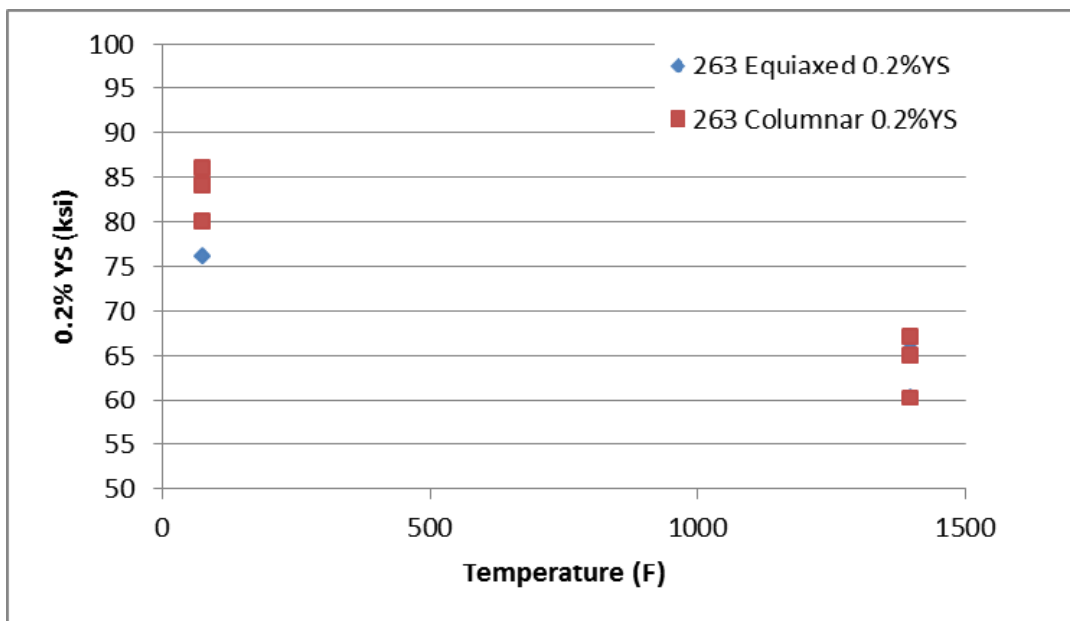


Figure 5: Cast structure influence on N263 0.2% YS at RT and 1400°F (760°C)

Figures 6 and 7 plots, show the influence of melt super heat temperatures on Haynes 282 Tensile (UTS) and 0.2% YS. Differences in Tensile and 0.2% YS properties are minimal for 100°C-150°C, super heat range temperatures, which are typical foundry casting pouring temperature selection practices.

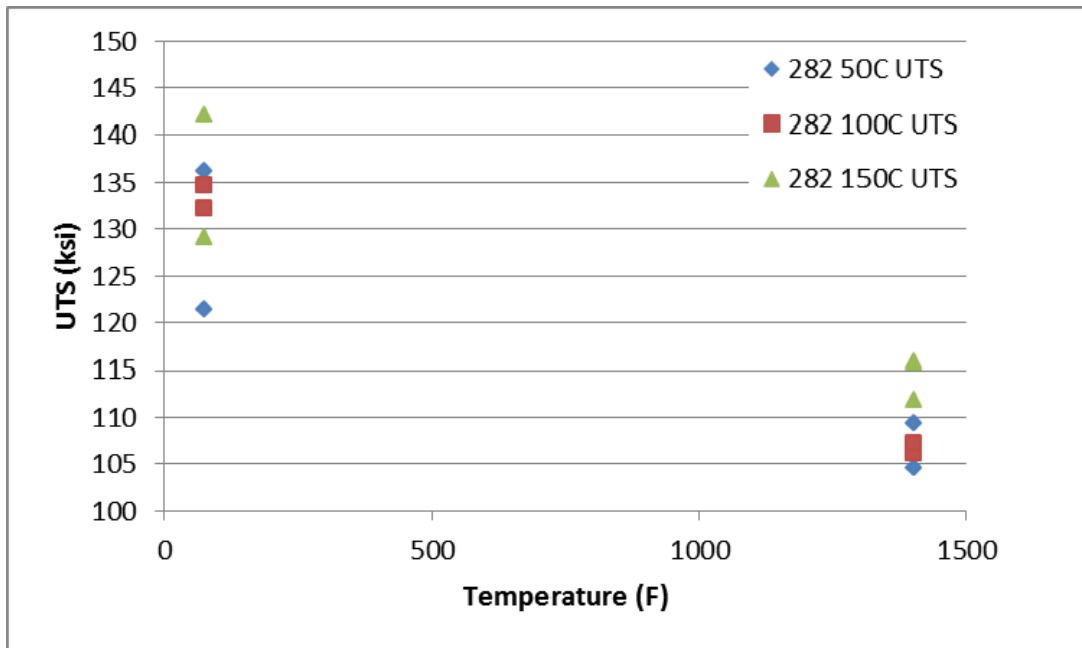


Figure 6: Super heat influence on H 282 Tensile strength at RT and 1400°F (760°C)

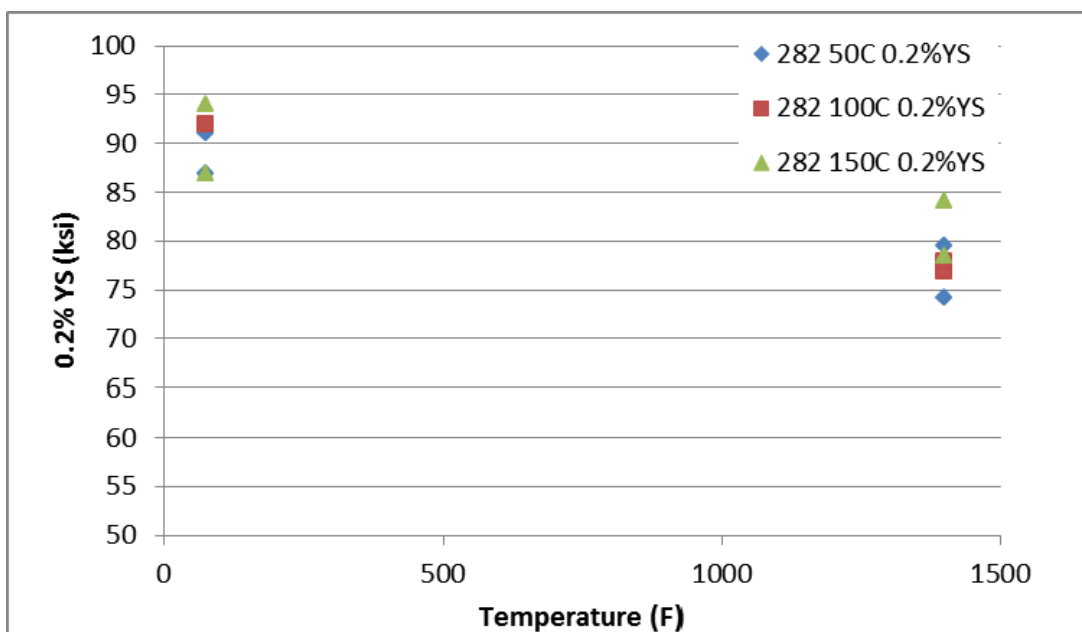


Figure 7: Super heat influence on H 282- 0.2% YS at RT and 1400°F (760°C)

Figures 8 and 9 plots, show the influence of cast structure on Haynes 282 Tensile (UTS) and 0.2% YS. Columnar as cast structures show higher tensile and 0.2% YS values at all temperatures.

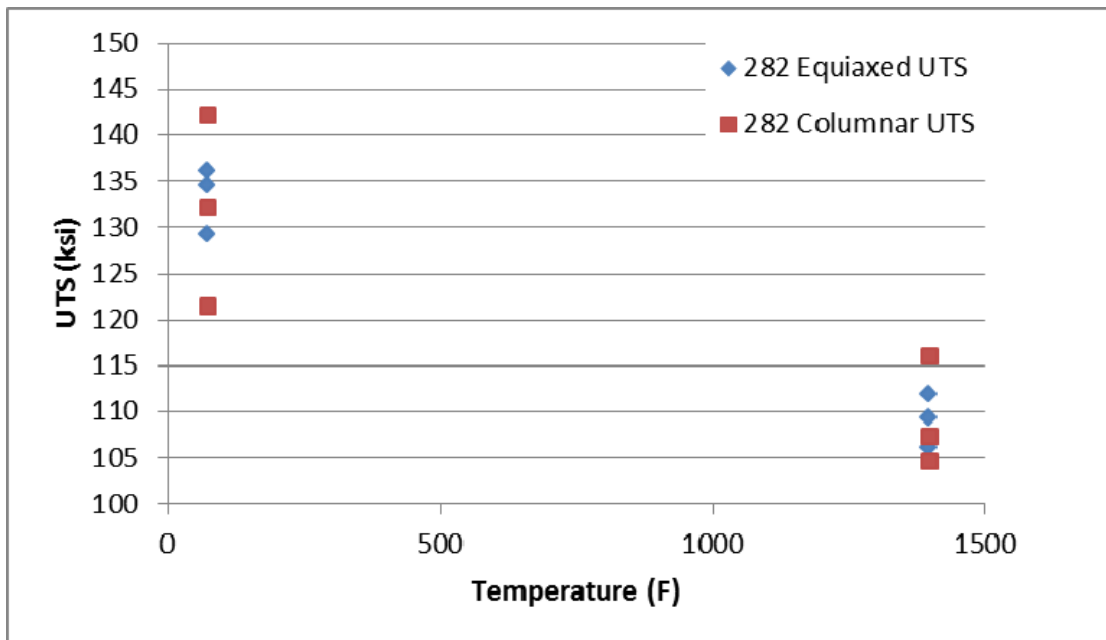


Figure 8: Cast structure influence on H 282 Tensile strength at RT and 1400°F (760°C)

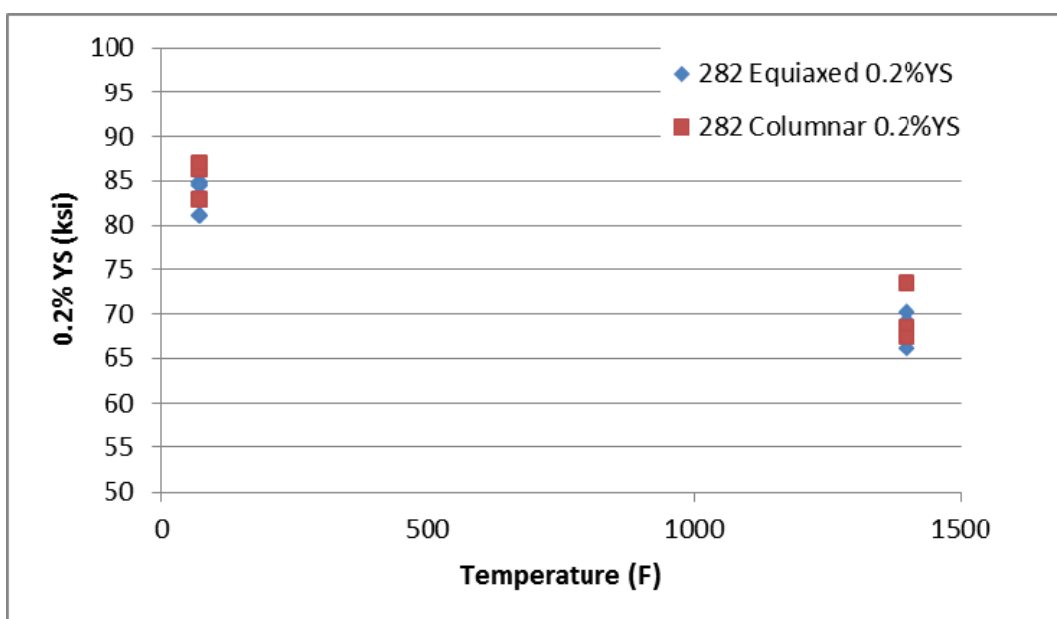


Figure 9: Cast structure influence on H 282 0.2% YS at RT and 1400°F (760°C)

Figures 10 and 11 show the influence of Super heat and cast structure on Nimonic 263 LCF properties.

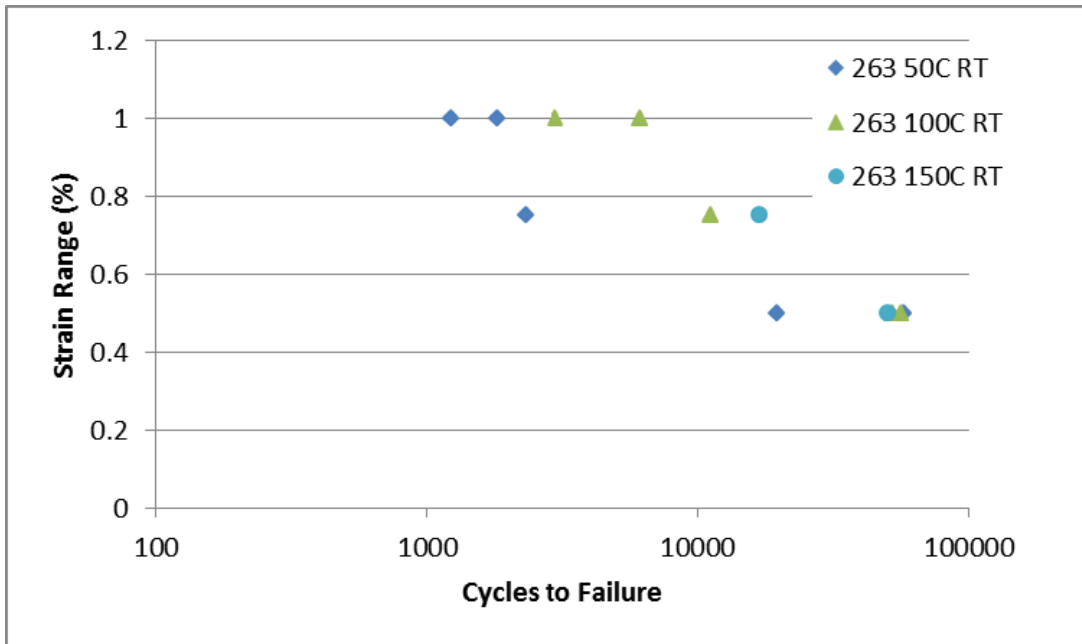


Figure 10: Super heat influence on N263 LCF at RT. Higher super heat temperatures of 150°C provides improved LCF properties

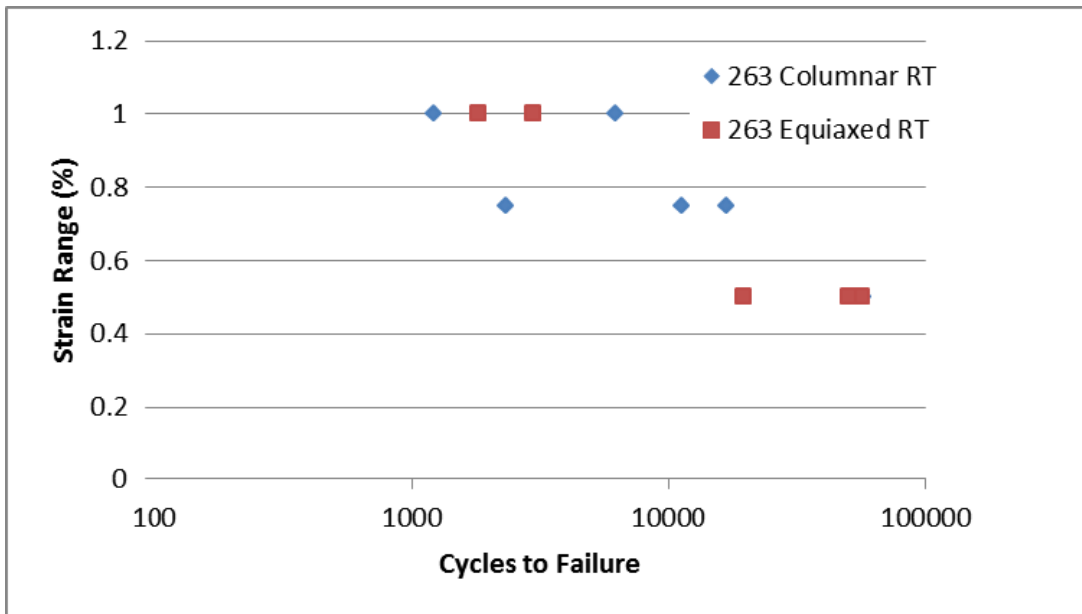


Figure 11: Cast structure influence on N263 LCF at RT. Columnar cast structures tend to provide better LCF properties.

Figures 12 and 13 show the influence of Super heat and cast structure on Haynes 282 LCF properties.

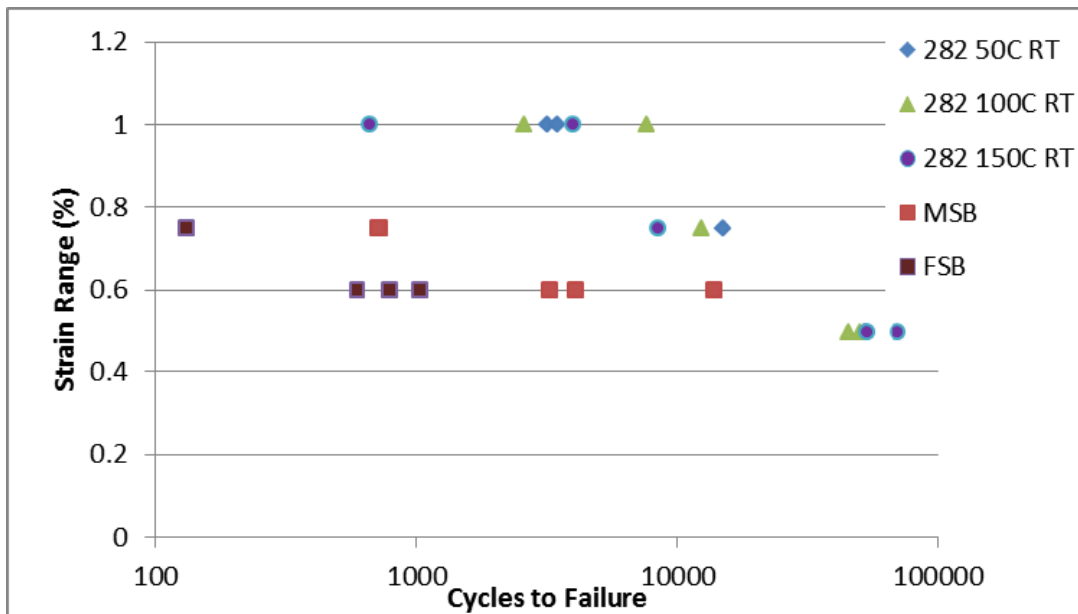


Figure 12: Super heat influence on H282 LCF at RT. Higher super heat pour temperatures of 100°C-150°C shows improved LCF properties

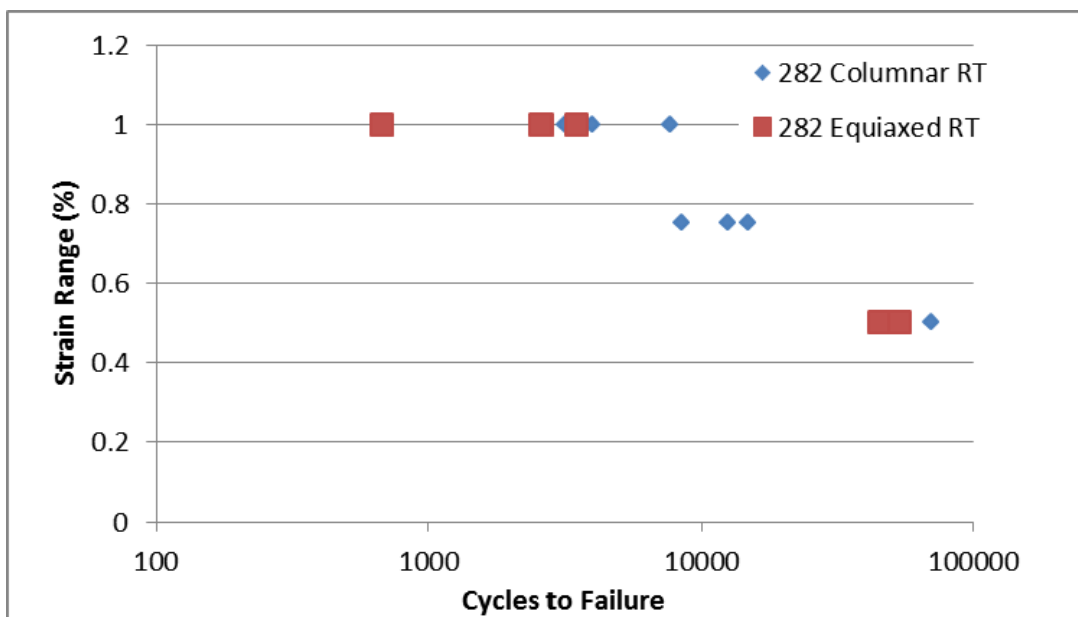


Figure 13: Cast Structure influence on H 282 LCF at RT. Columnar as cast structures shows improved LCF properties at RT.

Figures 14 and 15 show the influence of Super heat and cast structure on Nimonic 263 LCF properties at 1400°F (760°C) compared with forging property

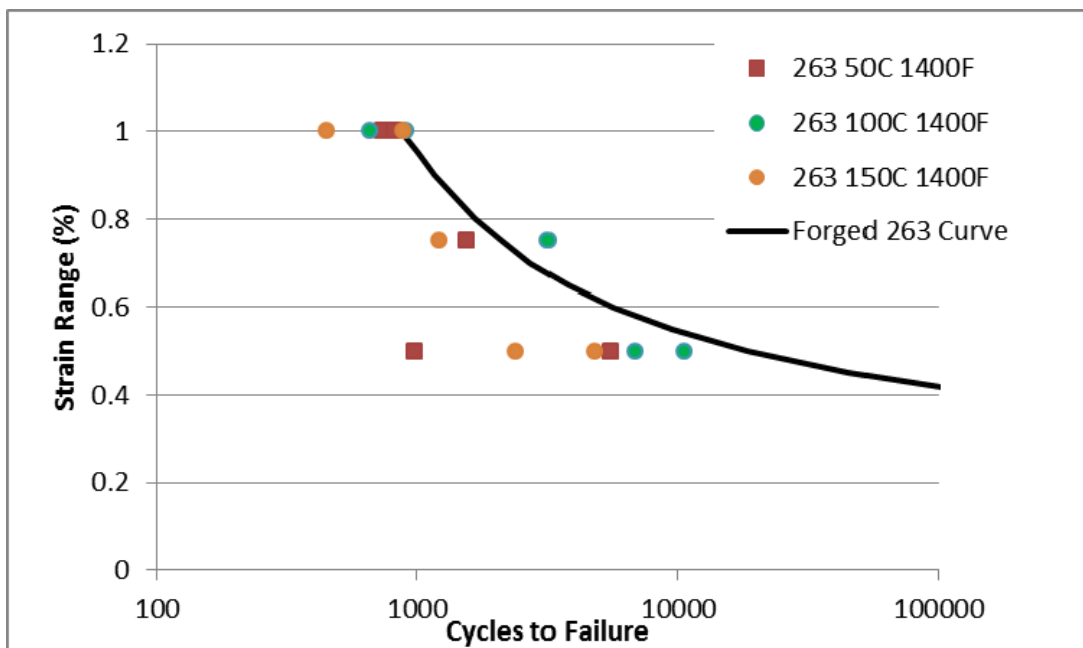


Figure 14: Super heat influence on N263 LCF at 1400F compared with Forged 263. 100°C-150°C super heat pour temperatures shows improved LCF properties at 1400°F (760°C)

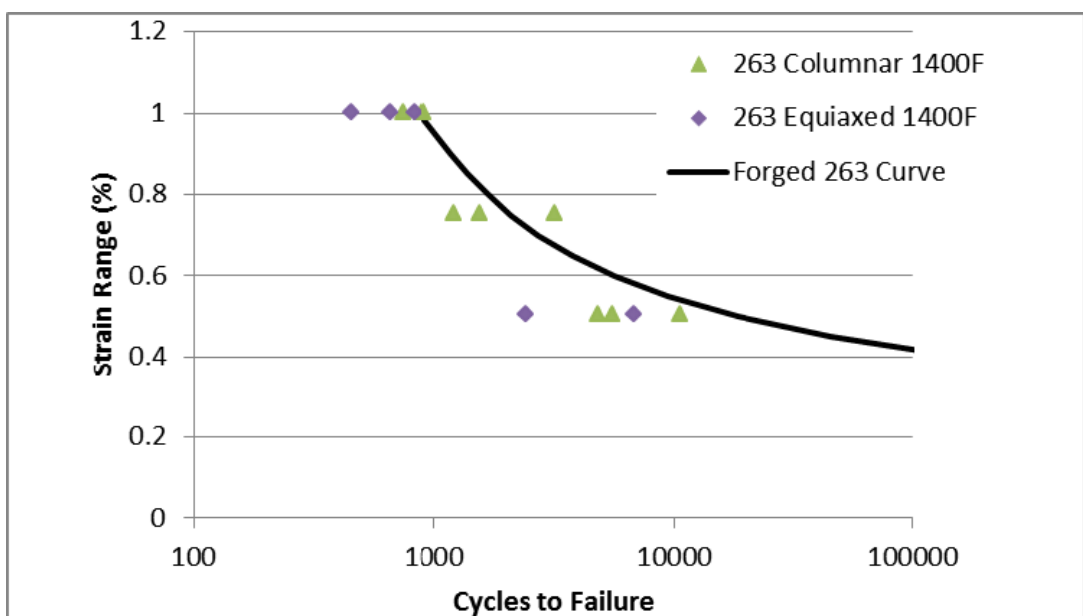


Figure 15: Cast structure influence on N263 LCF at 1400F compared with Forged 263

Figures 16 and 17 show the influence of Super heat and cast structure on Haynes 282 LCF properties at 1400°F (760°C) compared with forging property.

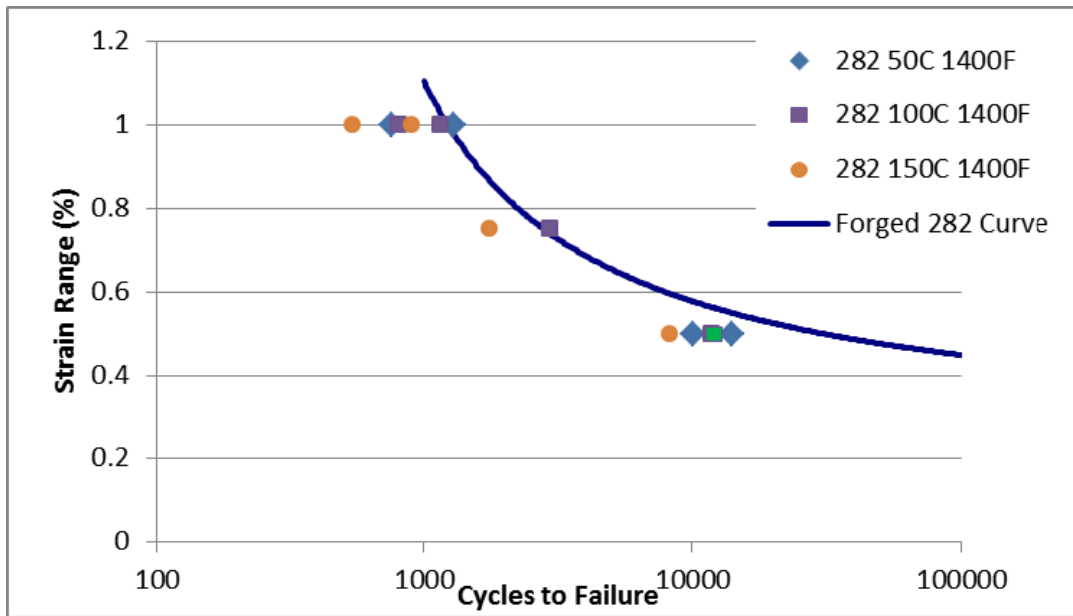


Figure 16: Super heat influence on H 282 LCF at 1400°F (760°C) compared with Forged H282 data. 100°C super heat pours indicate comparable LCF to forged 282 data at 1400°F

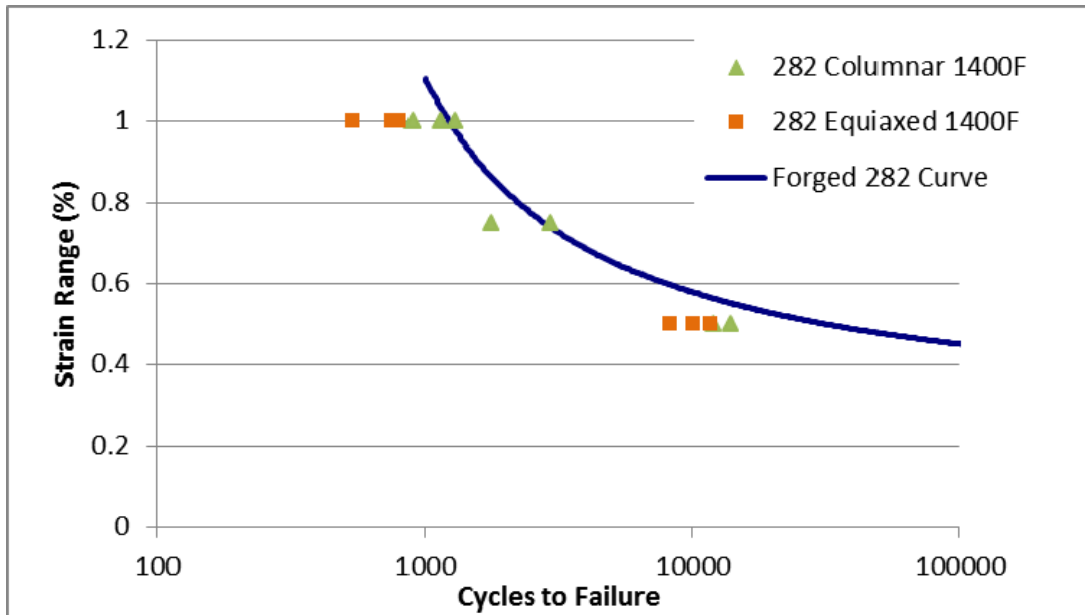


Figure 17: Cast structure influence on H282 LCF at 1400°F (760°C) compared with Forged H282. Columnar as cast structure provides improved LCF at 1400°F compared with equiaxed cast structure.

Conclusion: This test program confirms that 100°C to 150°C Melt super heat temperature is recommended practice depending on casting geometry for Haynes 282

STEP BLOCK CASTING OF HAYNES 282

Two separate Step block castings were poured at two foundry suppliers with different section sizes and casting gating and feeding methods.

MT Foundry Step block dimensions shown in Figure 18 and uses bottom gating and top feeder methods as shown in Figure 19. FS Foundry step block dimensions and horizontal gating method is shown in Figure 20.

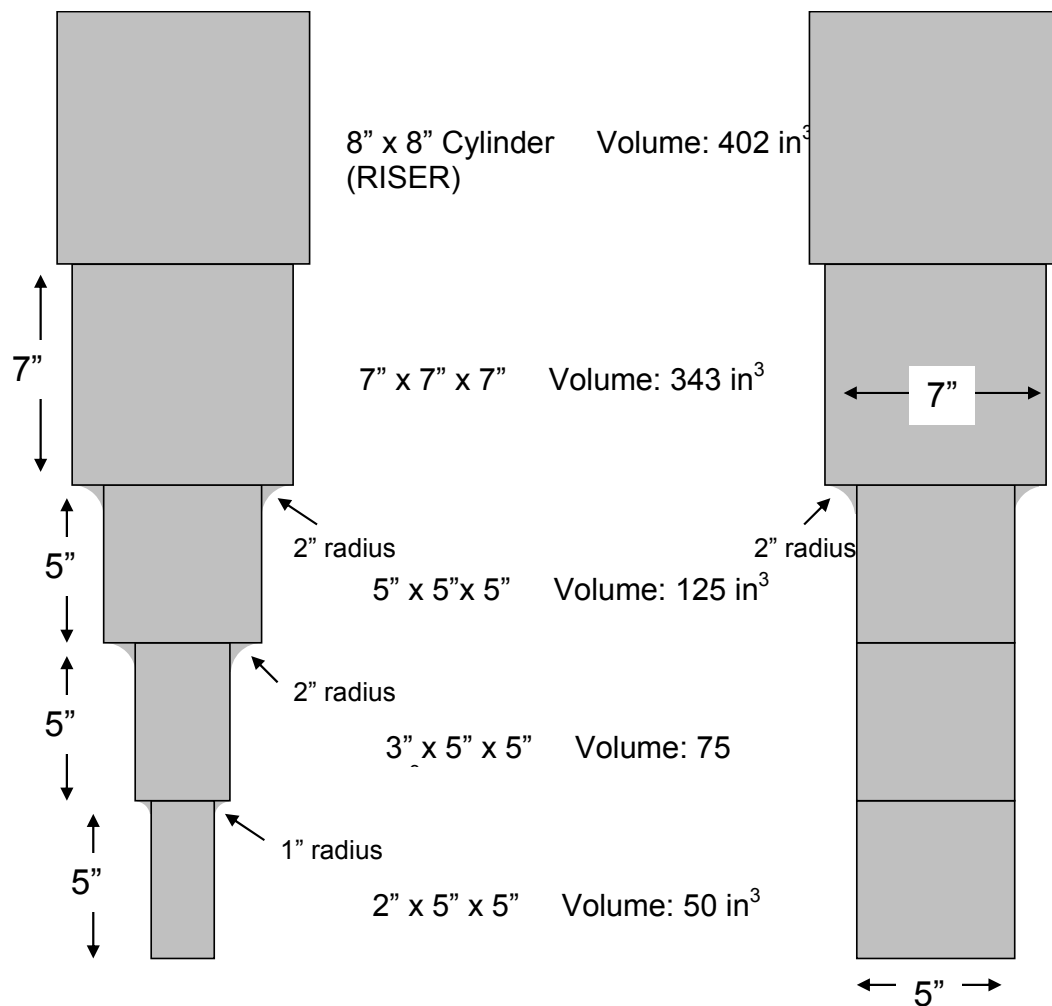


Figure 18: Schematic of the MetalTek 300 lbs. Haynes 282 step block casting with dimensions



Figure 19: MetalTek 300 lbs. Haynes 282 step block casting after mold shake out and shot blast cleaning operations. Bottom gated with casting top feeder arrangement shown.

Heat Treat Cycles: To justify the thermal cycle applied to the step blocks, microprobe analysis was performed on the casting as-cast and after a series of homogenization cycles to model the effect of the secondary dendrite arm spacing had on the extent of remaining segregation. Those cycles attempted to optimize a thermal cycle for homogenization while trading over time.

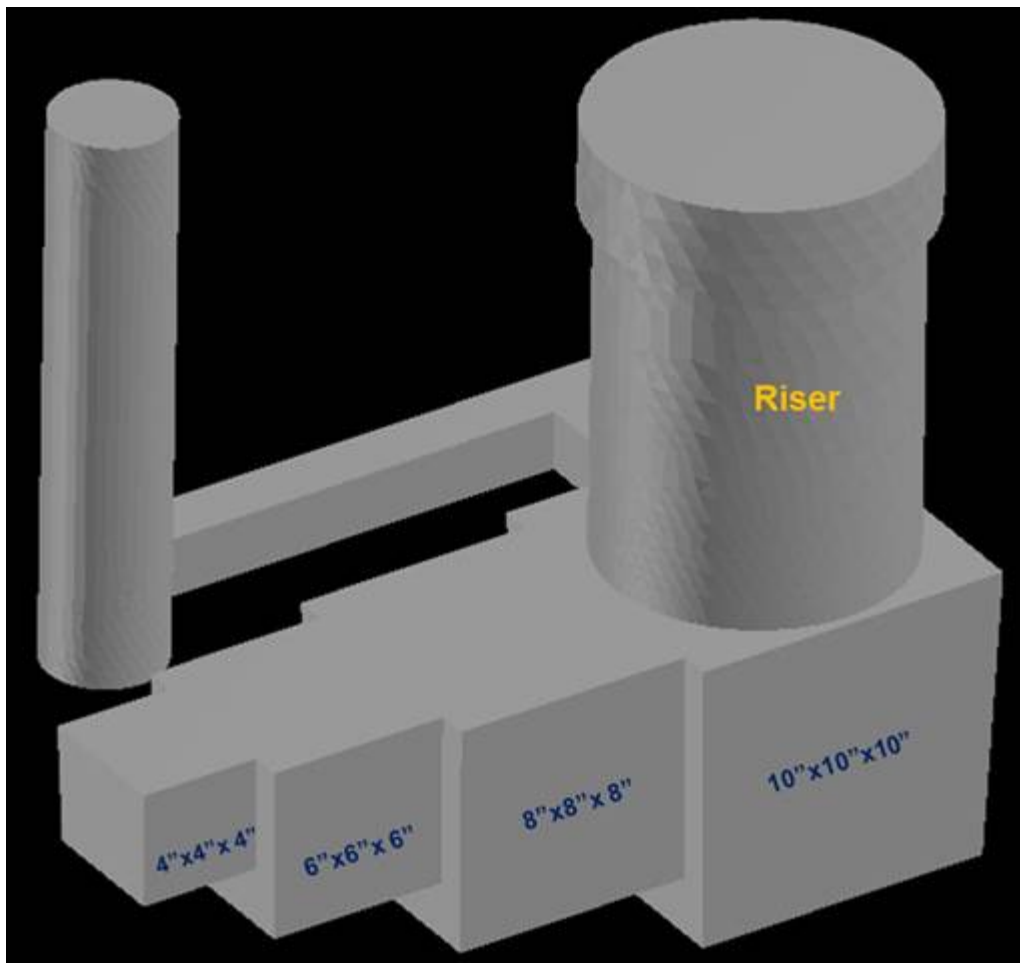


Figure 20: Schematic of Flowserve Step block. Top feeder with section modulus controlled feeding.

The core sections were tested for tensile, impact, and LCF properties as a baseline for future studies.

Both tensile and ductility values were lower compared with the smaller section cast cylinders data. The debit in mechanical properties are due to the in appropriate homogenization heat treatment cycles for the step block.

STEP CASTING OF NIMONIC 263

GE manufactured a large step block (SB) casting of Nimonic 263, with a pour weight of 1280 lbs. cast at Flowserve foundry and carried out multi step Homogenizing and Aging heat treatments followed by casting evaluation test program.

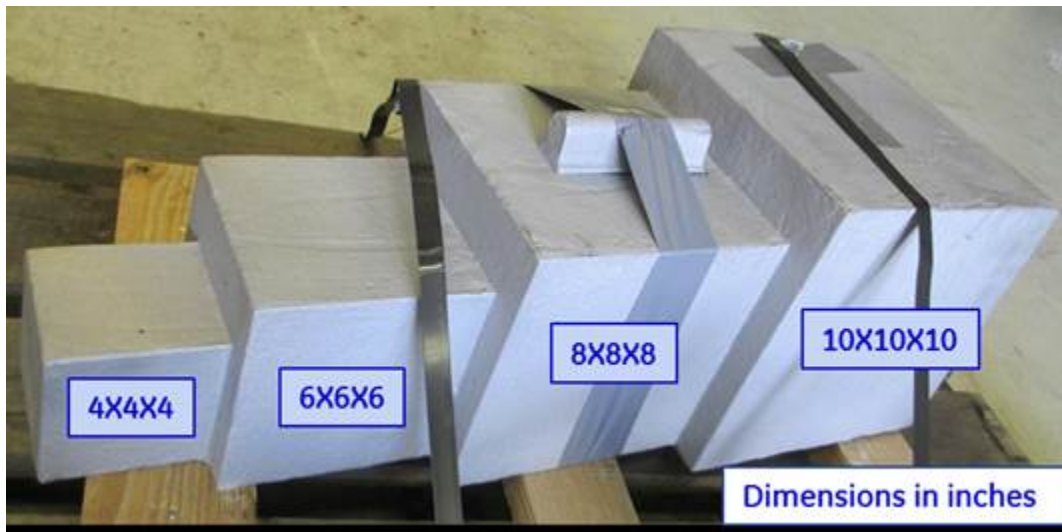


Figure 21: Nimonic 263 step block test casting, weighing 605 lbs. Completed optimized Homogenizing and Age hardening heat treatments

The test program evaluated casting solidification simulation analysis [Figure 23] NDT inspection methods [Figure 30], planned and executed detailed test matrix for chemical, mechanical property section sensitivity studies at RT and at elevated temperatures. Figure 26 - 27 provides the Test matrix. Trepan sample extraction location and orientations provided in [Figure 24-25].

N263 does not exhibit section sensitivity with respect to UTS, 0.2% YS, Hardness, stress rupture. However, section thickness influenced the ductility, LCF and Charpy impact energy properties. In addition, casting processing parameters such as gating, feeding, mold and melt processing steps, solidification cooling rate, and heat treatment cycles (Homogenizing & Aging) demonstrated influence on mechanical properties.

The Casting methods, mold, melt, pouring, processing steps and heat treatment are the main foundry process key characteristics:

- Casting gating & feeder methods to ensure free from Shrinkage, porosity-cavity defects.
- Mold zircon refractory coat painting is essential to minimize mold metal interaction related defects. Followed by adequate preheating of molds and ladles to dry refractory
- Argon cover of liquid metal during melt processing and Argon purging of pouring launders, ladles, molds are essential to avoid gas blow hole sub surface casting defects
- Heat treat parameters: Solutionizing optimized to within +/- 5% of composition variation recommended, considering the incipient melt temperatures at various stages.

Findings and Observations Summary:

No significant variation in chemistry when compared with section thermal centers [Figure 28].

Plots of UTS and 0.02% YS as a function of section thickness and temperature are shown below. All data falls within a tighter band at 1400°F-1500°F (760°C - 816°C) elevated temperature range. [Figures 33-37]

% Elongation as a function of temperature for various section thicknesses exhibit a wide variation as shown below [Figure 38].

% RA trend in smaller sections show a wide variation at elevated temperatures [Figure 39].

Hardness variation trend is not section thickness dependent, [Figure 54, Table-12]

CVN spread is larger in 10 inch section in comparison with 8 & 6 inch sections [Figure 53, Table-11].

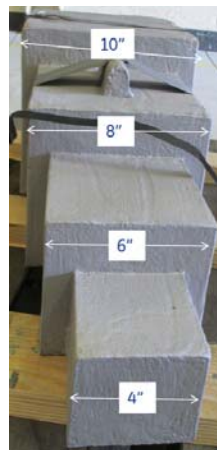
Plots of cycles to failure and Total strain range (%) for the 10" and 6" thick sections at RT are shown below. The 10 inch section shows a debit in comparison with 6 inch section.

Plots of cycles to failure and Total strain range (%) for the 10" and 6" thick sections at 1400°F (760°C) are shown below. The 10 inch section shows increased debit in comparison with 6 inch section, while 6 inch section shows degradation [Figures 41-42].

No significant changes in stress rupture data with section thickness [Figure 43, Table-8]

Non-destructive testing (NDT) inspection methods are limited to RT, LPT and Acoustic Emission since UT inspection was not effective for the Haynes263 SB casting.

Kq, the conditional fracture toughness values are minimally influenced with temperature raise up to 6 inch cast wall thickness. [Figure 44, Table-10]



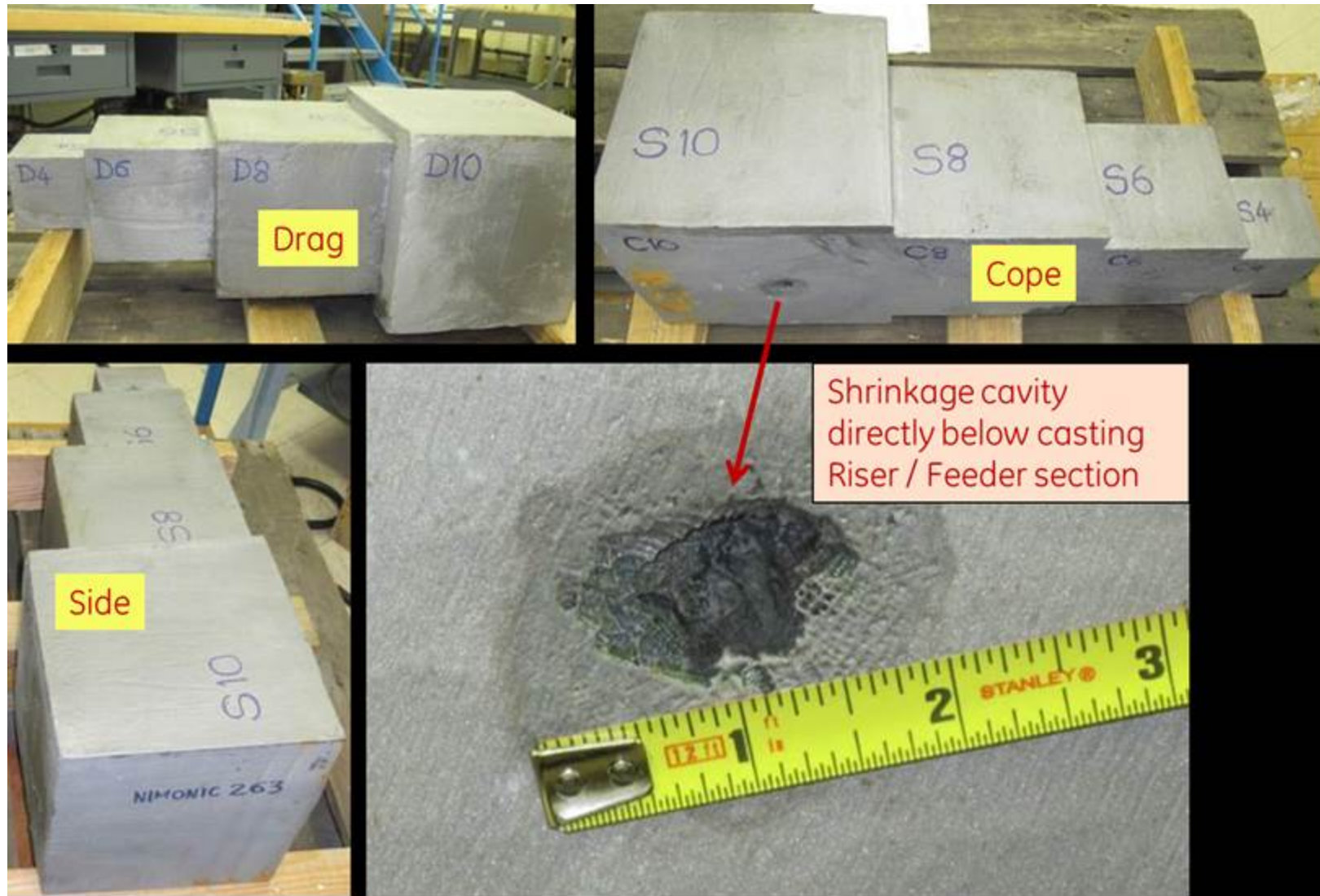


Figure 22: Picture showing the N263 casting and the associated shrink cavity below the rise/feeder section

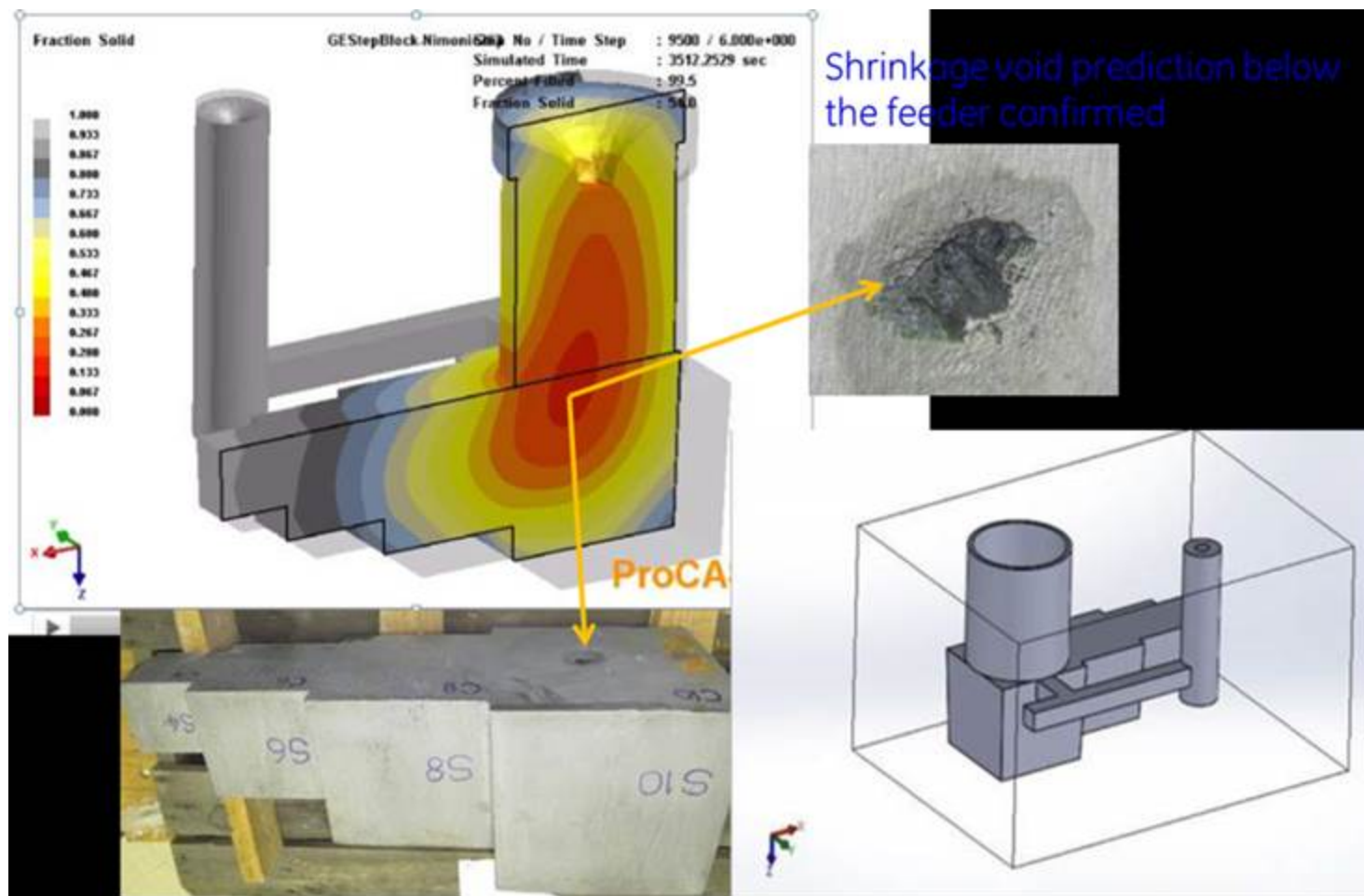


Figure 23: Casting solidification simulation analysis showing the hot spot location and the associated casting shrinkage defect. Shrinkage associated with Feeder section piping phenomena due to the thermal gradients established

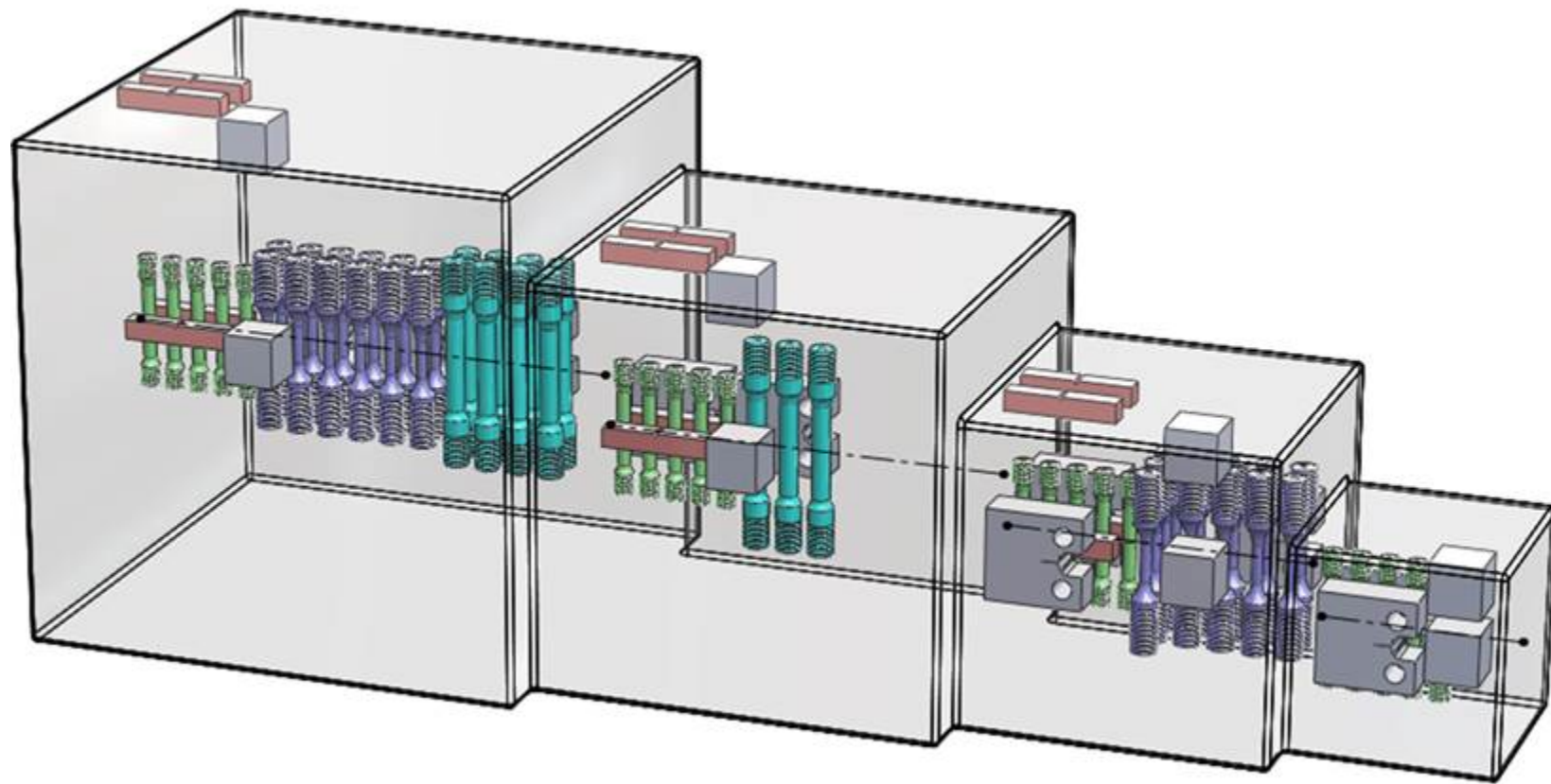


Figure 24: Nimonic 263 test casting, CAD layout of specimen extraction isometric views from step block cast sections

Specimens Centered on DL Line – 1" below surface

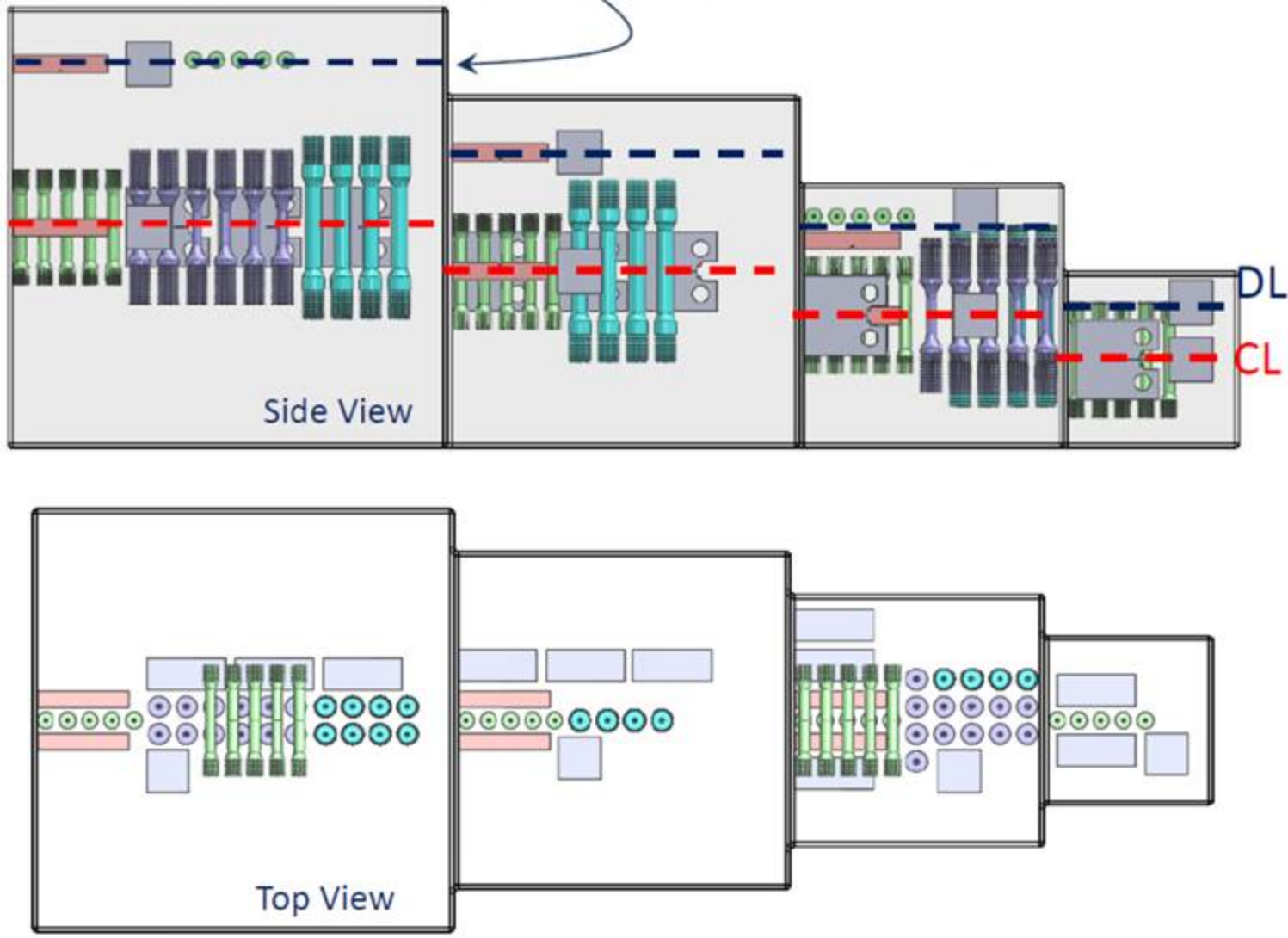


Figure 25: Orientation and specimen layout of various test specimens from N263 test block

Nimonic 263 step block test matrix:					Specimens Identification			
Test #	Test Type	Test condition	Step sections	Total Tests	Specimen ID / Step section			
1	Tensile Test (TS, YS, % EL, %RA) Tensile Specimen: MPE-TNSL-001 P4 30 specimens	Temperature deg.F	10"/8"/6"/4"	1 Test/section in CL plane in vertical orientation	10 inch	8 inch	6 inch	4 inch
			RT/ 75 deg. F		4	10-TN-CL-RT	8-TN-CL-RT	6-TN-CL-RT
			500 deg. F		4	10-TN-CL-500	8-TN-CL-500	6-TN-CL-500
			1000 deg.F		4	10-TN-CL-1000	8-TN-CL-1000	6-TN-CL-1000
			1250 deg.F		4	10-TN-CL-1250	8-TN-CL-1250	6-TN-CL-1250
			1500 deg F		4	10-TN-CL-1500	8-TN-CL-1500	6-TN-CL-1500
		RT/ 75 deg. F	1 Test/section in DL plane in Horizontal orientation (1" above Drag / bottom surface)	2	10-TN-DL-RT	NIL	6-TN-DL-RT	NIL
				2	10-TN-DL-500	NIL	6-TN-DL-500	NIL
				2	10-TN-DL-1000	NIL	6-TN-DL-1000	NIL
				2	10-TN-DL-1250	NIL	6-TN-DL-1250	NIL
				2	10-TN-DL-1500	NIL	6-TN-DL-1500	NIL
2	Charpy V Notch Impact Impact Energy (J); % Shear, Lateral Expansion 12 Specimens	RT/ 75 deg F	2 Tests at Centre CL plane vertical per section	6	10-CVN-RT-C1	8-CVN-RT-C1	6-CVN-RT-C1	NIL
					10-CVN-RT-C2	8-CVN-RT-C2	6-CVN-RT-C2	NIL
					10-CVN-RT-T1	8-CVN-RT-T1	6-CVN-RT-T1	NIL
			2 Tests at DL horizontal plane per section	6	10-CVN-RT-T2	8-CVN-RT-T2	6-CVN-RT-T2	NIL
3	LCF Data Frequency: 20 cpm Waveform: Triangular A Strain 1, TSR% (1.0; 0.90; 0.80; 0.70; 0.60; 0.50) 2 temperatures: RT & 1400 deg. F. Specimen Drg. # 4013195-741 24 specimens	RT/ 75 deg F	A strain / TSR (%)					
			1 / 1.00	2	10-LCF-01	NIL	6-LCF-01	NIL
			1 / 0.90	2	10-LCF-02	NIL	6-LCF-02	NIL
			1 / 0.80	2	10-LCF-03	NIL	6-LCF-03	NIL
			1 / 0.70	2	10-LCF-04	NIL	6-LCF-04	NIL
			1 / 0.60	2	10-LCF-05	NIL	6-LCF-05	NIL
			1 / 0.50	2	10-LCF-06	NIL	6-LCF-06	NIL
		1400 deg F	1 / 1.00	2	10-LCF-07	NIL	6-LCF-07	NIL
			1 / 0.90	2	10-LCF-08	NIL	6-LCF-08	NIL
			1 / 0.80	2	10-LCF-09	NIL	6-LCF-09	NIL
			1 / 0.70	2	10-LCF-10	NIL	6-LCF-10	NIL
			1 / 0.60	2	10-LCF-11	NIL	6-LCF-11	NIL
			1 / 0.50	2	10-LCF-12	NIL	6-LCF-12	NIL

Figure 26: Test matrix for Tensile, Charpy impact energy and LCF properties with specimen identification

Nimonic 263 step block test matrix:					Specimens Identification			
Test #	Test Type	Test condition	Step sections	Total Tests	Specimen ID / Step section			
4	Stress rupture Specimen per MPE-RUP 003-P3 16 specimens (Creep data not required)	Temperature deg.F	10"/8"/6"/4"		10 inch	8 inch	6 inch	4 inch
		Temperature deg.F	Stress					
		1472	40	1	10-RUP-01	NIL	NIL	NIL
		1472	35	1	10-RUP-02	NIL	NIL	NIL
		1472	30	1	10-RUP-03	NIL	NIL	NIL
		1472	25	1	10-RUP-04	NIL	NIL	NIL
		1400	45	3	10-RUP-05	8-RUP-01	6-RUP-01	NIL
		1400	40	3	10-RUP-06	8-RUP-02	6-RUP-02	NIL
		1400	35	3	10-RUP-07	8-RUP-03	6-RUP-03	NIL
		1400	30	3	10-RUP-08	8-RUP-04	6-RUP-04	NIL
5	Fracture Toughness Specimen per # 8024 J1C -11 specimens	RT/ 75 deg. F		4	10-J1c-01	8-J1c-01	6-J1c-01	4-J1c-01
		1000 deg.F		3	10-J1c-02	8-J1c-02	6-J1c-02	NIL
		1400 deg F		4	10-J1c-03	8-J1c-03	6-J1c-03	4-J1c-02
6	Chemical Analysis 8 Specimens	Ni,Cr,Co,Mo,Ti,Al,Fe, Mn,Si,C,B,P,S & Cu	Thermal Center	4	10-C-1	8-C-1	6-C-1	4-C-1
			1" above drag	4	10-D-1	8-D-1	6-D-1	4-D-1

Figure 27: Test matrix for Stress rupture, Fracture toughness and Chemical analysis with specimen identification

Chemical Analysis: (Wt. %)	Nimonic 263 N07263 SB - Casting	GJOJ-263-TB-1	Step block casting section locations Chemical composition values (Wt. %)							
			10 inch		8 inch		6 inch		4 inch	
			Thermal-C	Drag-1"	Thermal-C	Drag-1"	Thermal-C	Drag-1"	Thermal-C	Drag-1"
	Flowserve Heat	Cast on coupon	10-C-1	10-D-1	8-C-1	8-D-1	6-C-1	6-D-1	4-C-1	4-D-1
C	0.06	0.01	0.01	0.01	0.01	0.01	0.01	0.01	0.02	0.01
Mn	0.31	0.3	0.29	0.3	0.29	0.3	0.3	0.3	0.3	0.3
Si	0.61*	0.65	0.59	0.66	0.63	0.64	0.66	0.66	0.65	0.66
P	-	<0.010	<0.10	<0.10	<0.10	<0.10	<0.10	<0.10	<0.10	<0.10
S	-	<0.001	<0.001	<0.001	<0.001	<0.001	<0.001	<0.001	<0.001	<0.001
Cr	19.4	20.2	19.97	20.12	20.14	20.07	20.09	20.15	20.12	20.08
NI	Bal.	50.25	50.23	50.3	50.45	50.5	50.19	50.14	50.18	50.48
Mo	5.8	5.56	5.72	5.67	5.66	5.6	5.8	5.77	5.82	5.55
Co	20.2	19.82	20.14	19.68	19.76	19.67	19.78	19.73	19.67	19.71
Fe	0.45	0.45	0.5	0.48	0.49	0.48	0.46	0.47	0.47	0.48
Cu	0.02	0.02	0.02	0.02	0.02	0.02	0.02	0.02	0.02	0.02
B		0.005	0.005	0.005	0.005	0.005	0.005	0.005	0.005	0.005
Al	0.4	0.34	0.31	0.31	0.32	0.33	0.32	0.32	0.32	0.34
Ti	2.12	2.12	2	2.18	1.97	2.13	2.11	2.16	2.17	2.12

Figure 28: Step block casting thermal center trepanned section chemical analysis. No significant variation in chemistry when compared with casting section Thermal center analysis

Homogenizing Heat Treatment (Note: As-Cast Incipient MP is 2102°F)

- Part should be loaded into a room temperature furnace with contact thermocouples for recording homogenization HT cycle. Also furnace thermocouples HT cycle record.
- Ramp furnace at a rate not exceeding 350°F/Hour
- **Hold at 1900°F ± 25°F for four hours**
- Ramp furnace to 1960°F
- **Hold at 1960°F ± 25°F for four hours.**
- Ramp furnace to 2012°F.
- **Hold at 2012°F ± 25°F for ONE hour**
 - (Note: Theoretical Incipient MP is now 2291°F)
- Ramp furnace to 2090°F
- **Hold at 2090°F ± 10°F for Four hours**
- Ramp to 2175°F
- **Hold at 2175°F ± 10°F for 44 Hours**
 - (Note: Theoretical Incipient MP is now 2410°F)
- Forced Air Cool to RT with fans, keeping contact thermocouples attached for measuring cooling rate

AGING- HT Cycle

- Ramp furnace at a rate not exceeding 350°F/Hour
- **Hold at 1472°F ± 25°F for 8 Hours**
- Forced Air Cool with Fans measuring cooing rate with contact thermocouples attached.

Figure 29: Homogenizing and Aging Heat treatment cycles Optimized to within +/- 5% of nominal chemistry variation (NETL)

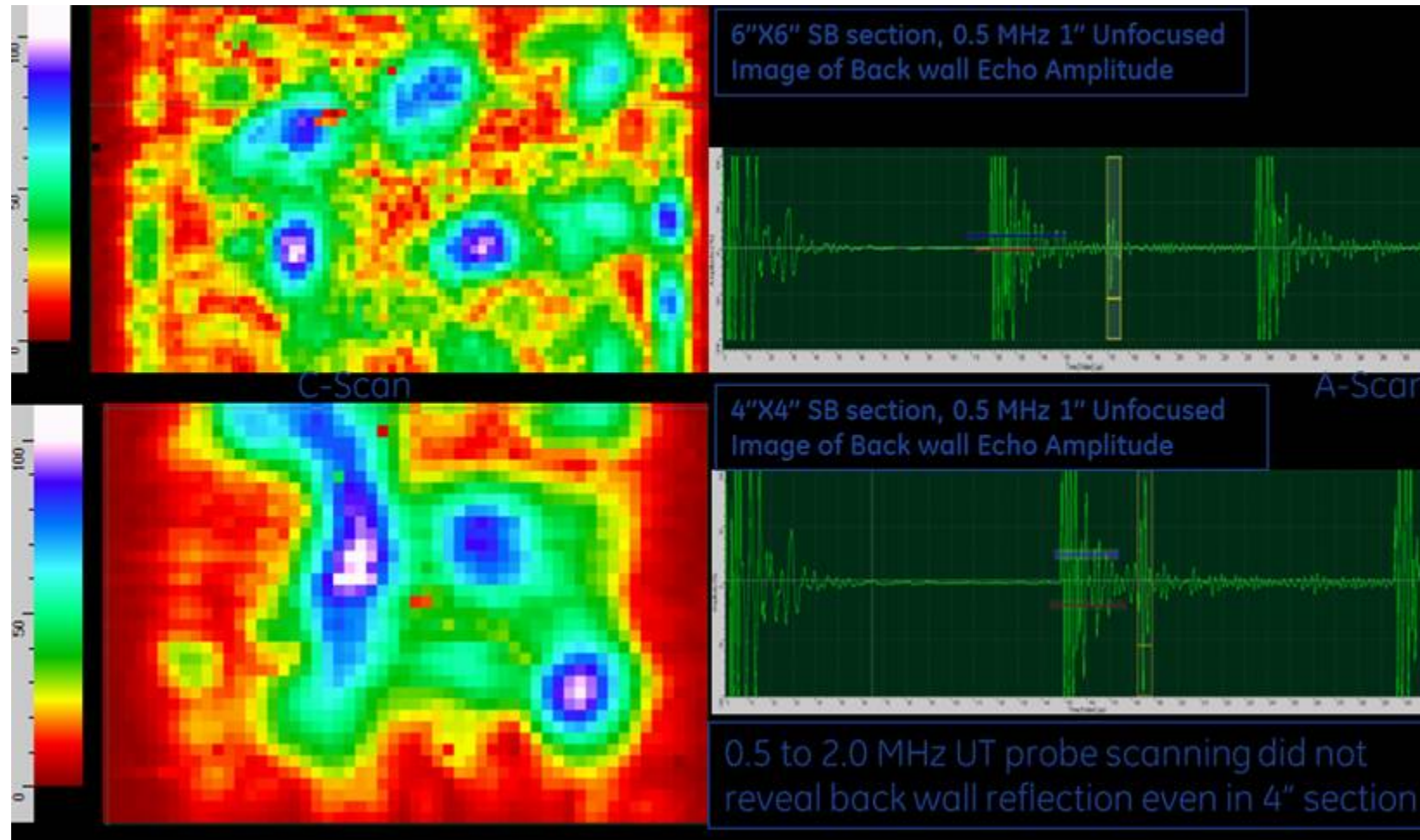


Figure 30: UT immersion scans of N263 step block casting 6 inch and 4 inch sections showing the inherent issue of achieving a superior back wall reflection in thick walled super alloy castings

MISTRAS GROUP INC.

2 MILLBURY STREET
AUBURN, MA. 01501
TELEPHONE (508) 832-5500
FAX (508) 832-5557

Figure 31: Radiographic Scan Plan

MISTRAS GROUP INC

2 Millbury Street
Auburn, Massachusetts 01501
(508) 832-5500 Fax (508) 832-5557

RADIOGRAPHIC REPORT

PAGE 1 OF 1

LOCATIONS NATIONWIDE

BRANCH LABORATORY
SPRINGFIELD, MA.

(413) 734-6648 FAX: (413) 734-2810

Nondestructive Testing - QA/QC Services - Chemical Testing - Mechanical Testing - Metallurgical Testing & Failure Analysis

Figure 32: Radiographic Test Report confirming no other casting defect in other cast sections, except the surface cavity defect in 10 inch section under the casting feeder.

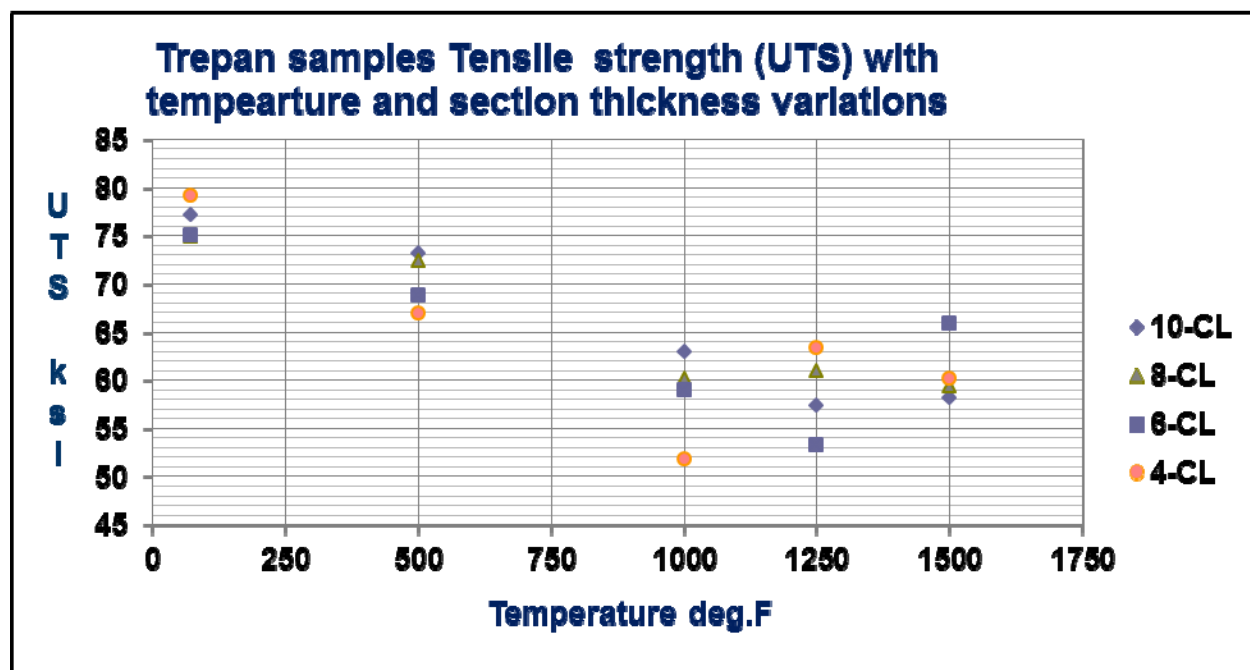


Figure 33: UTS plot with temperature and trepanned casting section thickness variation

Table 1: N263 Step block trepan cast sections tensile strength (UTS) vs temperature data

N263 Step Block trepan cast sections UTS vs. Temperature						
Section thickness (inches)	10-CL (10)	10-DL (10)	8-CL (8)	6-CL (6)	6-DL (6)	4-CL (4)
Temperature °F	(ksi)	(ksi)	(ksi)	(ksi)	(ksi)	(ksi)
72°F	77.2	71.1	74.9	75	70.5	79.2
500°F	73.2	67.3	72.4	68.8	60	66.9
1000°F	63	69.1	60.1	58.9	58.9	51.8
1250°F	57.4	57.6	61	53.3	68.8	63.3
1500°F	58.2	52.4	59.4	65.8	60	60.2

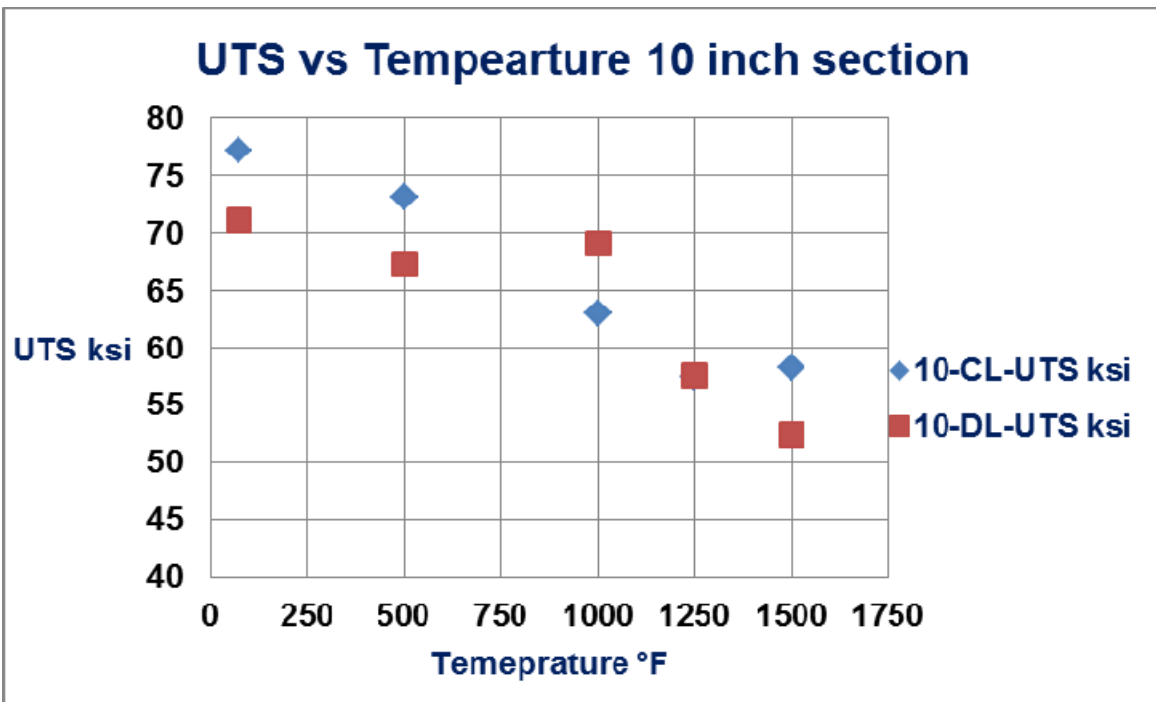


Figure 34: UTS vs temperature plot for 10 inch section CL and DL location trepans

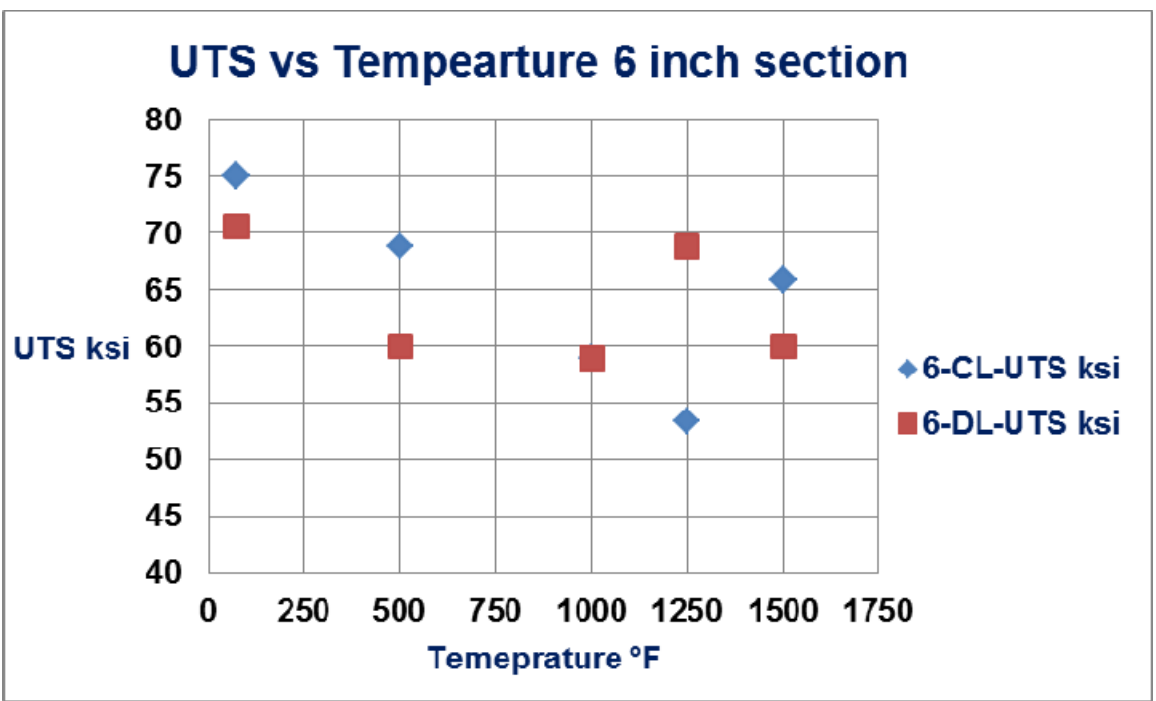


Figure 35 UTS vs temperature plot for 6 inch section CL and DL location trepans

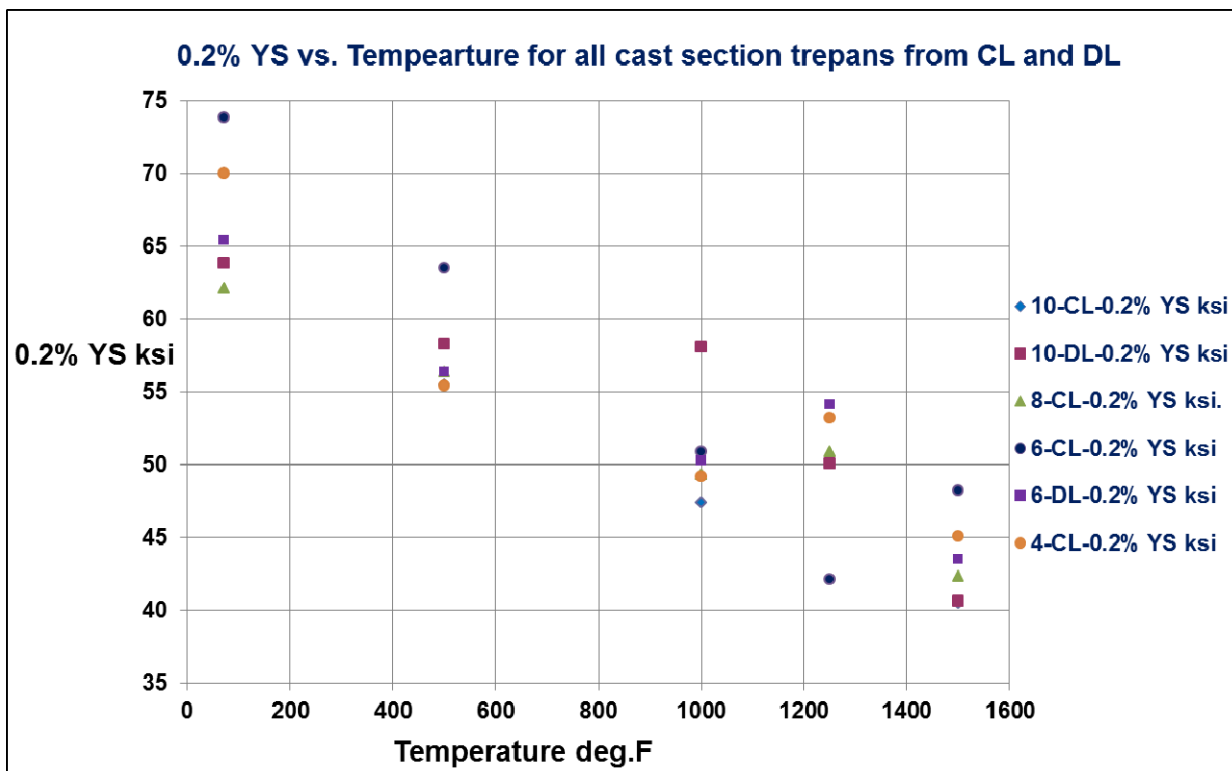


Figure 36: 0.2 % YS vs. Temperature for all N263 step block cast section trepans. The 0.2% YS vs. temperature trend plot shows tighter band trepan CL values at elevated temperatures for all section thicknesses

Table 2: N263 Step block trepan cast sections 0.2% Yield strength vs temperature data

N263 Step Block trepan cast sections 0.2% YS vs. Temperature						
Section thickness (inches)	10-CL (10)	10-DL (10)	8-CL (8)	6-CL (6)	6-DL (6)	4-CL (4)
Temperature °F	(ksi)	(ksi)	(ksi)	(ksi)	(ksi)	(ksi)
72°F	70	63.8	62.1	73.8	65.4	70
500°F	55.5	58.3	56.4	63.5	56.4	55.4
1000°F	47.4	58.1	49.3	50.9	50.3	49.2
1250°F	50.2	50.1	50.9	42.1	54.1	53.2
1500°F	40.5	40.6	42.3	48.2	43.5	45.1

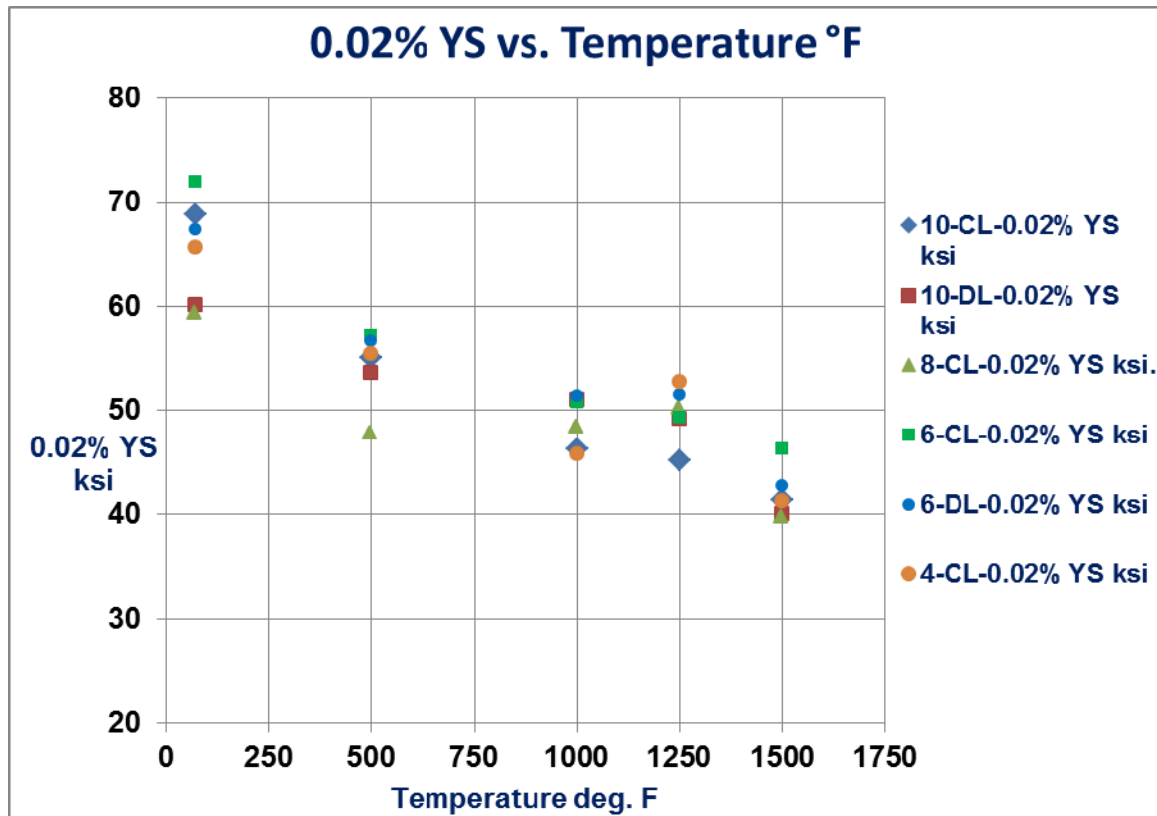


Figure 37: 0.02 % YS vs. Temperature for all N263 step block section trepans. The 0.02% YS vs. temperature trend plot shows tighter band at elevated temperatures for all section thicknesses

Table 3: N263 Step block trepan cast sections 0.02% Yield strength vs temperature data

N263 Step Block trepan cast sections 0.02% YS vs. Temperature						
Section thickness (inches)	10-CL (10)	10-DL (10)	8-CL (8)	6-CL (6)	6-DL (6)	4-CL (4)
Temperature °F	(ksi)	(ksi)	(ksi)	(ksi)	(ksi)	(ksi)
72°F	68.8	60.1	59.4	71.9	67.3	65.6
500°F	55	53.6	47.8	57.1	56.6	55.4
1000°F	46.3	51	48.4	50.7	51.4	45.8
1250°F	45.1	49.2	50.3	49.3	51.5	52.7
1500°F	41.4	40	39.8	46.3	42.7	41.3

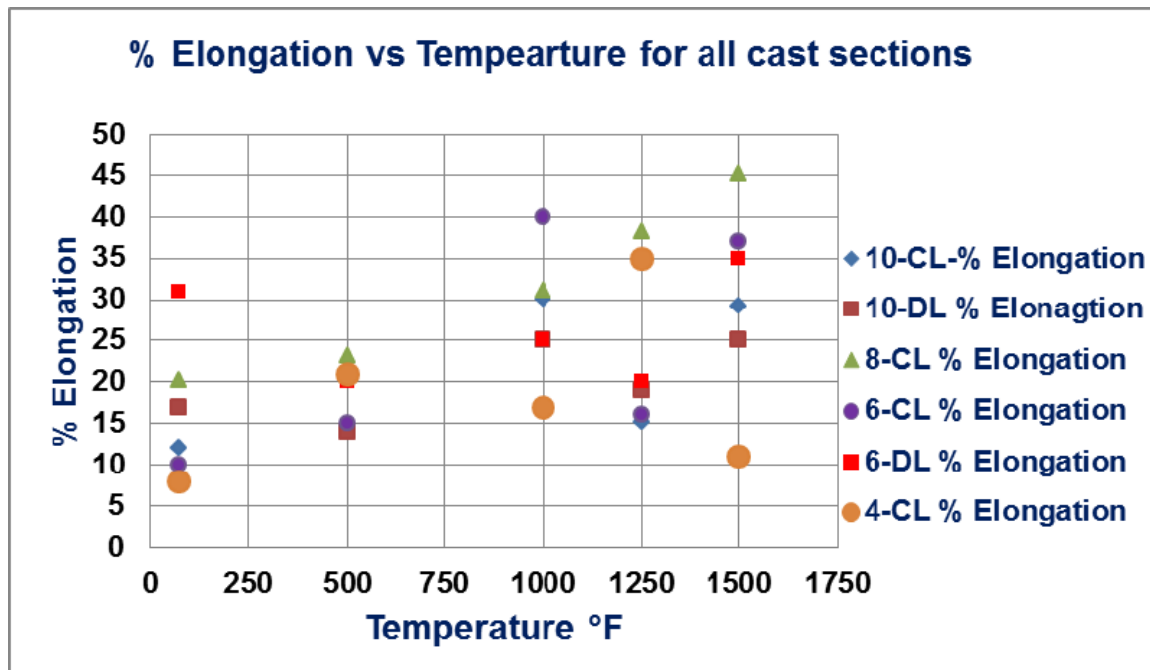


Figure 38: N263 step block cast section trepan samples % Elongation vs. Temperature

Table 4: N263 step block trepan section samples % Elongation values

Trepan sample % Elongation with temperature and section size						
Temperature (deg. F)	10-CL (%)	10-DL (%)	8-CL (%)	6-CL (%)	6-DL (%)	4-CL (%)
72	12	17	20	10	31	8
500	21	14	23	15	20	21
1000	30	25	31	40	25	17
1250	15	19	38	16	20	35
1500	29	25	45	37	35	11

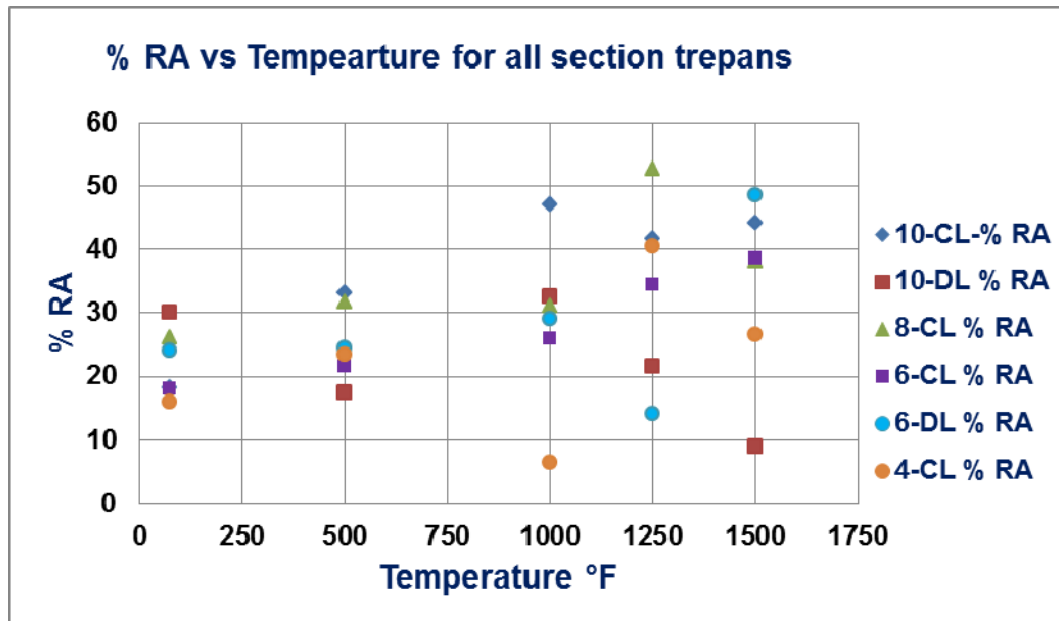


Figure 39: N263 %RA Vs Temperature plots for all section trepans

Table 5: N263 Step Block section Trepan sample % RA values data

Trepan sample % RA values with temperature and section size						
Temperature	10-CL	10-DL	8-CL	6-CL	6-DL	4-CL
(deg. F)	(%)	(%)	(%)	(%)	(%)	(%)
72	18	30	26	18	24	16
500	33	17.5	31.5	21.5	24.5	23.5
1000	47	32.5	31	26	29	6.5
1250	41.5	21.5	52.5	34.5	14	40.5
1500	44	9	38	38.5	48.5	26.5

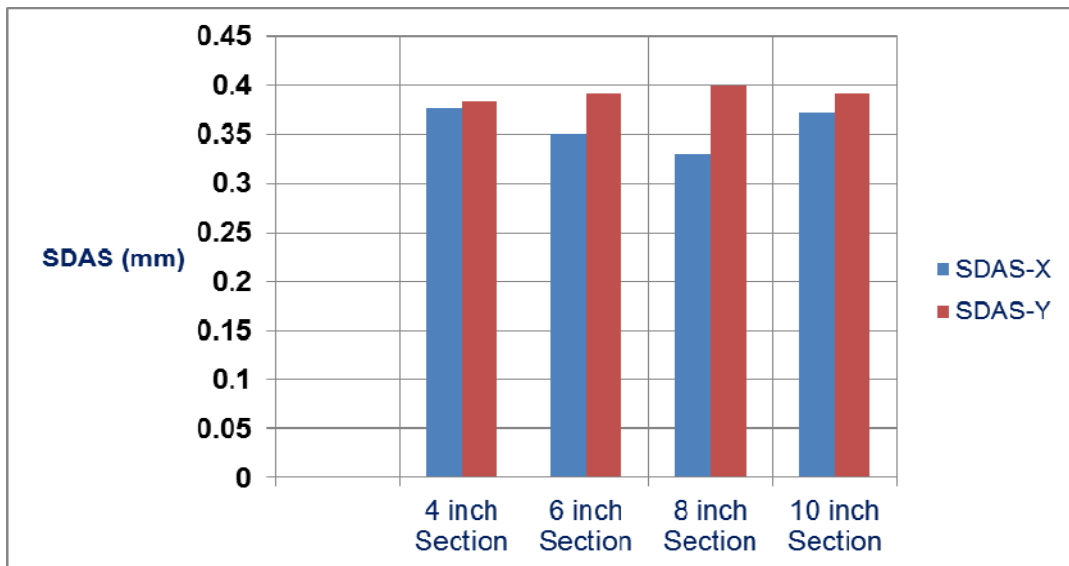
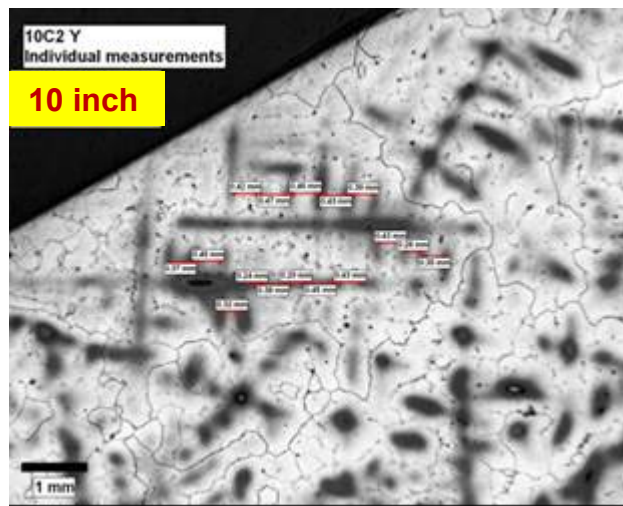
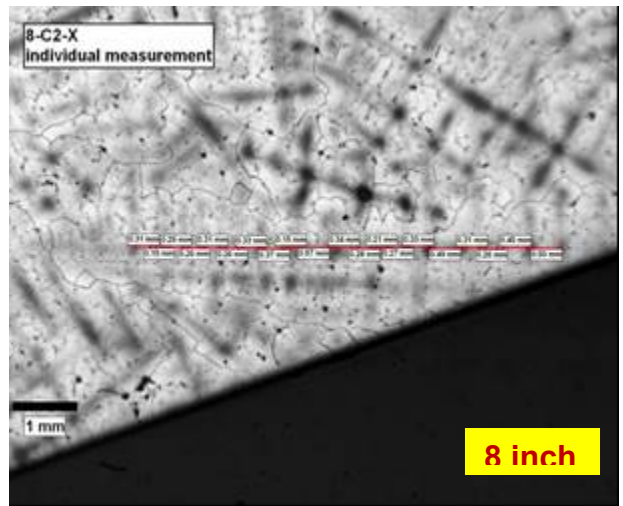
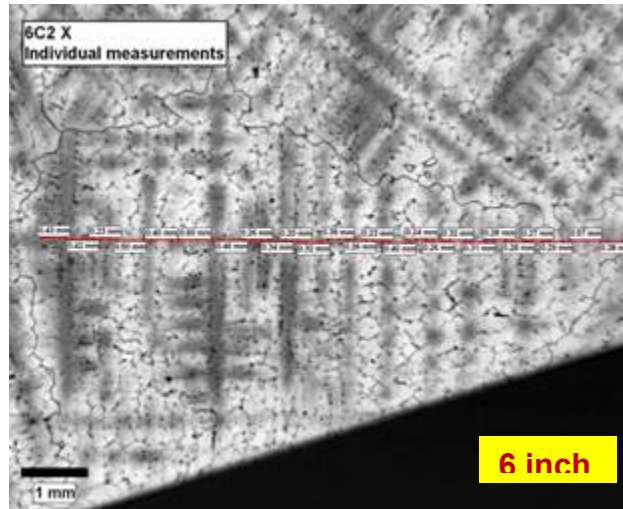
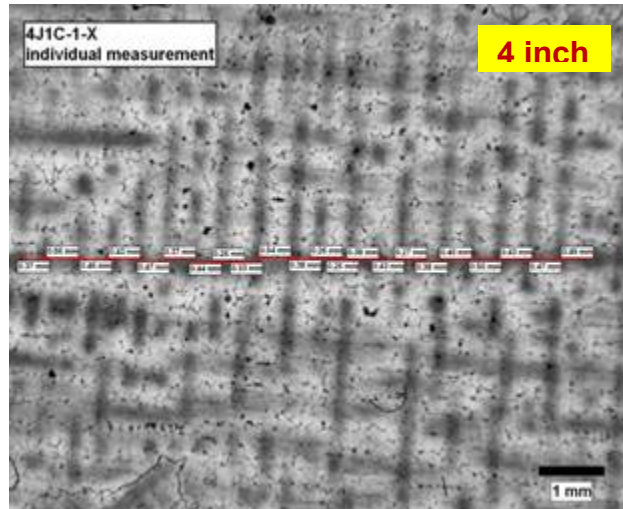


Figure 40: Nimonic 263 step block casting SDAS measurements with section size

Table 6: Nimonic 263 Step block cast sections SDAS Measurements. Consistently in the range of 0.35 to 0.40 mm for 100 to 250 mm cast sections

N263 SB Casting SDAS Measurements				
Section thickness	SDAS Counts #		SDAS Average value (mm)	
	X	Y	SDAS-X	SDAS-Y
4 Inch Section	32	29	0.38	0.38
6 Inch Section	25	30	0.35	0.39
8 Inch Section	27	27	0.33	0.40
10 Inch Section	27	25	0.37	0.39

Table 7: Nimonic 263 Step block cast section thermal center trepanned samples SDAS values show independent of casting section thickness and orientation



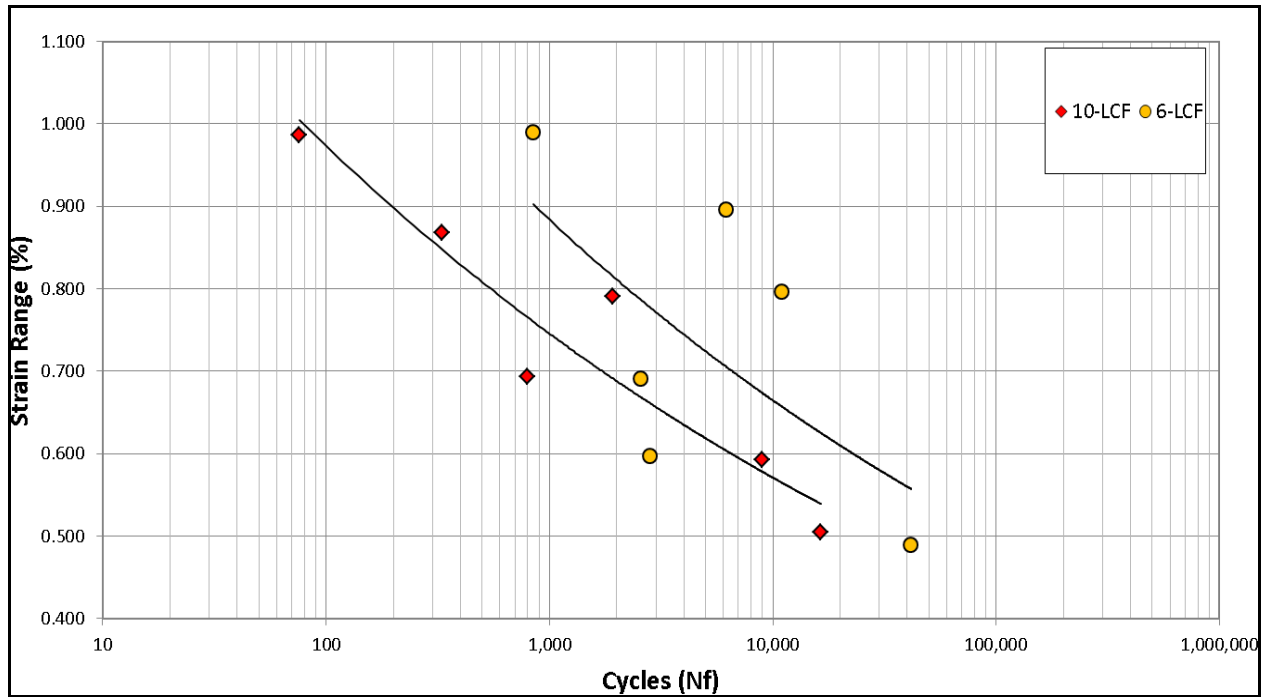


Figure 41: N263 Step block 10 inch and 6 inch sections cycles to failure compared at RT, A-ratio 1. The 10 inch section shows a debit in comparison with 6 inch section

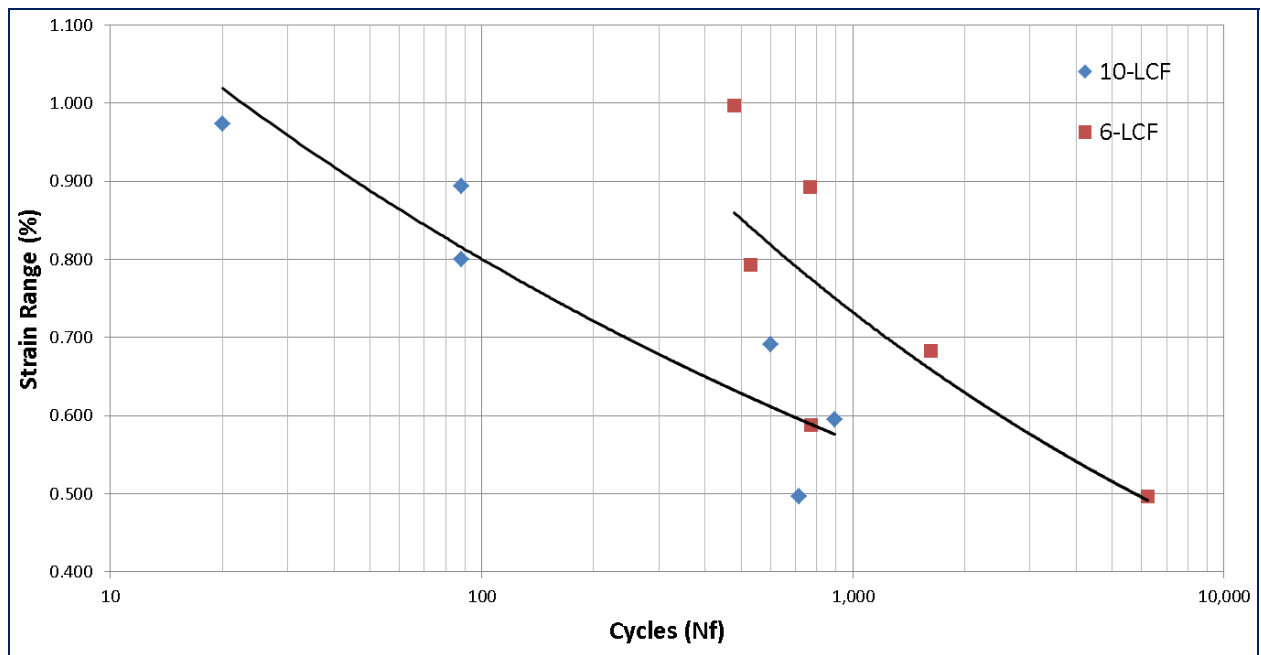


Figure 42: N263 Step block 10 inch and 6 inch sections cycles to failure compared at 1400°F (760°C), A-Ratio 1. The 10 inch section shows increased debit in comparison with 6 inch section, while 6 inch section shows degradation

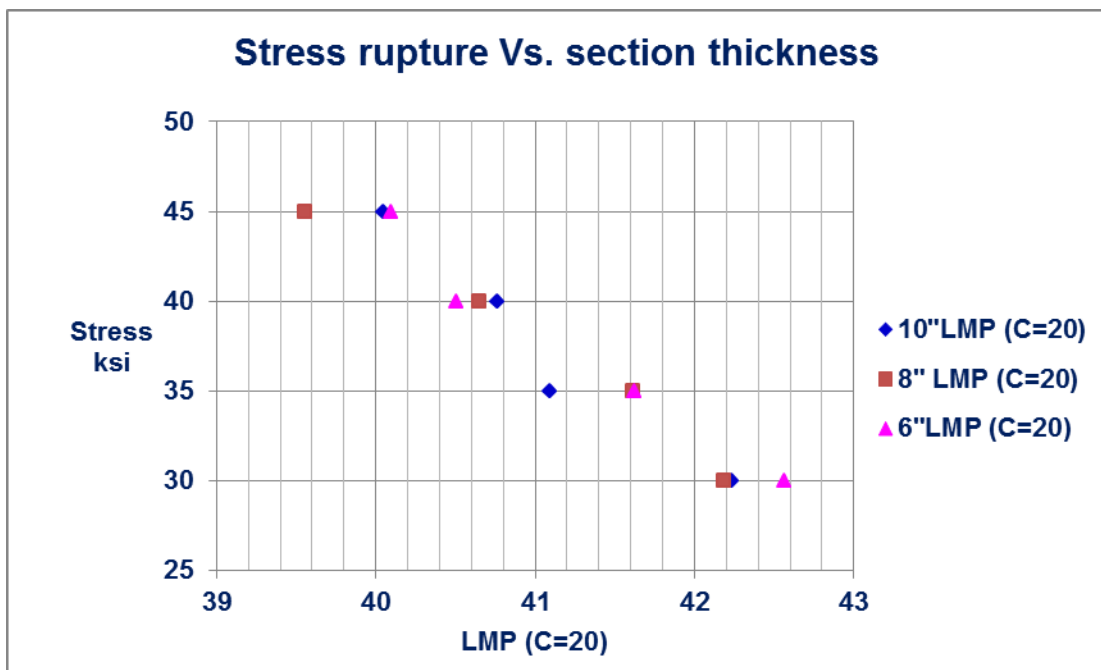


Figure 43: N263 Stress rupture strength vs, LMP (C=20) with section thickness. No significant changes in stress rupture data with section thickness variation

Table 8: Stress rupture test results raw data

Sample ID	Temp. °F	Time (hrs)	Elong %	RA %	Stress (ksi)	LMP
10-RUP-01	1472	1.8	9.3	19.2	40	39.13
10-RUP-02	1472	35.2	21.2	39.0	35	41.63
10-RUP-03	1472	49.2	14.5	27.6	30	41.91
10-RUP-04	1472	209.8	19.0	34.4	25	43.13
10-RUP-05	1400	33.9	15.7	14.4	45	40.05
10-RUP-06	1400	82.5	12.9	22.0	40	40.76
10-RUP-07	1400	123.6	11.3	22.3	35	41.09
10-RUP-08	1400	508.1	16.9	30.4	30	42.23
8-RUP-01	1400	18.4	15.3	41.2	45	39.55
8-RUP-02	1400	71.8	12.4	23.2	40	40.65
8-RUP-03	1400	235.5	15.3	18.1	35	41.61
8-RUP-04	1400	479.9	17.9	38.2	30	42.19
6-RUP-01	1400	36.0	12.8	17.9	45	40.09
6-RUP-02	1400	59.7	13.6	39.0	40	40.50
6-RUP-03	1400	238.3	11.7	14.9	35	41.62
6-RUP-04	1400	761.8	9.0	27.3	30	42.56

Table 9: Nimonic 263 Step block sections J-Integral Test results at RT; 1000°F (538°C) and 1400°F (760°C) summarized

Specimen	Testlog Number	Temperature	J_Q (in lb/in ²)	K_{J_Q} (ksi/in)	K_{Ic} Determination (Annex 5)		Unstable
					P_0 (lb)	K_0 (ksi/in)	
10-JIC-01	T46793	Room	273.85	102.57	5046.9	62.3	No
8-JIC-01	T46794	Room	623.19	146.56	4402.0	48.8	No
6-JIC-01	T46795	Room	327.07	105.57	4017.5	49.4	No
4-JIC-01	T46796	Room	531.87	136.16	4765.0	56.0	No
10-JIC-02	T46797	1000°F	479.30	119.34	3313.4	39.3	No
8-JIC-02	T46798	1000°F	642.31	139.60	4542.9	50.7	No
6-JIC-02	T46799	1000°F	467.36	113.85	3779.3	49.0	No
10-JIC-03	T46800	1400°F	272.22	83.74	3236.6	38.7	No
8-JIC-03	T46801	1400°F	621.48	123.59	3707.6	41.8	No
6-JIC-03	T46802	1400°F	336.48	90.25	3855.4	47.9	No
4-JIC-02	T46803	1400°F	550.07	115.68	4371.5	51.4	No

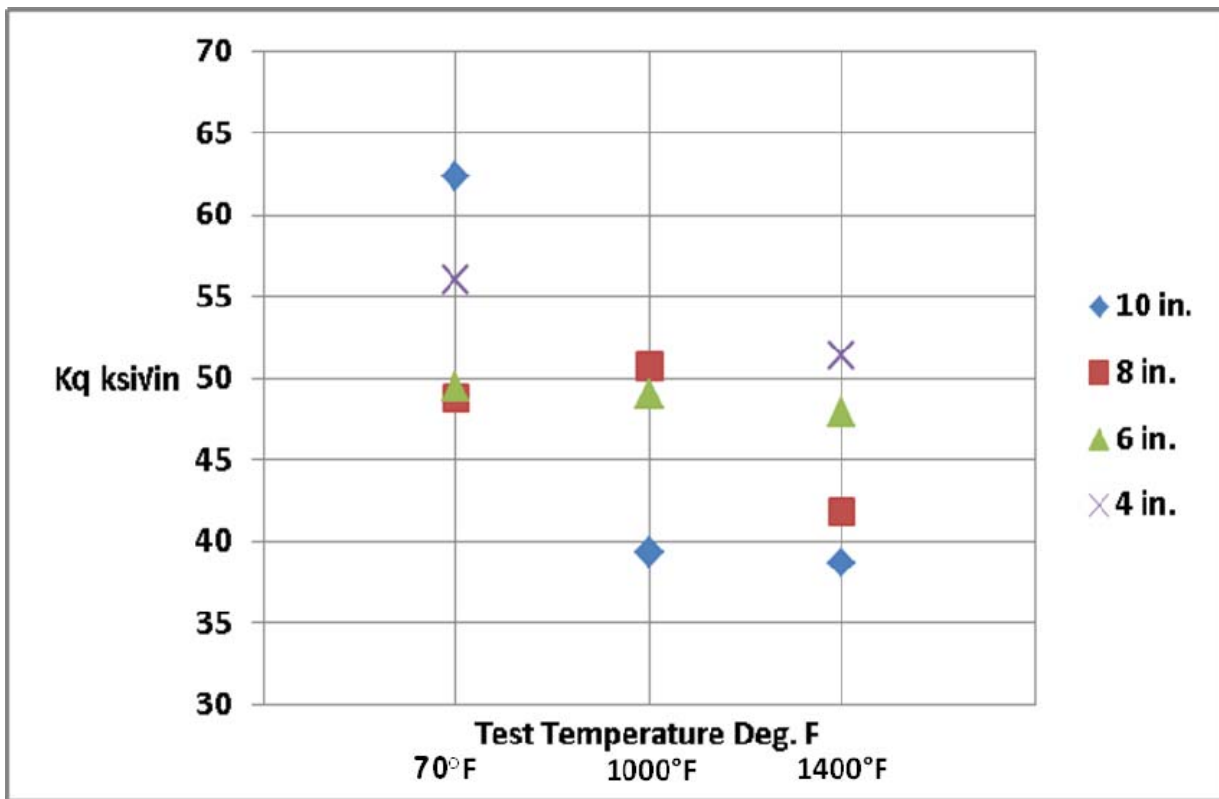


Figure 44: Plot showing Kq Fracture toughness value Vs. Temperature for various section sizes. Note that the conditional fracture toughness Kq values are minimum influenced with temperature raise up to 6 inch cast wall thickness

Table 10: Kq Fracture toughness @ RT, 1000°F (538°C) and 1400°F (760°C) temperatures vs. section size data

Kq ksivin Fracture toughness plot			
SB Section	70°F	1000°F	1400°F
10 in.	62.3	39.3	38.7
8 in.	48.8	50.7	41.8
6 in.	49.4	49	47.9
4 in.	56		51.4

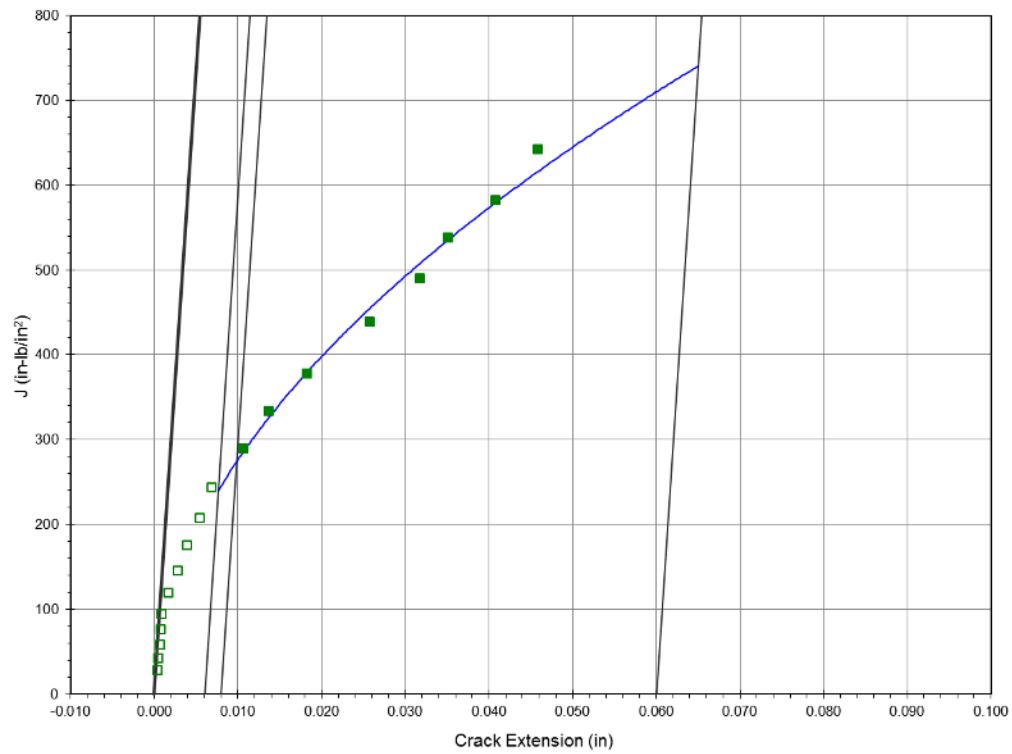


Figure 45: 10-J1C-01, J vs. a graph for 10 inch section tested at RT

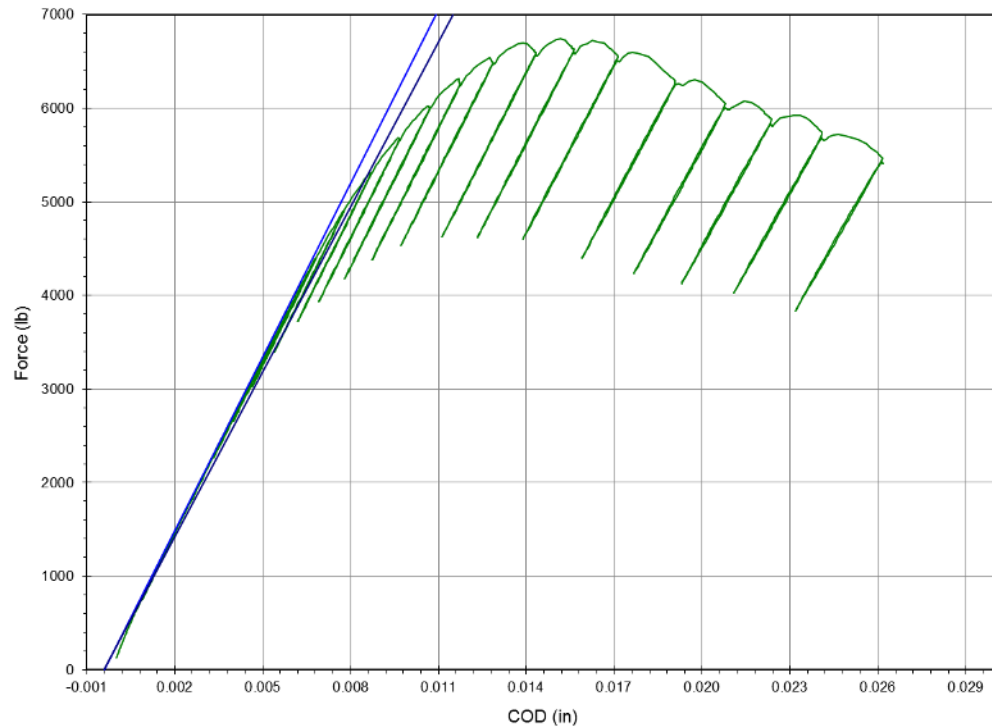


Figure 46: 10-J1C-01, Force vs. COD graph for 10 inch section tested at RT

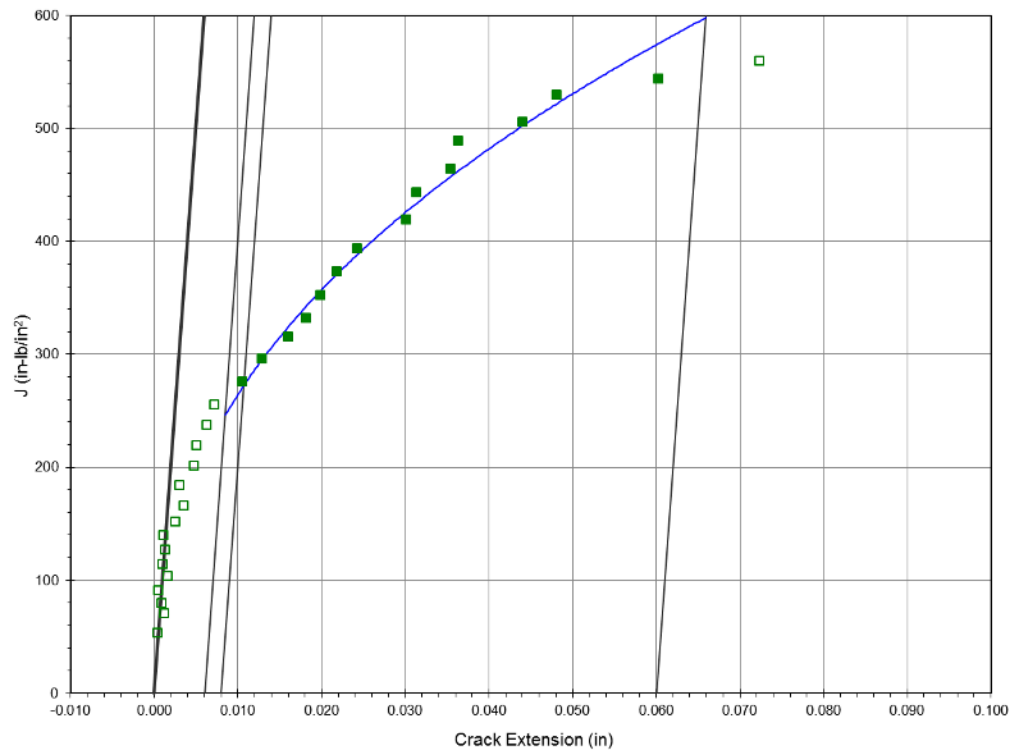


Figure 47: 10-J1C-03, J vs. a graph for 10 inch section tested at 1400°F (760°C)

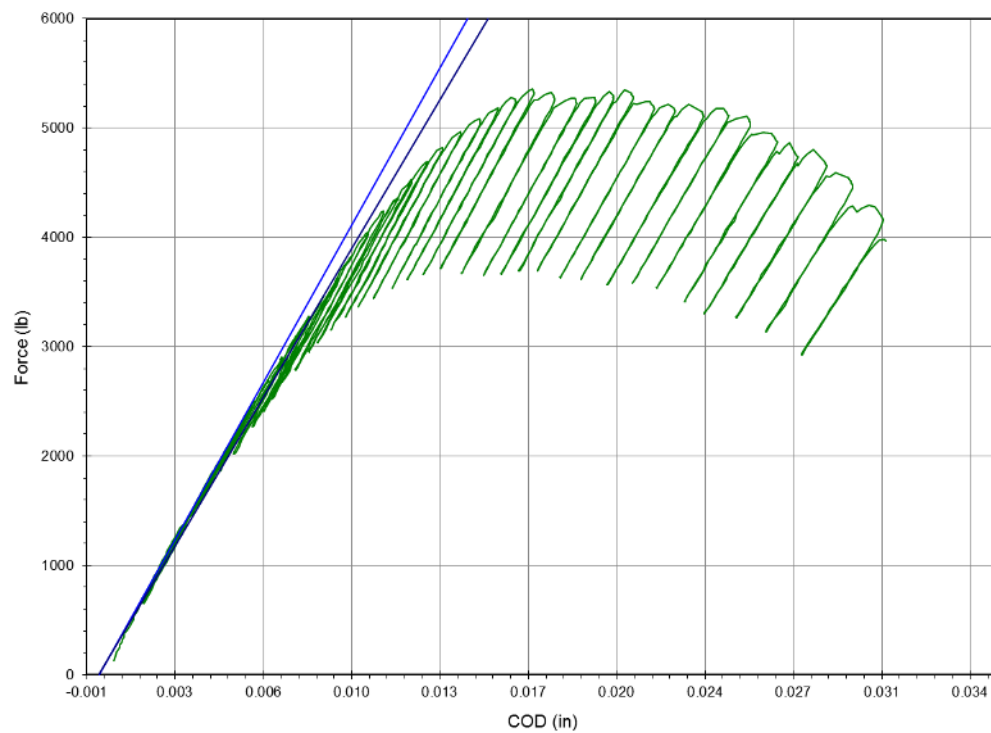


Figure 48: 10-J1C-03, Force vs. COD graph for 10 inch section tested at 1400°F (760°C)

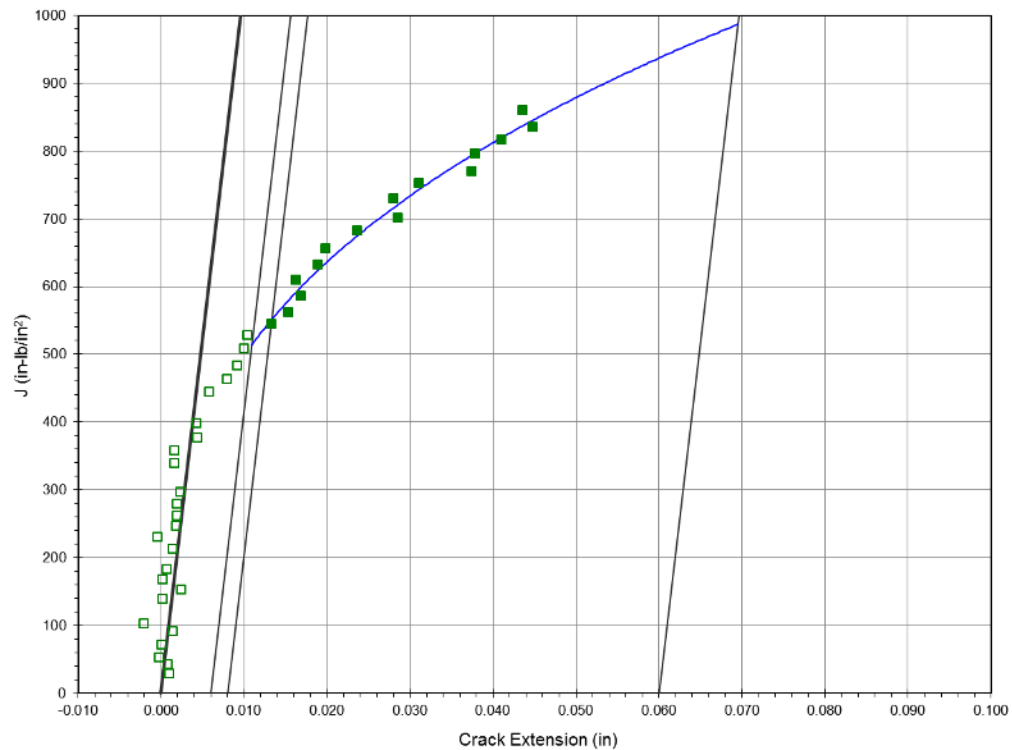


Figure 49: 4-J1C-02, J vs. a graph for 4 inch section tested at 1400°F (760°C)

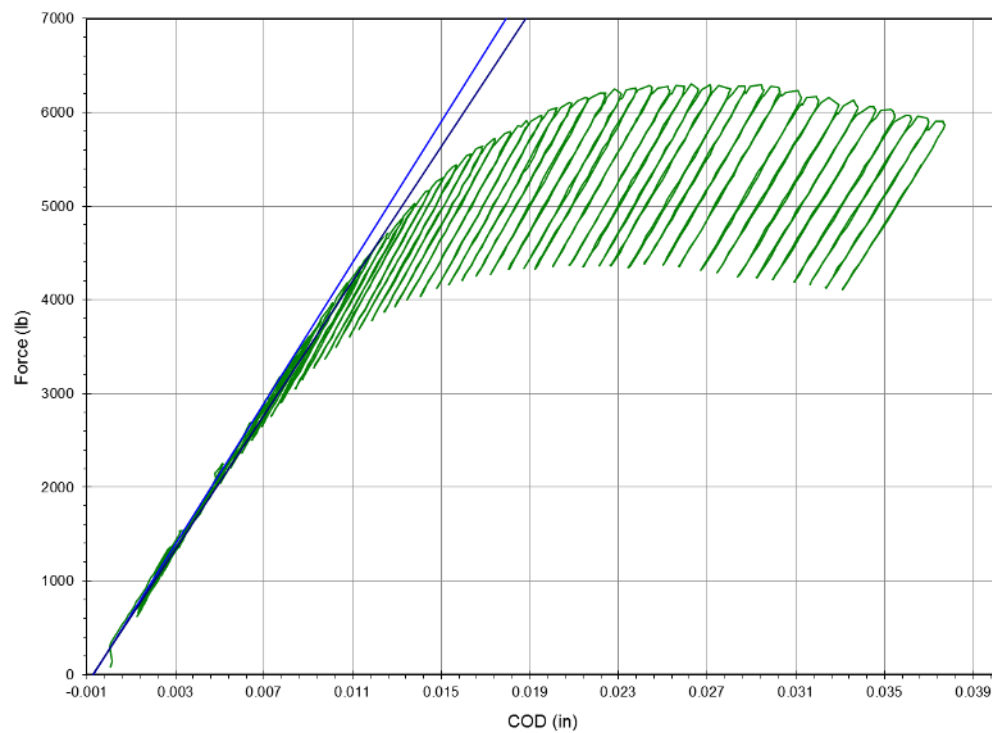


Figure 50: 4-J1C-02, Force vs. COD graph for 4 inch section tested at 1400°F (760°C)

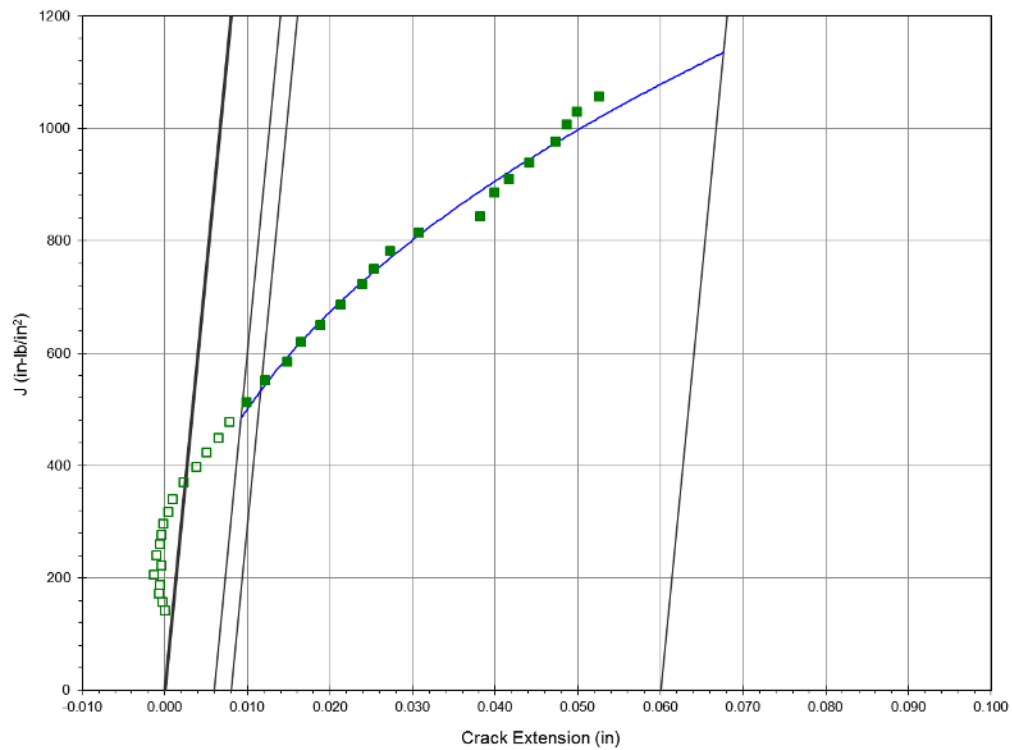


Figure 51: 4-J1C-01, J vs. a graph for 4 inch section tested at RT

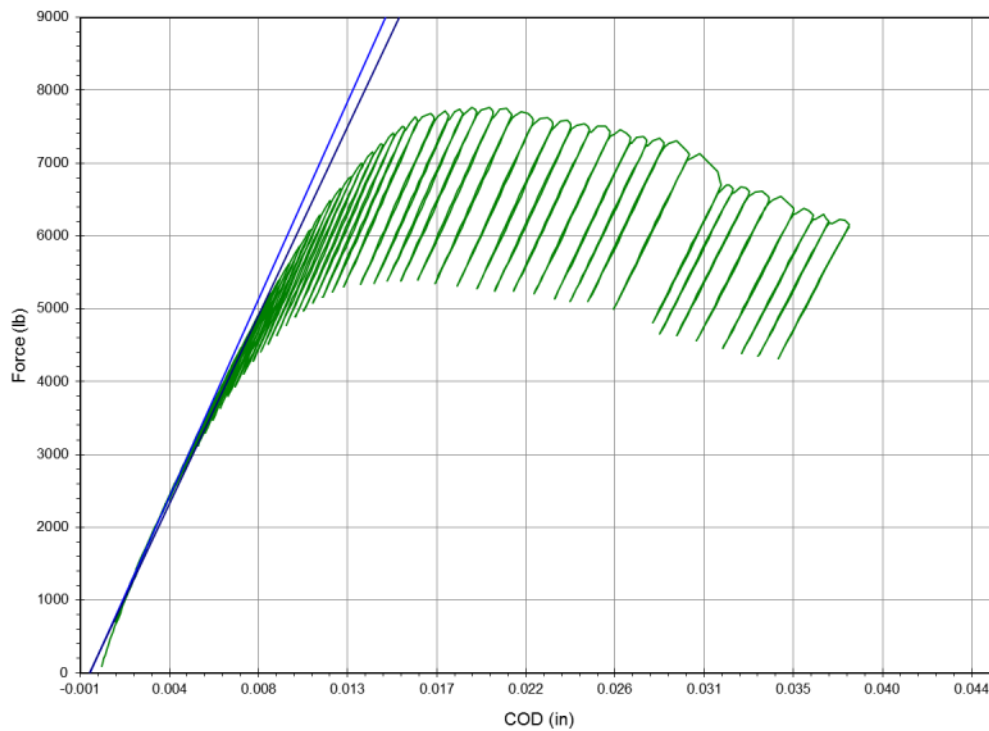
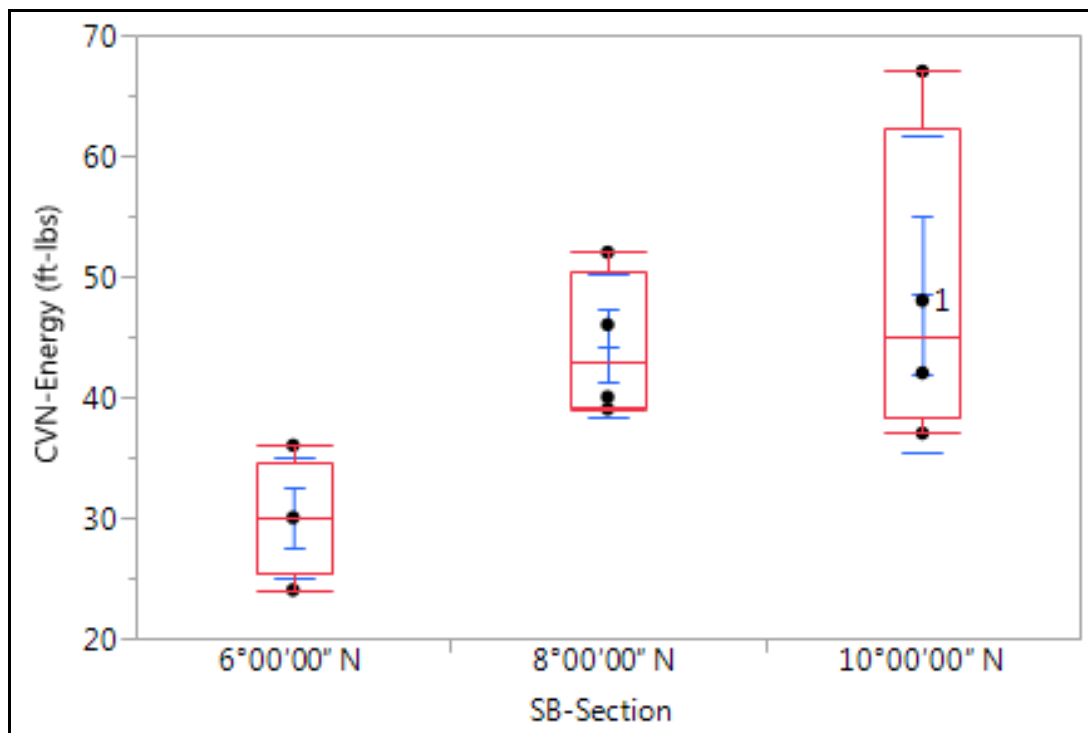


Figure 52: 4-J1C-01, Force vs. COD graph for 4 inch section tested at RT

Table 11: Charpy V-Notch Impact energy data for 10 inch, 8 inch, and 6 inch trepan samples

Sample ID	Temp	Energy		Mils
		°F°C	ft-lbs	
10-CVN-RT-C1	70/21	48	65.1	51
8-CVN-RT-C1	70/21	39	52.9	41
6-CVN-RT-C1	70/21	30	40.7	22
10-CVN-RT-C2	70/21	37	50.2	33
8-CVN-RT-C2	70/21	40	54.2	32
6-CVN-RT-C2	70/21	36	48.8	43
10-CVN-RT-T1	70/21	67	90.8	46
8-CVN-RT-T1	70/21	46	62.4	56
6-CVN-RT-T1	70/21	24	32.5	15
10-CVN-RT-T2	70/21	42	56.9	24
8-CVN-RT-T2	70/21	52	70.5	52
6-CVN-RT-T2	70/21	30	40.7	22



Section	No.	Mean	Std Dev	Std Err Mean	Lower 95%	Upper 95%
6 inch	4	30	4.899	2.4495	22.205	37.795
8 inch	4	44.25	6.0208	3.0104	34.67	53.83
10 inch	4	48.5	13.1276	6.5638	27.611	69.389

Figure 53: Charpy V notch Impact energy vs. section size combined data plot

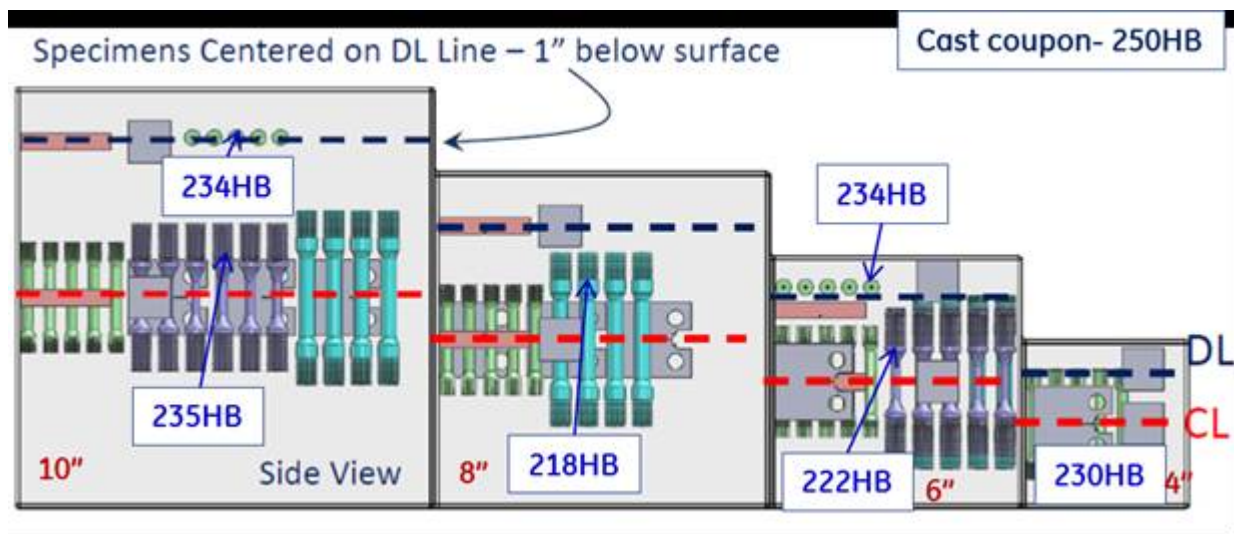


Figure 54: N263 Cast hardness values are not section thickness dependent

Table 12: N263 Casting section hardness values raw data

Sample ID	Hardness (HRBW/HRC)	Conversion (HBW)
10-TN-CL-RT-H	98.98 HRBW *	235 HBW
8-TN-CL-RT-H	96.58 HRBW *	218 HBW
6-TN-CL-RT-H	97.21 HRBW *	222 HBW
4-TN-CL-RT-H	98.36 HRBW *	230 HBW
10-TN-DL-RT-H	99.27 HRBW *	234 HBW
6-TN-DL-RT-H	20.82 HRC *	234 HBW
GJOJ-263-TB-RT-H	23.91 HRC *	250 HBW

CENTRIFUGAL CASTING OF HAYNES 282

A Vertically Spun Centrifugal Casting of Haynes 282, weighing 1400 lbs. with hybrid mold (half Graphite and half Chromite sand) mold assembly was cast at MetalTek WI, with vertical centrifugal casting process, Figure 55.

The 26 inch outer diameter (OD) and 21 inch height casting sectional view is shown in Figure 56. The mold is based in on a GE Aviation compressor casing for the CF34. This hybrid mold design was selected to illustrate the influence of different cast cooling rates during Centrifugal casting solidification and also the varied cast wall part dimensions influence on microstructural features.



Figure 55: Haynes 282 Test program Centrifugal casting

The Haynes 282 ingots were induction melted in air under Argon cover protection. Necessary Al and Ti additions were made to the melt to compensate for the melt losses. The centrifugal die was purged with Argon prior to pour and 35 G forces were maintained with die rotational rpm during casting and solidification process. Mold assembly view shown in Figure 57.

Casting solidification simulation analysis was carried out for cooling rate estimates. The surface indication on the casting inner diameter (ID) on the chromite sand mold side matched well with the FEM based solidification simulation analysis. Figure 58 provides simulation predicted casting cooling rates.

X-ray Radiographic inspections were reported clean except the visual ID surface, mid height level shrink that appeared primarily on the Chromite sand side mold. This is due to the differential thermal cooling rates caused by the hybrid mold materials since Graphite heat extraction rate is faster than Chromite.

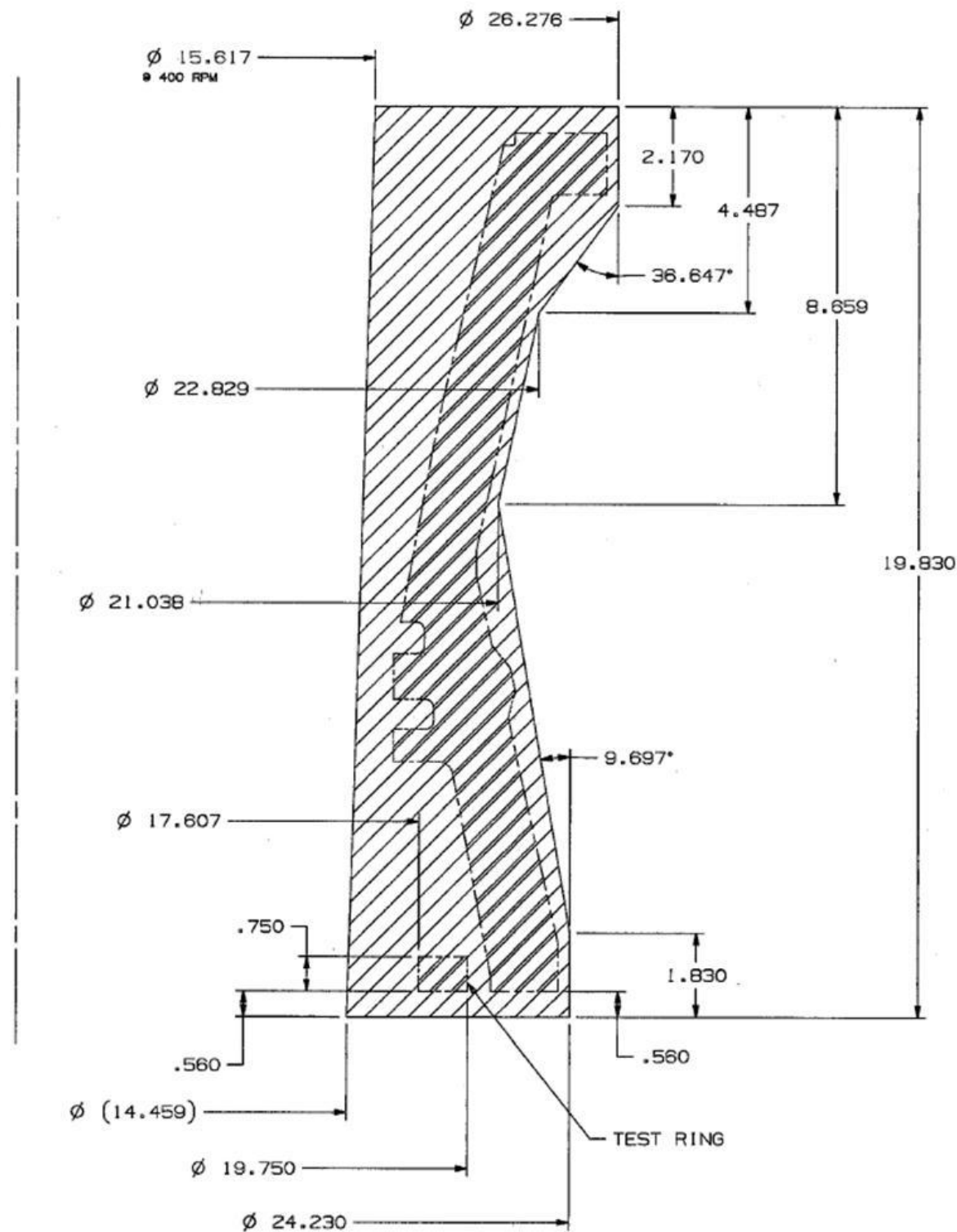
The Heat treatment cycles homogenizing and aging were determined by NETL based on the average SDAS of 70 μm .

The trepan specimen extraction lay out map of the centrifugally cast Haynes 282 casting wall is as shown in Figures 64 and 65.

Conclusion:

In general it is observed that Graphite mold out performs sand mold across all temperatures for 0.2% YS; %Elongation, %RA and UTS at 1400°F when compared with Chromite sand mold section. The Stress-LMP plot of Centrifugal Cast H282 compared to wrought H282 data. The data scatter is in line with the wrought alloy Figure 75. Also the conditional Fracture toughness Kq plot for the Haynes 282 cast data [Sand & Graphite] falls in the scatter of wrought alloy as shown in Figure 74

Figures 66 to 69 for tensile properties; Figures 70 to 73 for LCF and Figure 75 for the Stress rupture test plots confirm the above findings.



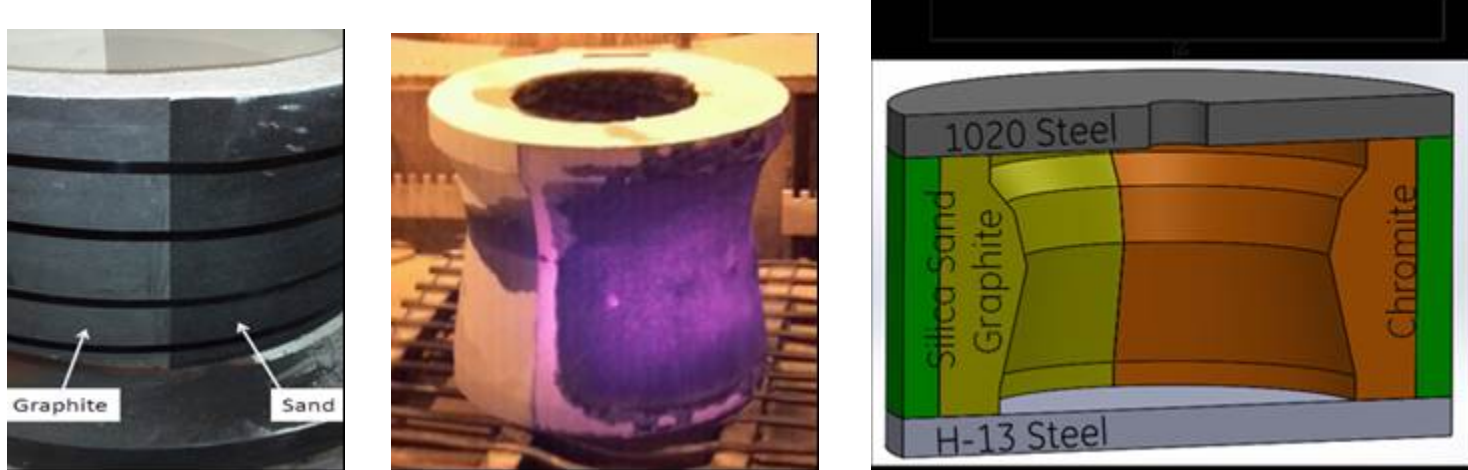


Figure 57: Haynes282 Centrifugal casting mold assembly comprising half mold Graphite and half mold Chromite sand

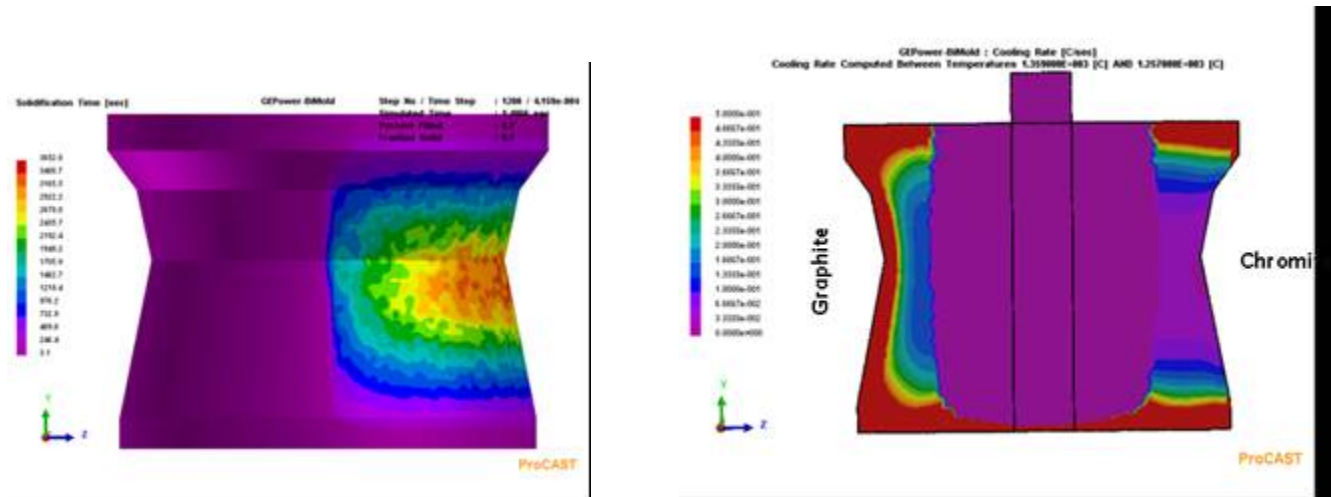


Figure 58: Casting simulation predicted cooling rates for Graphite and Chromite sand side molds

The casting sectioning and Heat treat sample extraction views are shown in Figures 92 and 93.

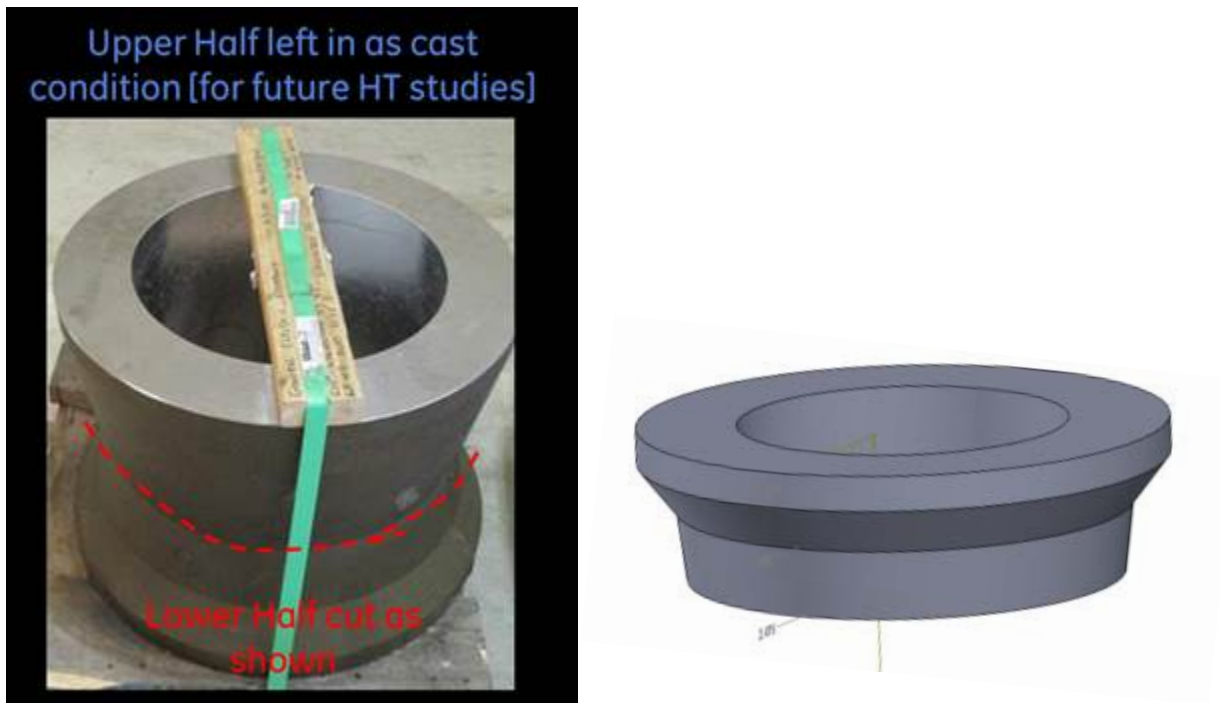


Figure 59: Picture showing the location of the casting utilized for micro-structural analysis and mechanical testing.

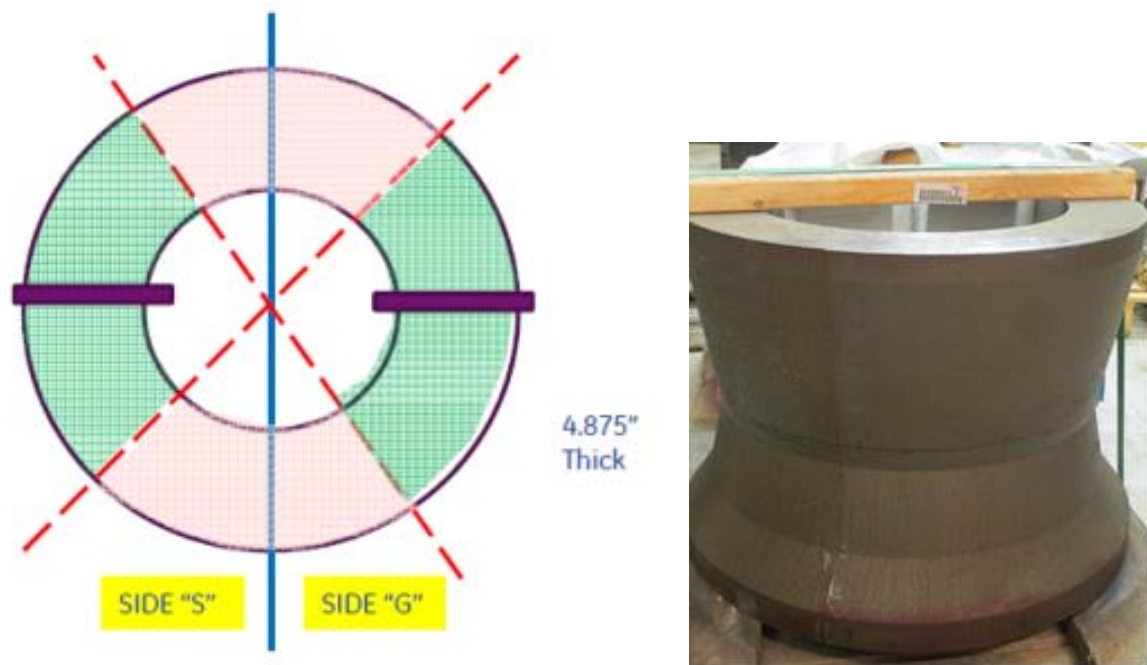


Figure 60: Picture showing the extraction of the slice for heat treatment and micro-structural analysis

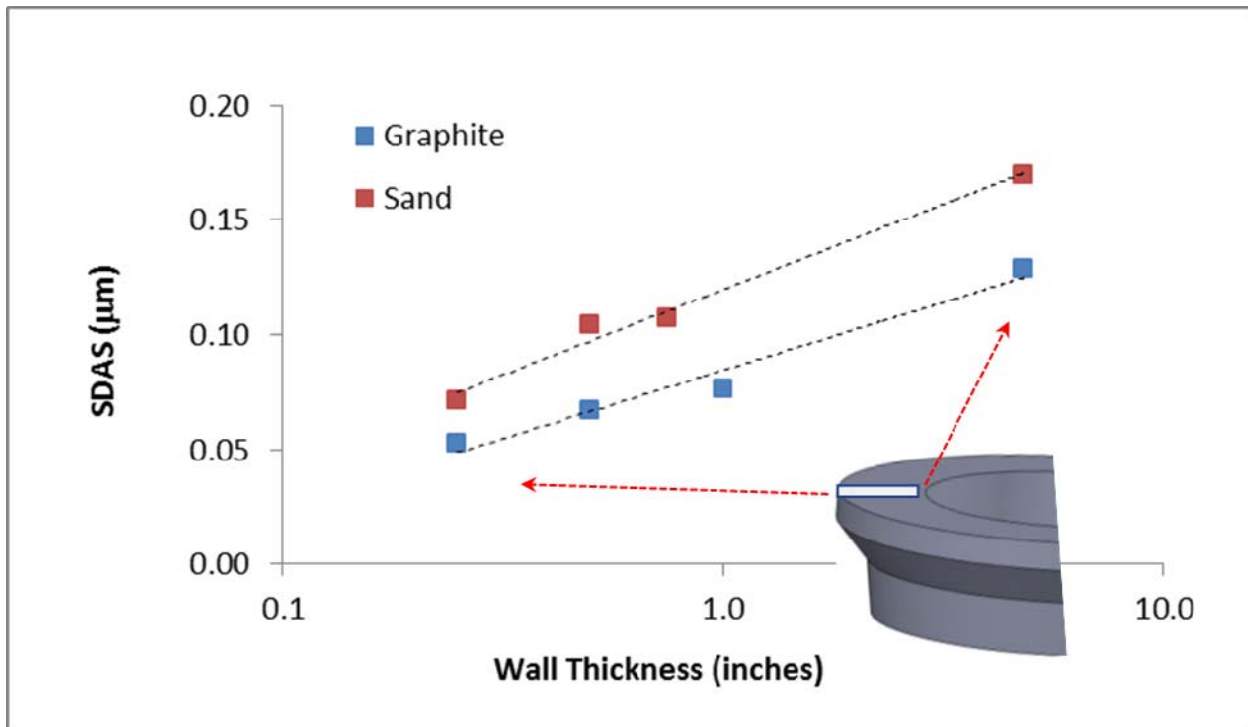
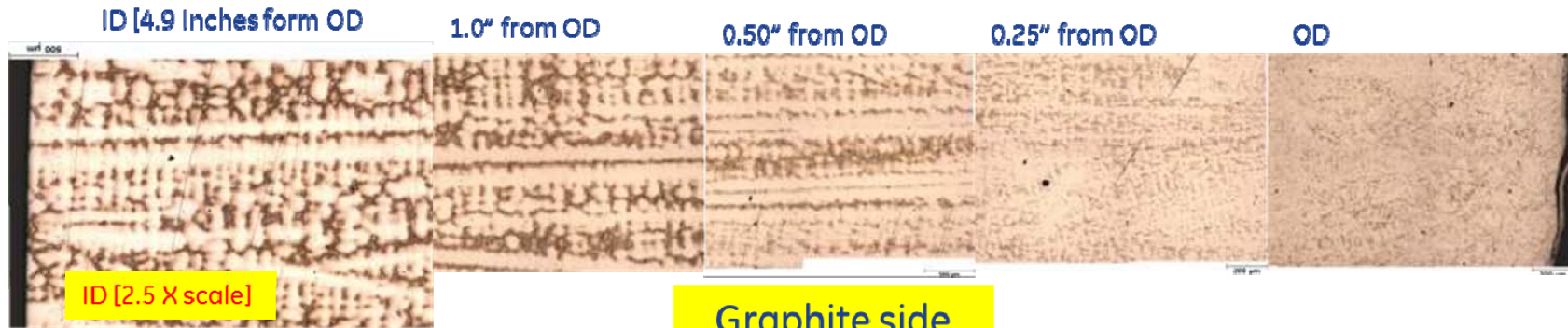


Figure 61: SDAS along the wall thickness for the two respective mold material.

The Microstructure evolution as a function of mold cooling rates for centrifugal castings are clearly established with Haynes 282 hybrid mold casting trials and the SDAS values for both Graphite mold and Chromite sand molds were plotted with ID (Hotter surface) to OD (Cooler mold interfaced surface) distance measurements as shown in Figures: 61 and 62.

The Grain boundary regions in as cast condition as shown in Figure 63 (SEM), indicating Ti, Cr and Mo rich precipitates.



Micro-structure evolution as a function of cooling rates and type of mold [Graphite versus Sand]

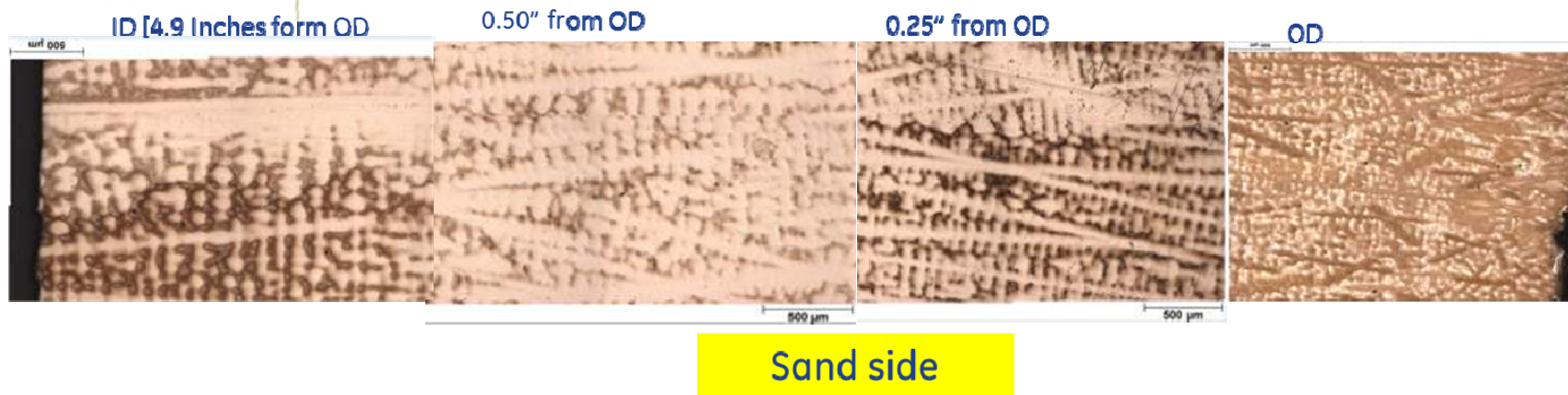


Figure 62 As cast microstructural evolution across the wall thickness for the two mold material

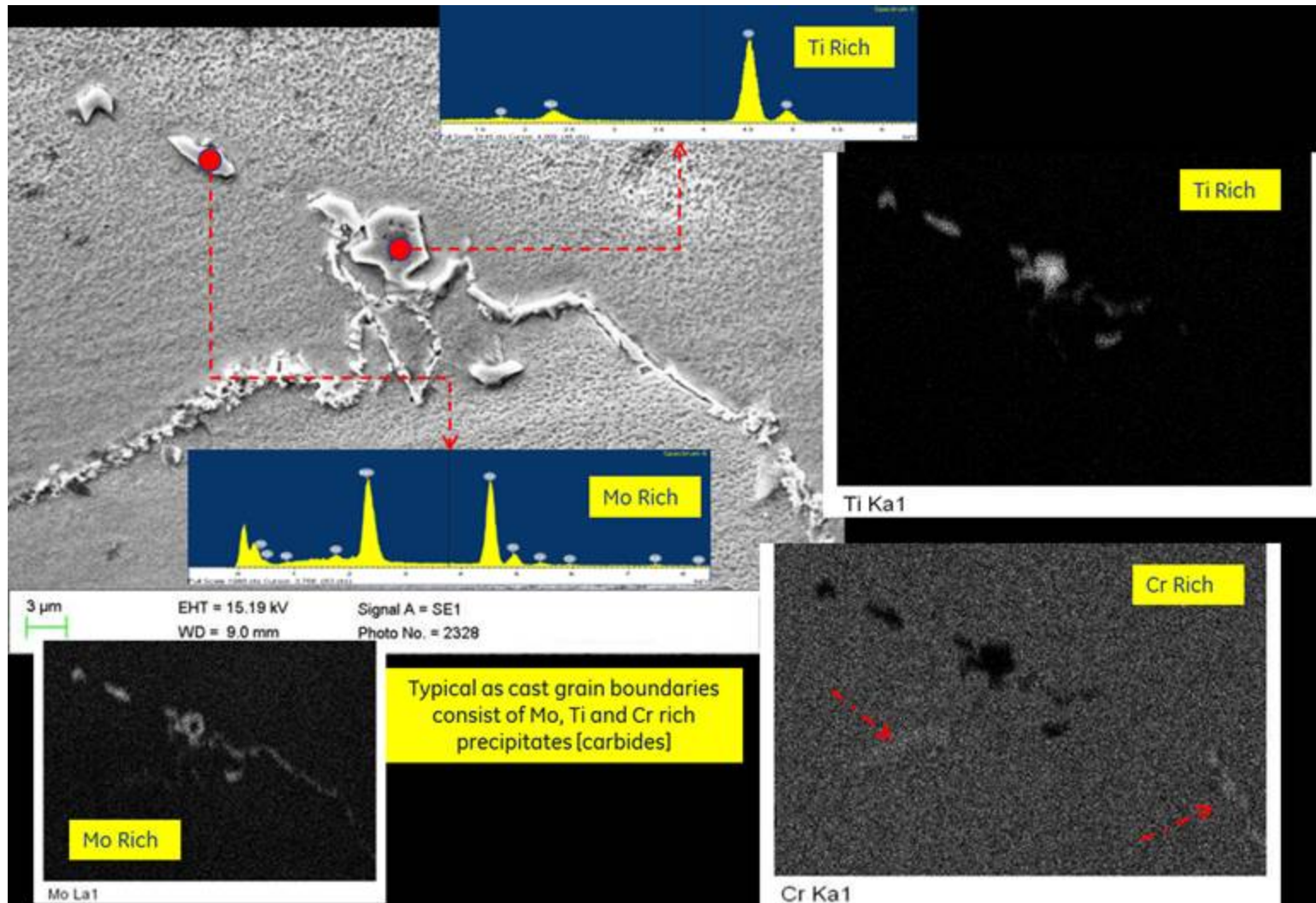


Figure 63 SEM image of grain boundary in as cast specimens. Most precipitates consists of Ti, Mo and Cr rich

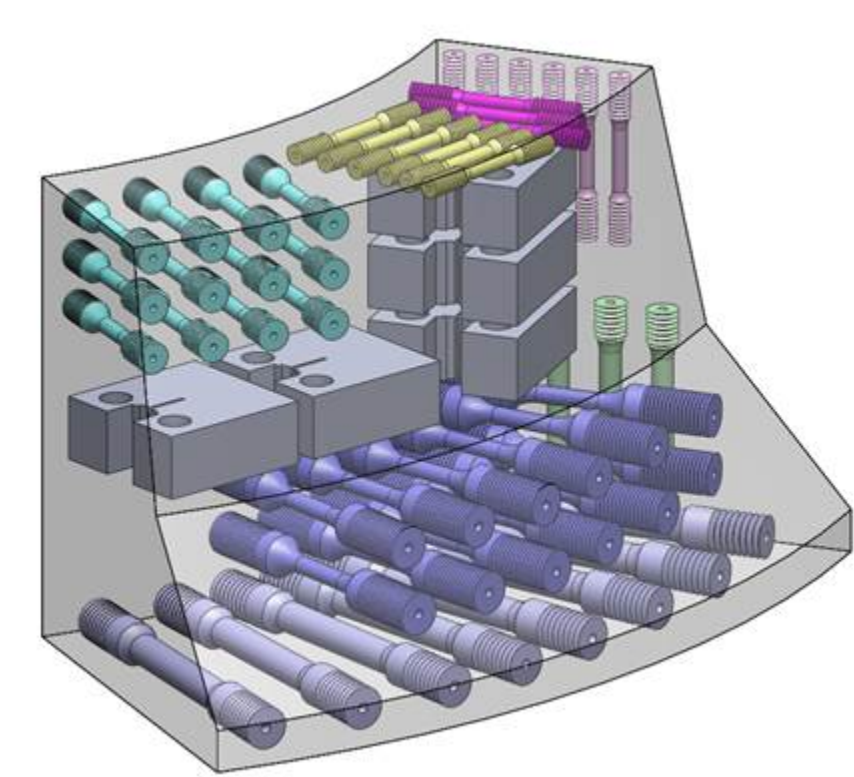


Figure 64: Complete map of specimen extraction from the centrifugally cast Haynes 282. The specimens include tensile, LCF and fracture toughness

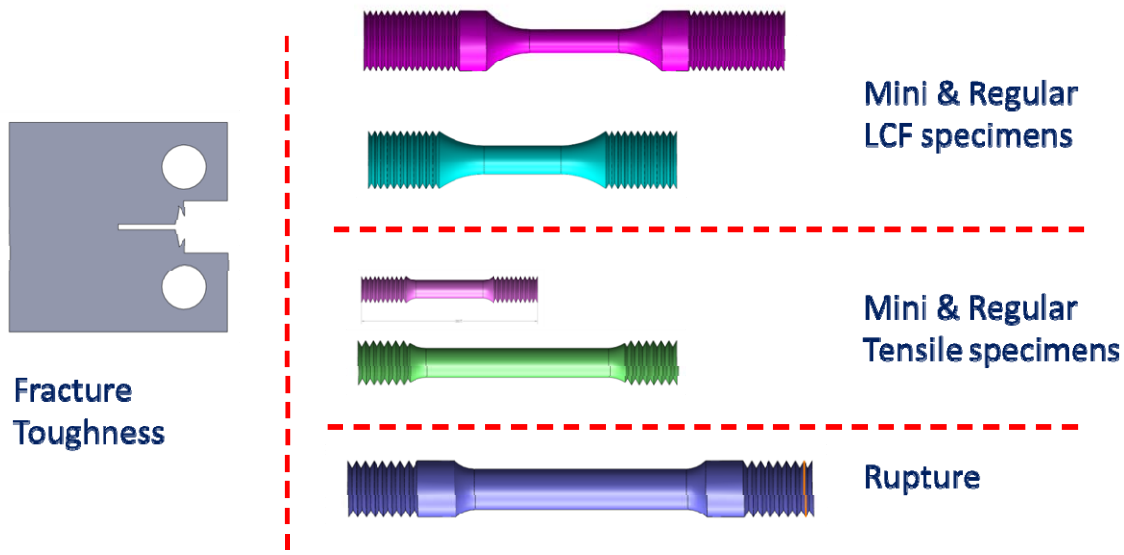


Figure 65: Color code of specimen type is as shown. All mini specimens are for the thinner wall thickness

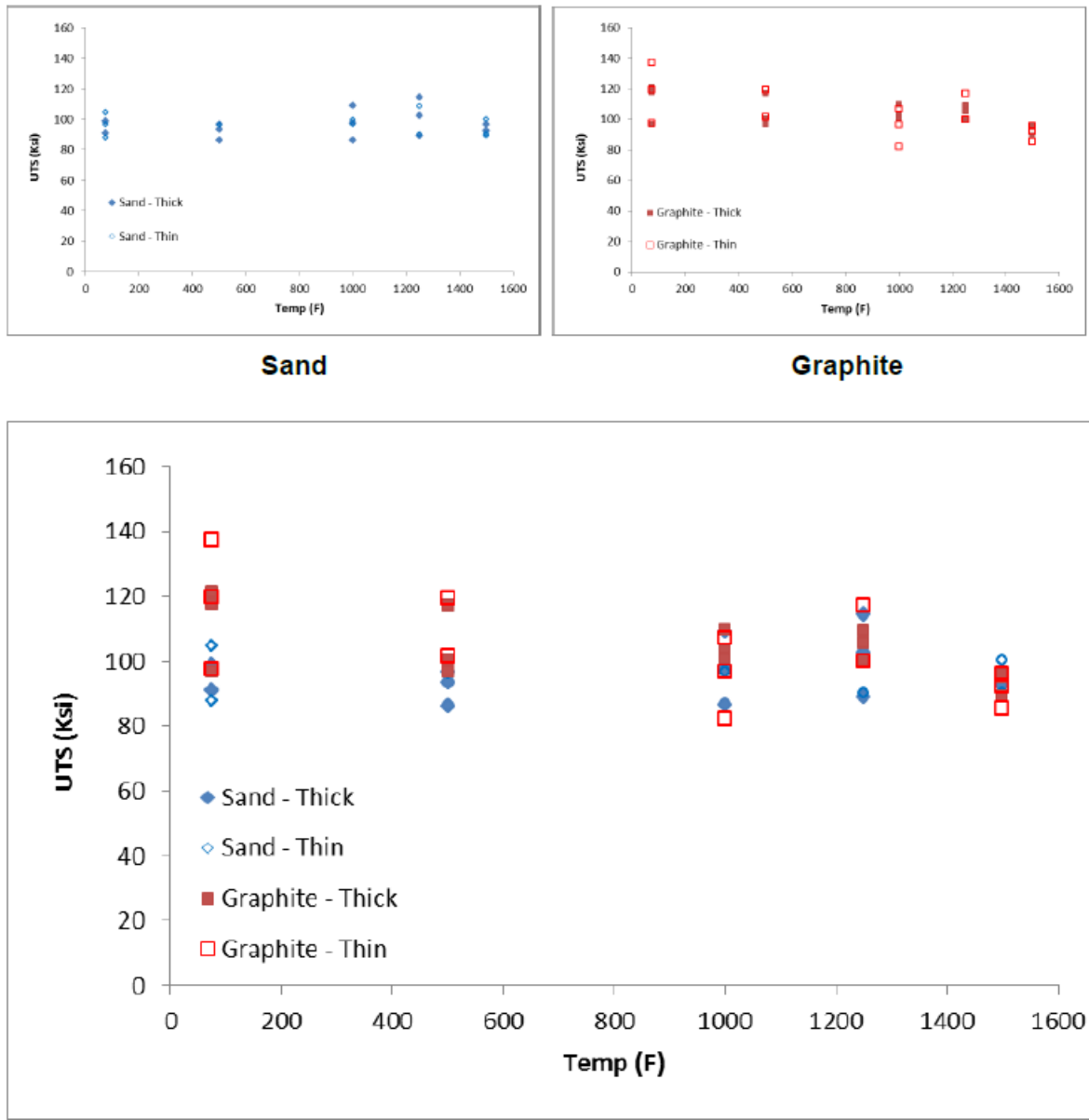
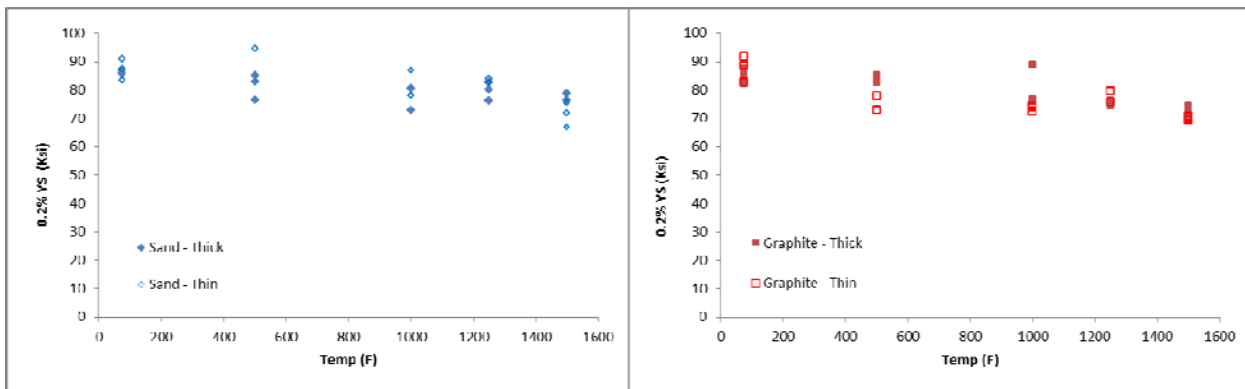


Figure 66: Plots of UTS as a function of temperature [Sand and Graphite mold]. In general, the variation between the thick and thin sections on the sand side has less variability, when compared to the graphite side. Graphite side has better RT properties when compared to the sand. However at 1400°F (760°C), all data falls within a very tight band.



Sand mold

Graphite mold

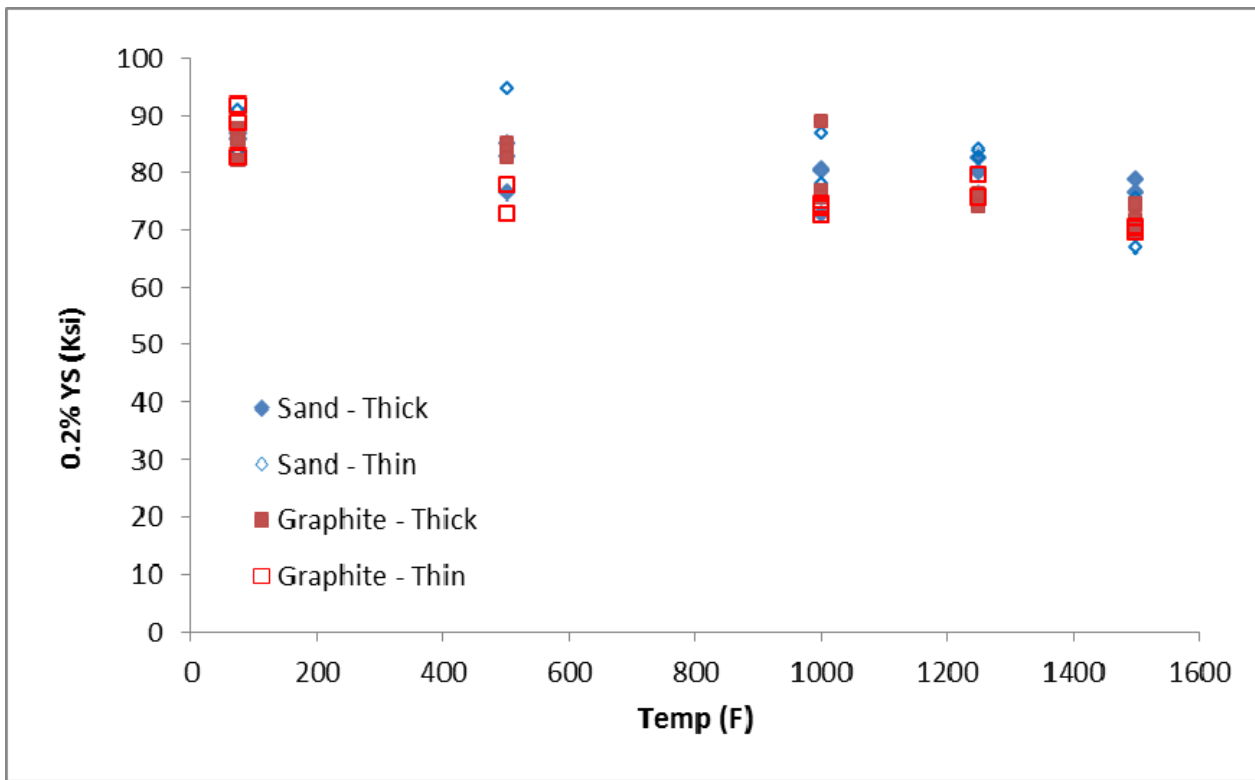
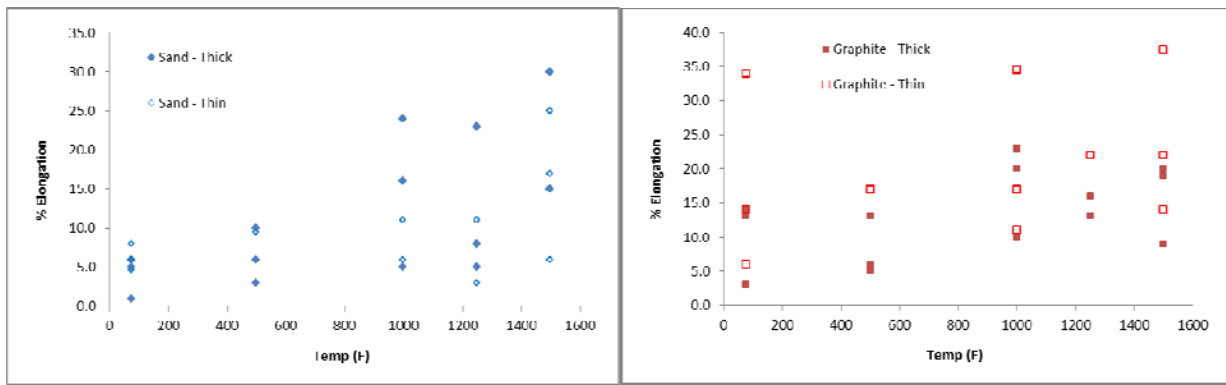


Figure 67: Plots of 0.2% YS as a function of temperature for various mold material. Unlike the variation in UTS, the 0.2% YS has a very tight range across all temperatures tested



Sand mold

Graphite mold

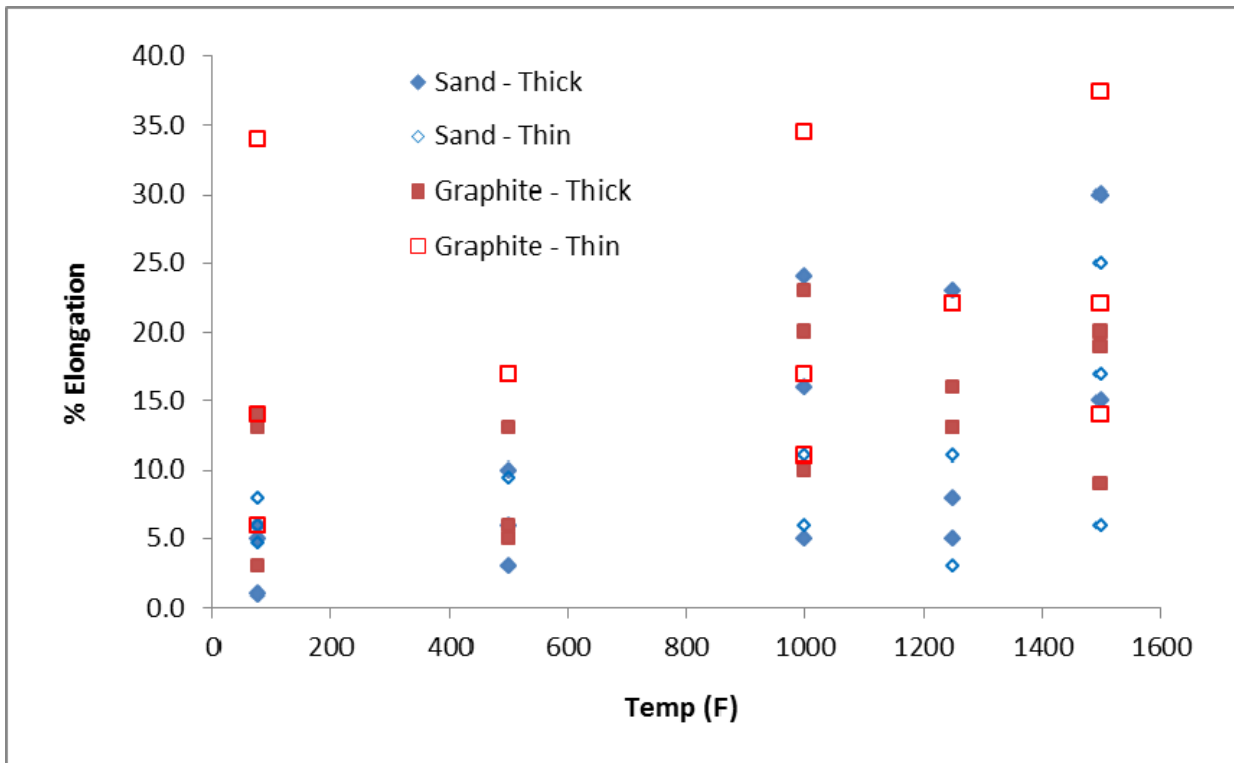
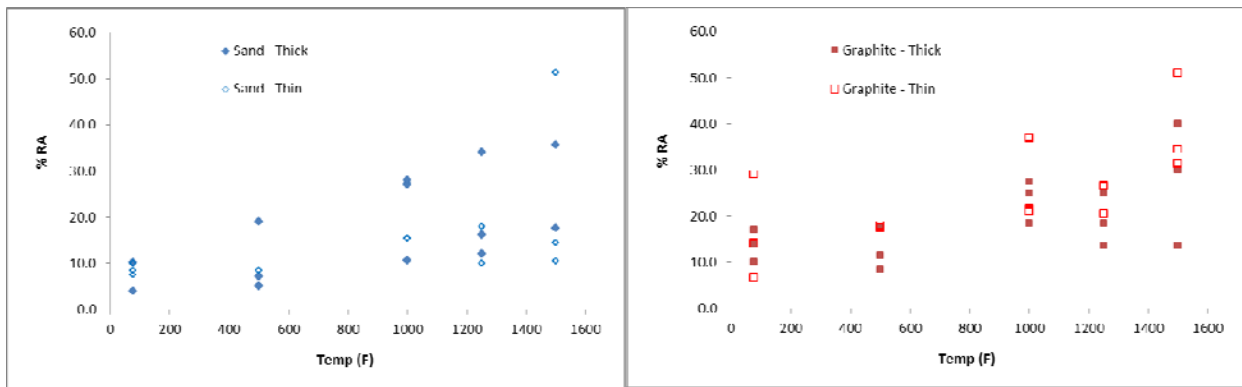


Figure 68: Plots of % Elongation as a function of temperature for various mold material. The plots clearly show a wide variation in % Elongation, with the graphite mold being better than the sand mold across all temperatures



Sand mold

Graphite mold

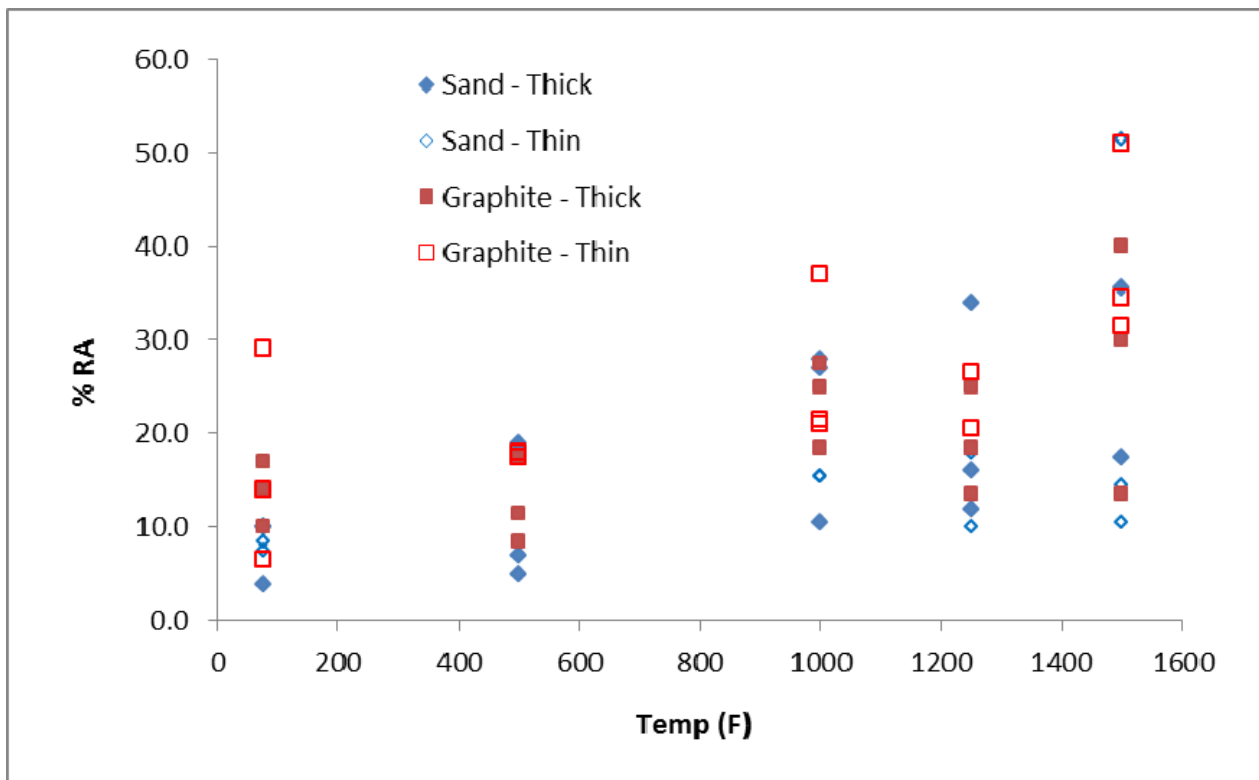


Figure 69: Plots of % RA as a function of temperature for various mold material. The plots clearly show a wide variation in % RA, and in general, graphite mold out performs sand mold across all temperatures

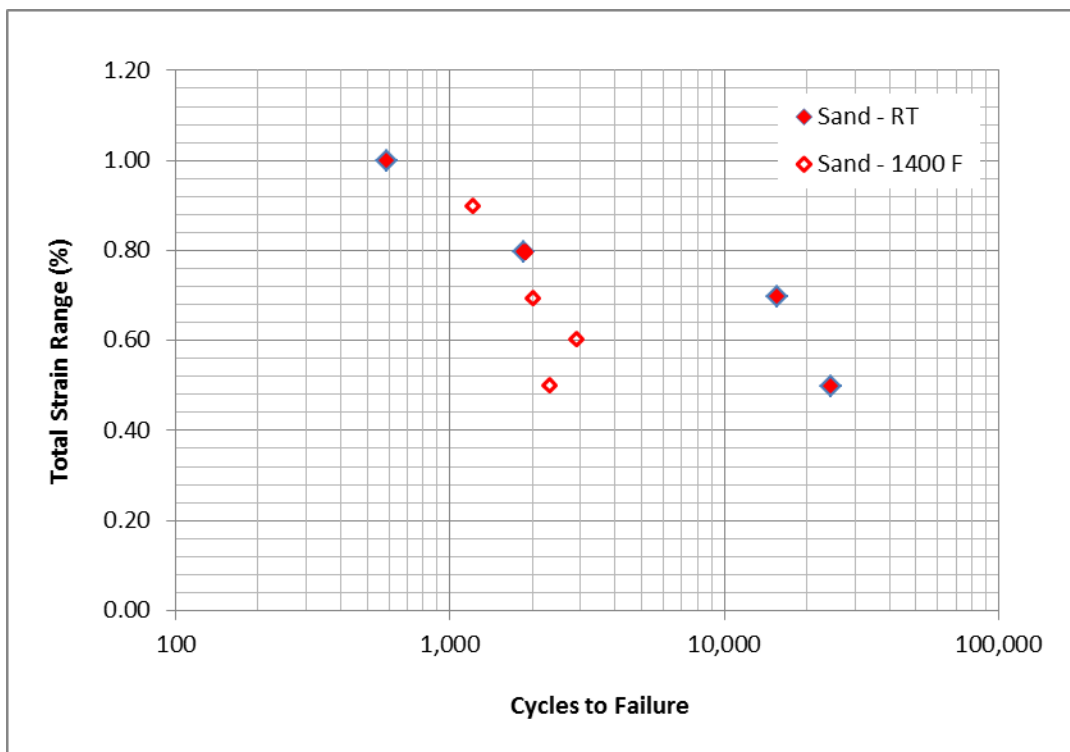
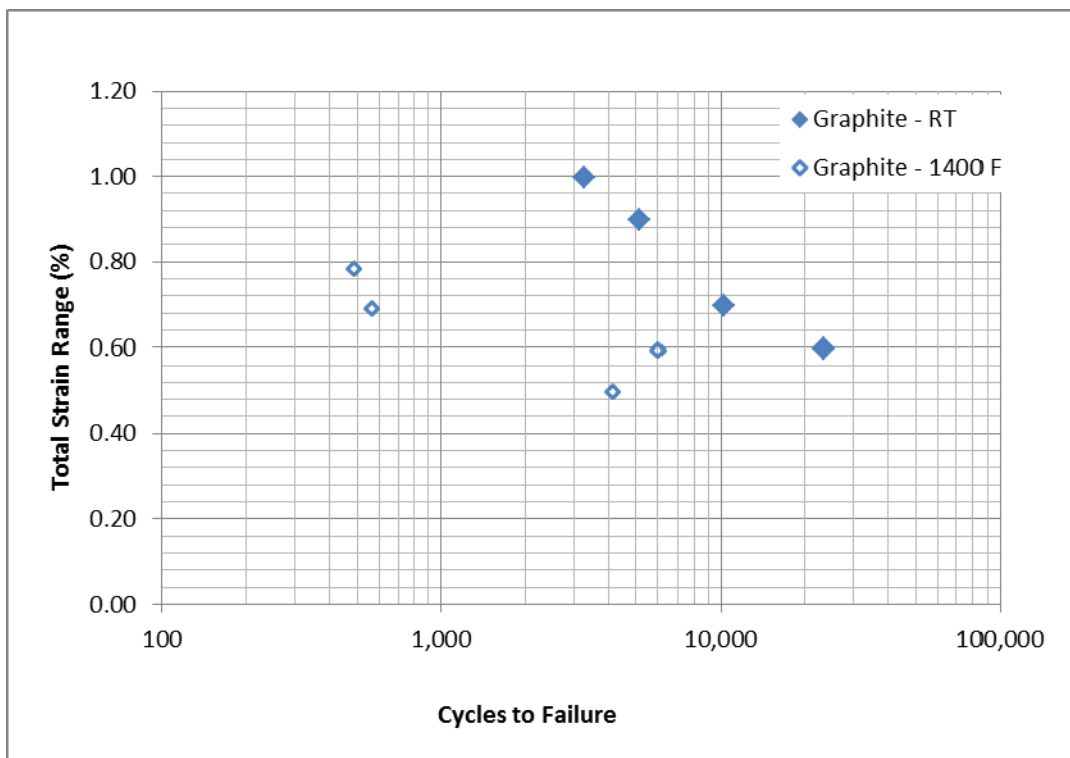


Figure 70: Plots of Cycles to Failure and Total Strain Range (%) for the Sand and Graphite molds at RT and 1400°F (760°C). The Graphite side shows a debit at 1400°F, while the sand side does degrade with the same severity

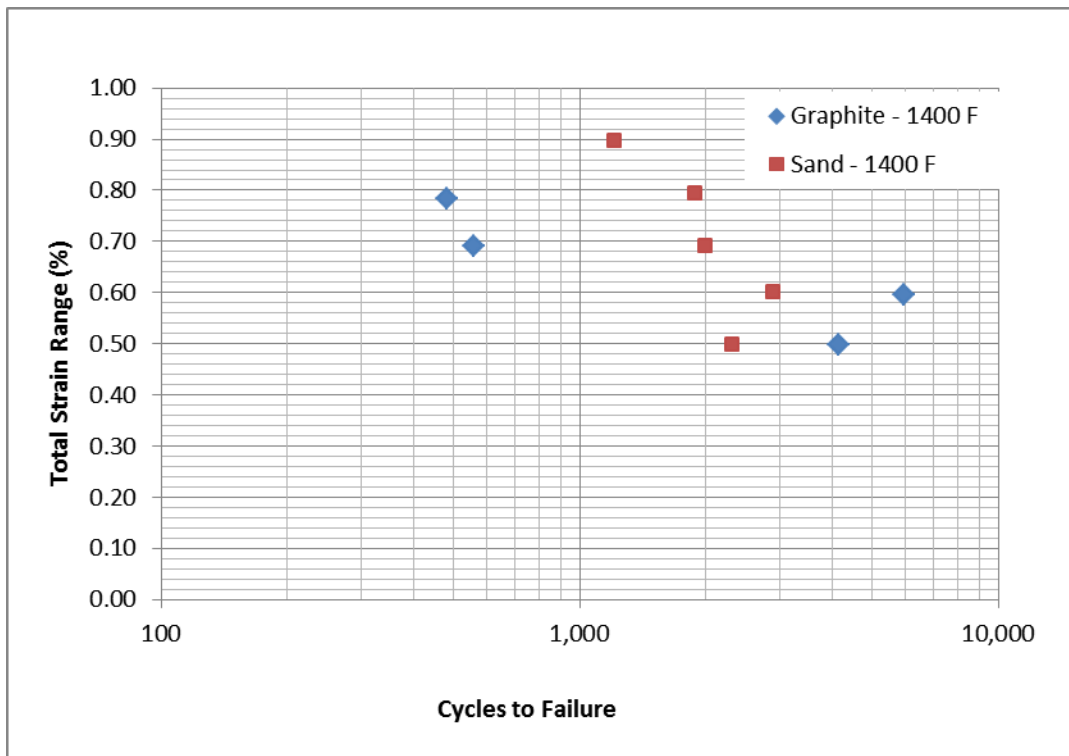
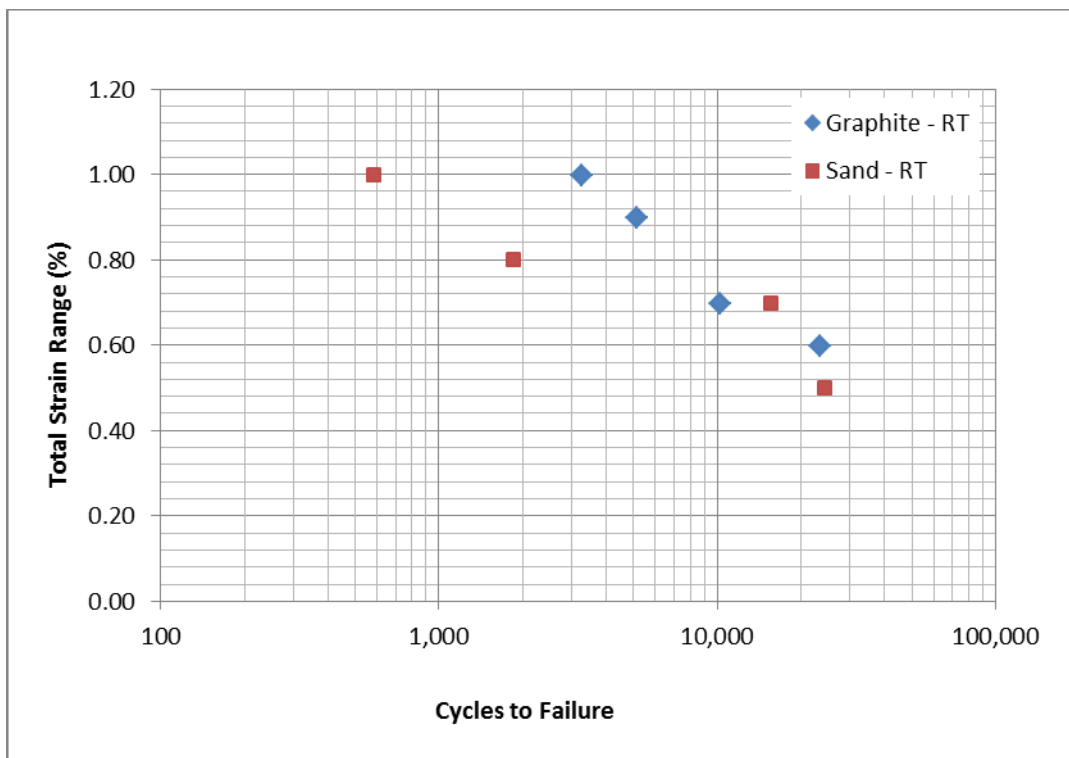


Figure 71: Plots of Cycles to Failure and Total Strain Range (%) for the Sand and Graphite molds at RT and 1400°F (760°C). The debit in the graphite compared to sand at high strains and 1400°F will need some further investigation

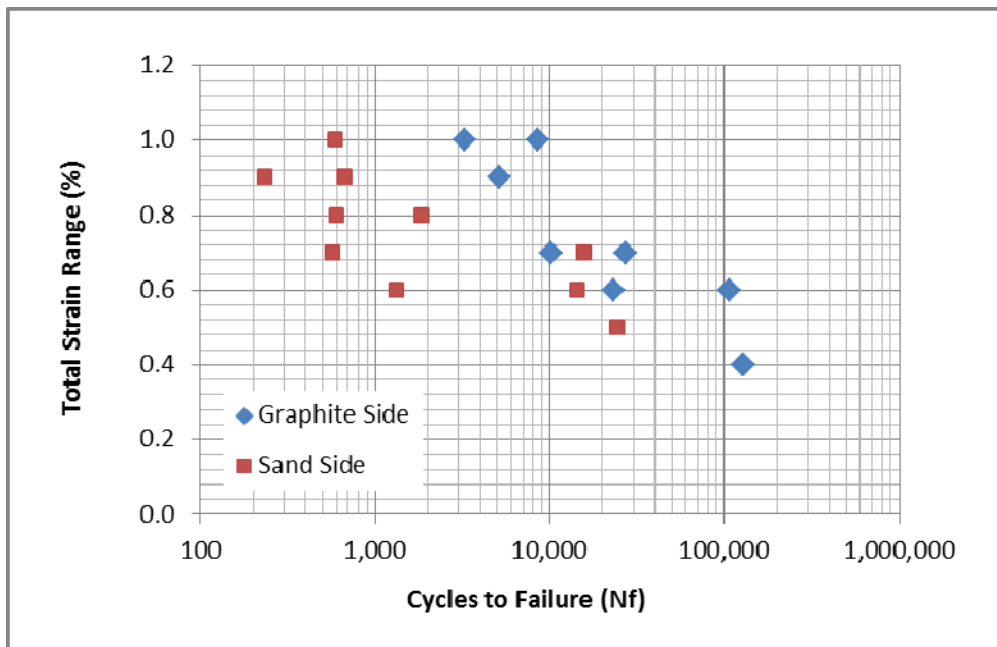


Figure 72: Plot of cycles to failure and total strain range from Table 4B-1. The graph clearly shows the better performance of faster cooling rates [finer SDAS in the graphite side] due to higher UTS at 75 F (+10 to 15 ksi increase in UTS on Graphite side]

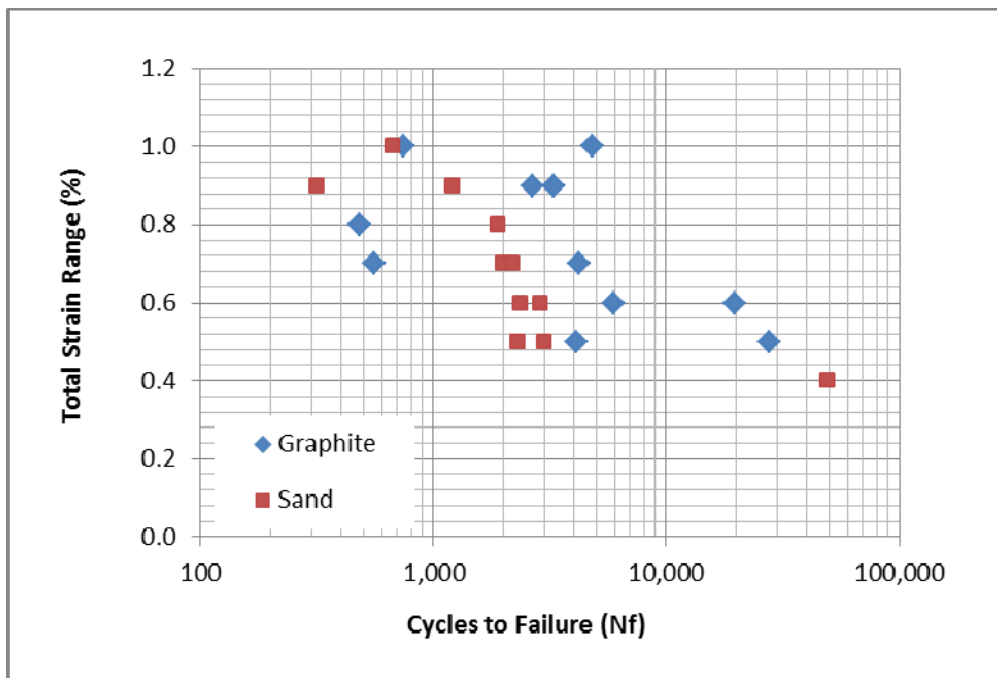


Figure 73: Plot of cycles to failure and total strain range from Table 4B-2. The graph clearly shows no performance difference at 1400°F (760°C) as the tensile properties of both sand and graphite are similar at 1400°F

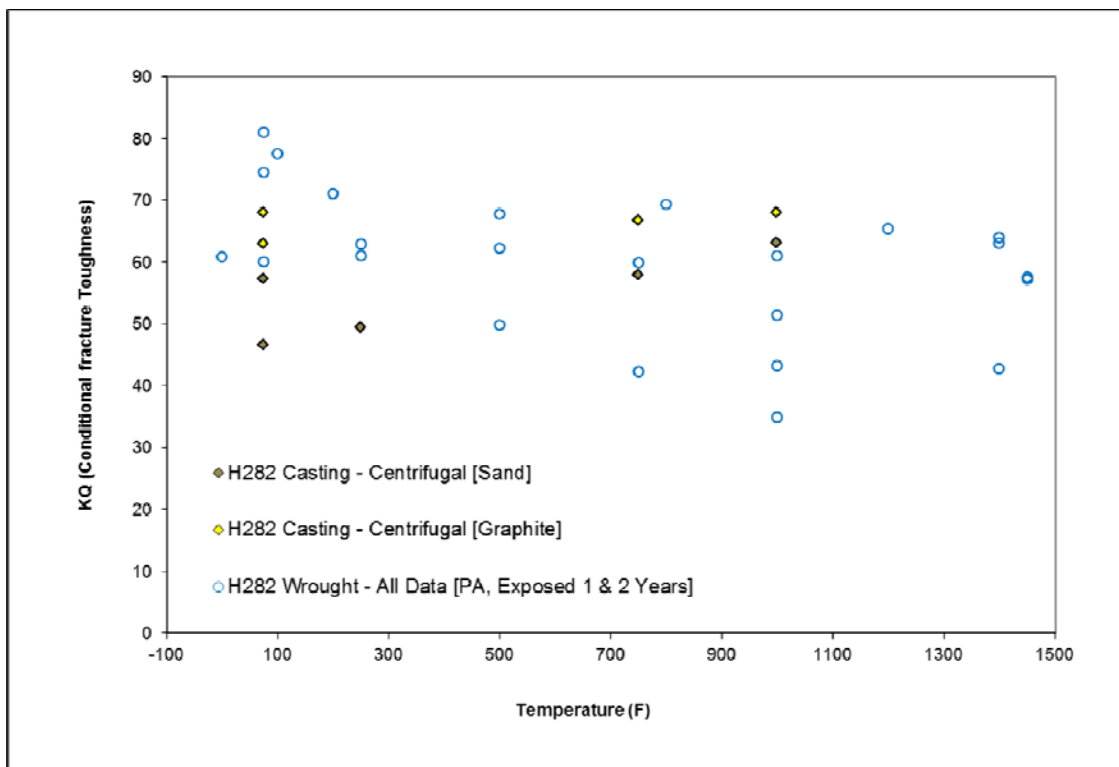


Figure 74: Conditional Fracture toughness (K_Q) of centrifugally cast Haynes 282. The cast data [Sand & Graphite] falls in the scatter of wrought alloy. The wrought data in the figure above consists of PA, and exposed for 1 & 2 years at 1425°F (774°C)

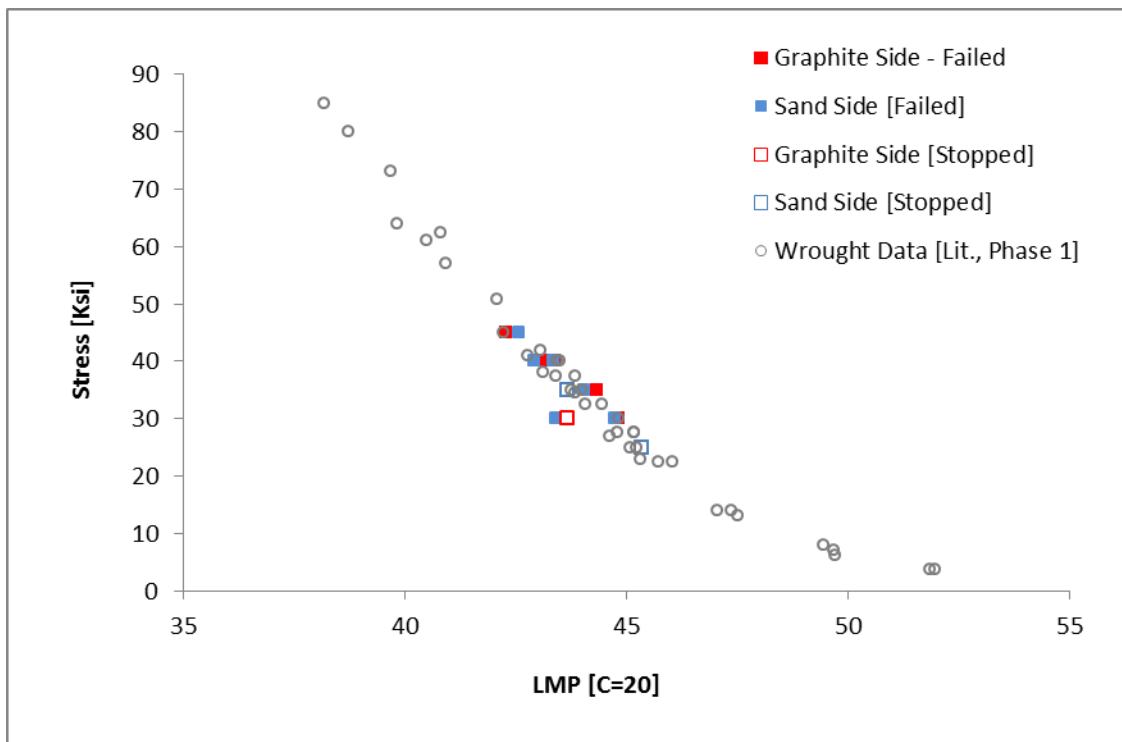


Figure 75: Stress-LMP plot of Centrifugal Cast H282 compared to wrought H282 data. The data scatter is in line with the wrought alloy.

FUNDAMENTAL STUDIES ON COOLING RATES AND SDAS

The objective was to study the effect of mold material on casting cooling rates and characterize the effect on SDAS spacing in the cast wall section as shown in schematic sketch, Figure 76.

Hence in this test program, evaluated the influence of 6 mold materials Silica, Chromite, Alumina, Silica with Indirect Chills, Zircon and Graphite on casting solidification cooling rates. [Figures 78-79] The molds layout schematic is shown in [Figure 77]. The molds assembly, thermocouples cable layout are shown in Figures 80-83. The thermocouples relative location in each mold is shown in Figure 85.

Actual Casting cooling rates through Liquidus to Solidus phase transition were measured with 3 different locations based thermocouples placed in each mold. [Figure 87]

Compared with solidification simulation cooling rates and measurement of SDAS, microstructure features were reported. [Figure 89] and simulation vs. measured cooling rates compared in Tables 13 and Table 15 provides the SDAS measurements. The test results provided engineered casting potential methods, applicable for heavy section Haynes 282 castings for optimal properties, with foundry process methods and tools.

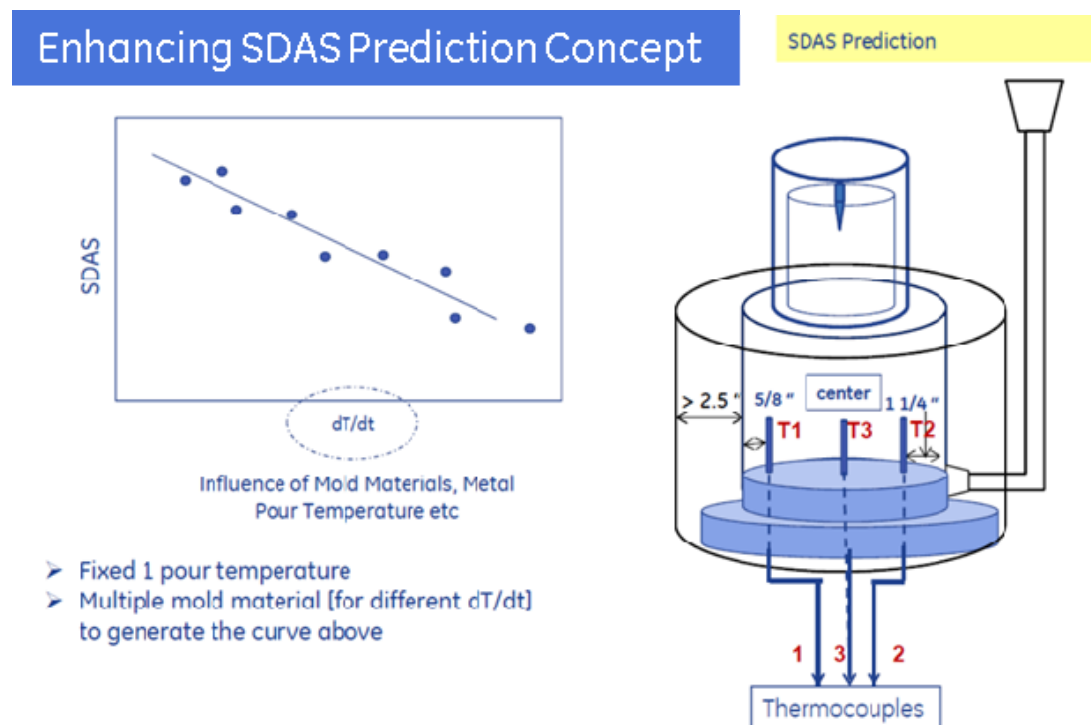


Figure 76: Enhancing SDAS prediction with casting solidification mold cooling rate studies. Six molds with different mold materials [to simulate different cooling rates] were poured with thermocouples located as shown to measure casting cooling rates

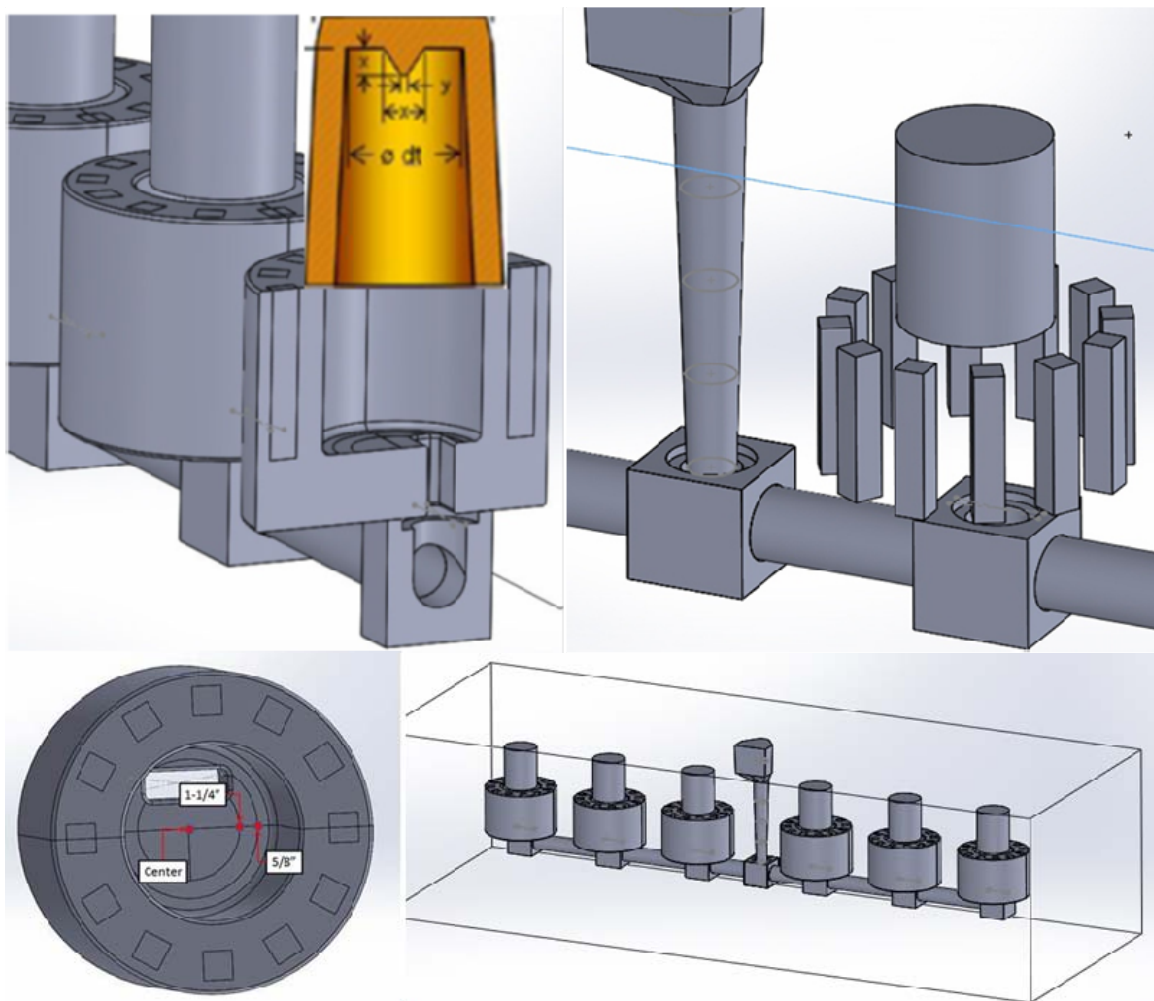


Figure 77: Detailed plan of casting solidification cooling rates measurement mold layout assembly

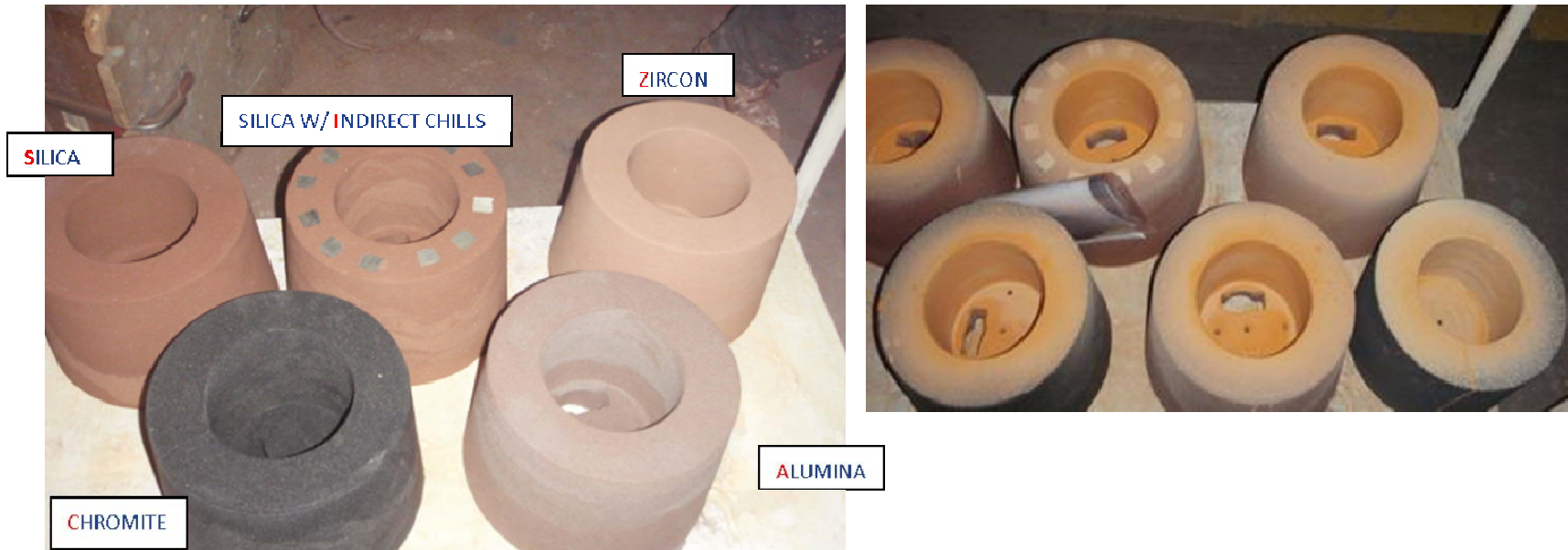


Figure 78: Sand molds from 5 different mold materials [left] coated with refractory paint and dried [right]. Six mold materials were evaluated: 1. Silica, 2. Chromite, 3. Graphite, 4. Alumina, 5. Zircon, 6. Silica with indirect chills placement.



Figure 79: Photograph of chills location in mold pattern prior to molding

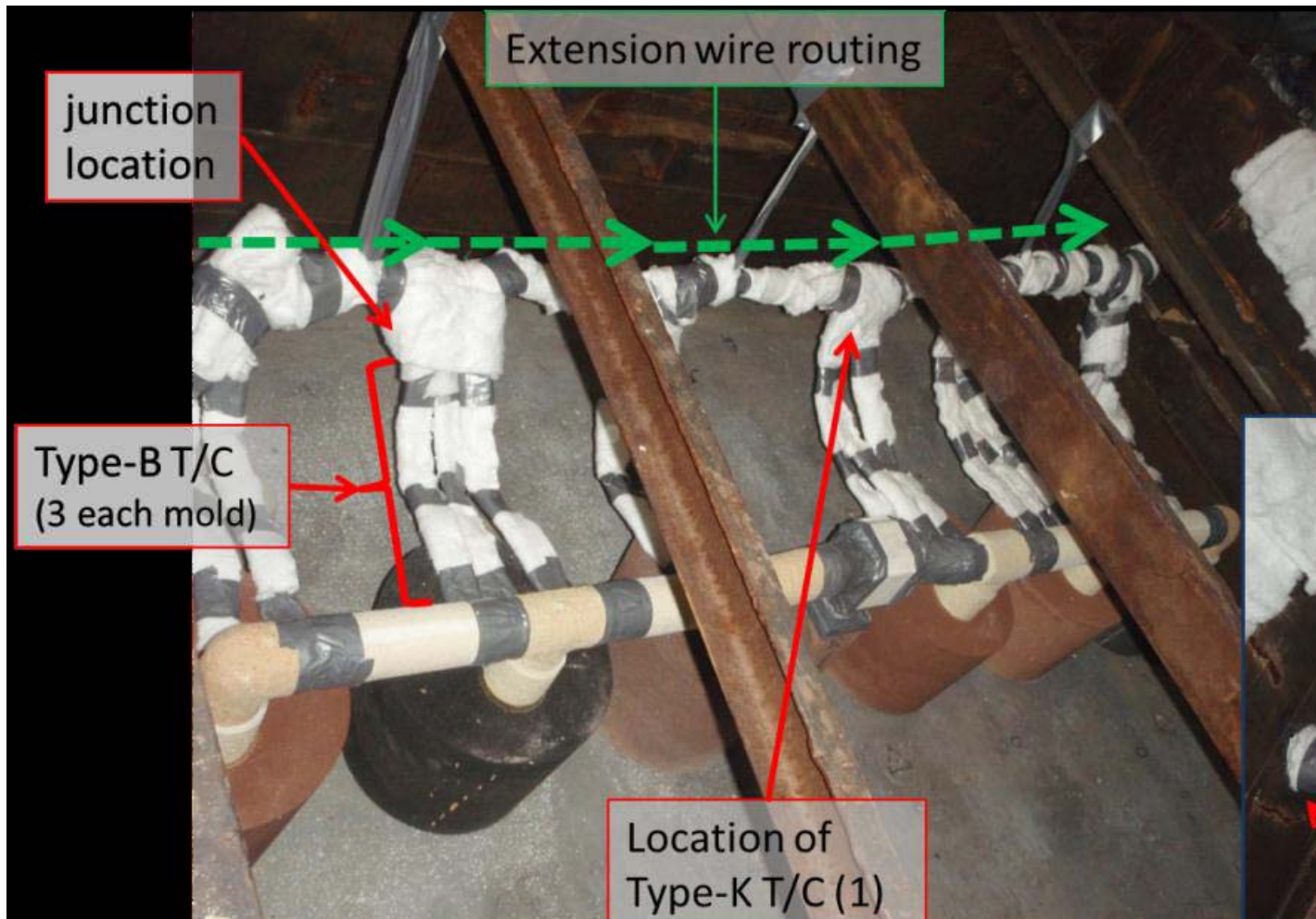


Figure 80: Thermocouples and extension wire were wrapped with Kaowool thermal insulation.



Figure 81: Photograph of thermocouple compensating cables routing within the drag mold

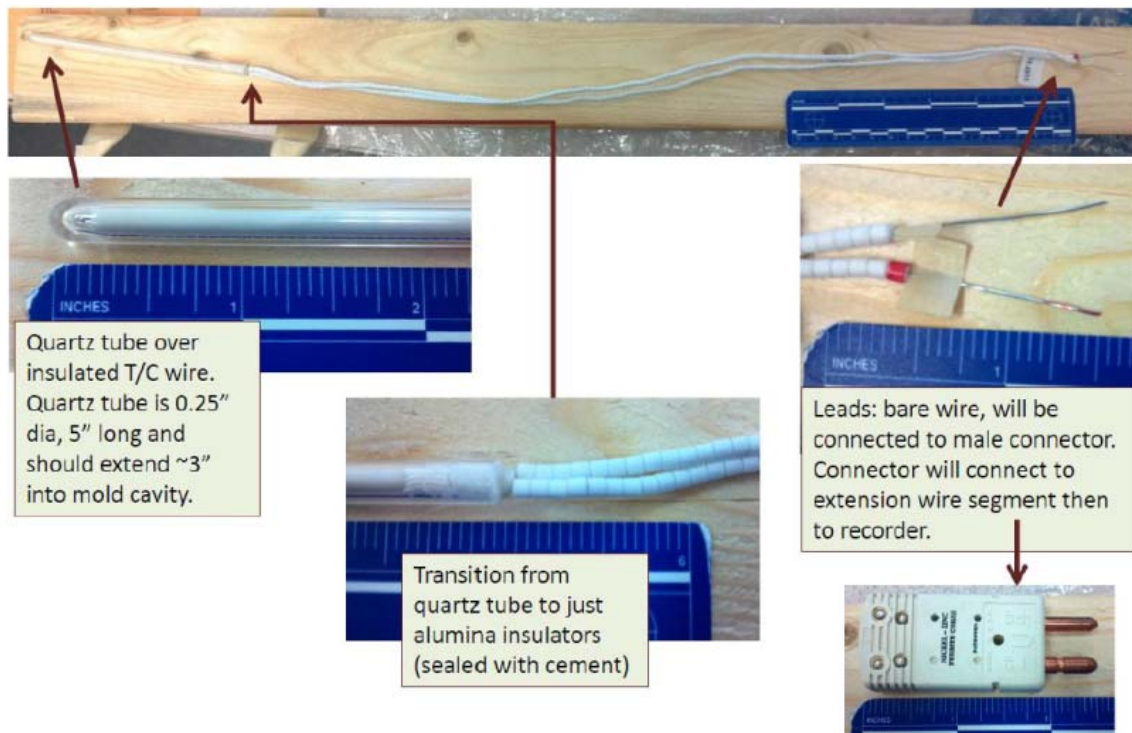


Figure 82: Type B Thermocouples, insulators and connectors assembly components

]



Figure 83: Photograph of completed mold ready for pour

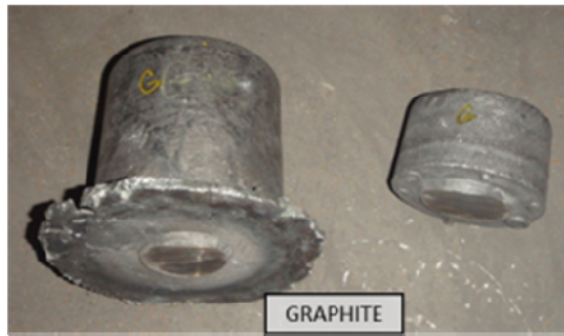
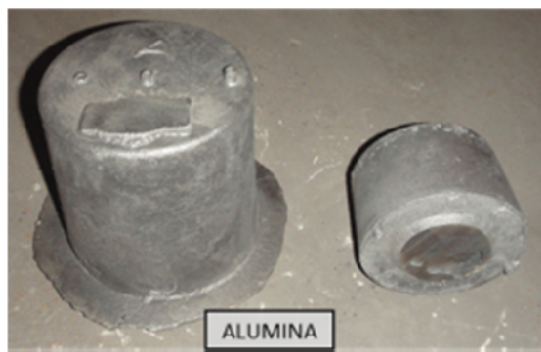
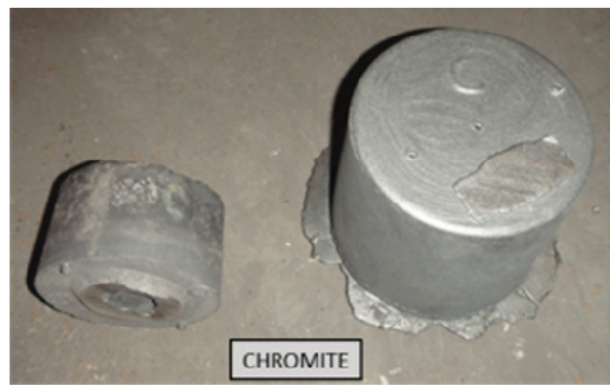


Figure 84: Photograph showing castings after mold shake out, gating and feeders removal

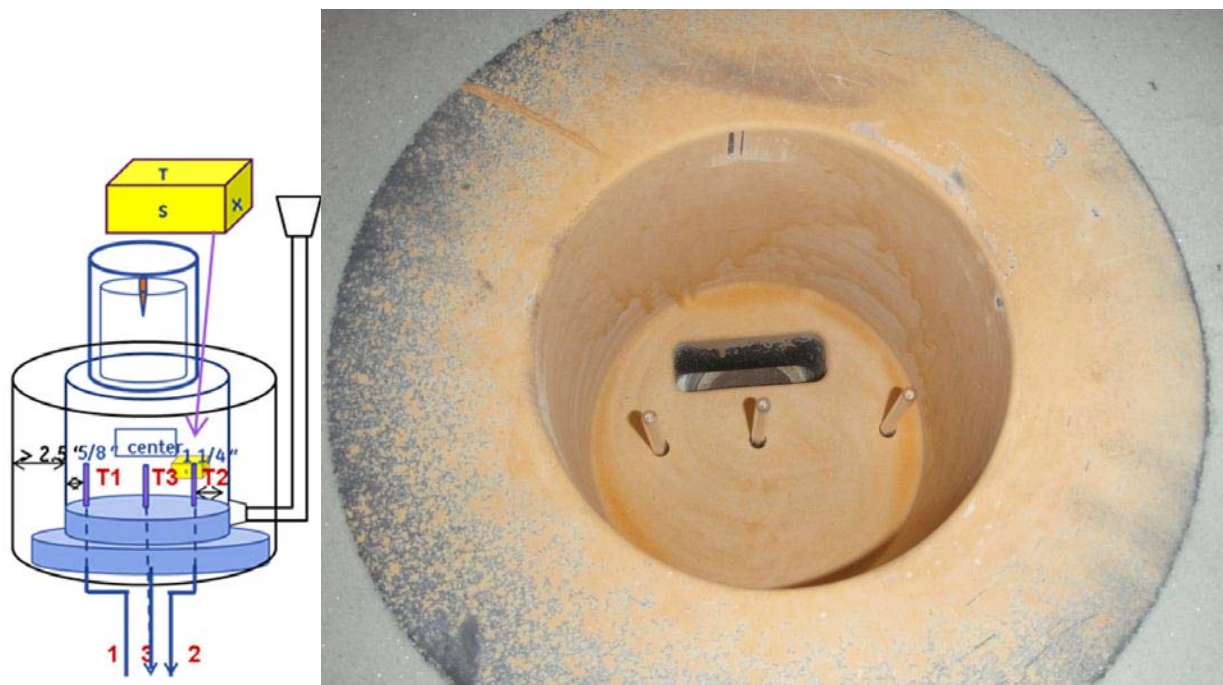


Figure 85: Haynes 282 cylinder castings thermocouple arrangements schematic view. Photograph showing Quartz sheathed Type-B thermocouples located within the molds

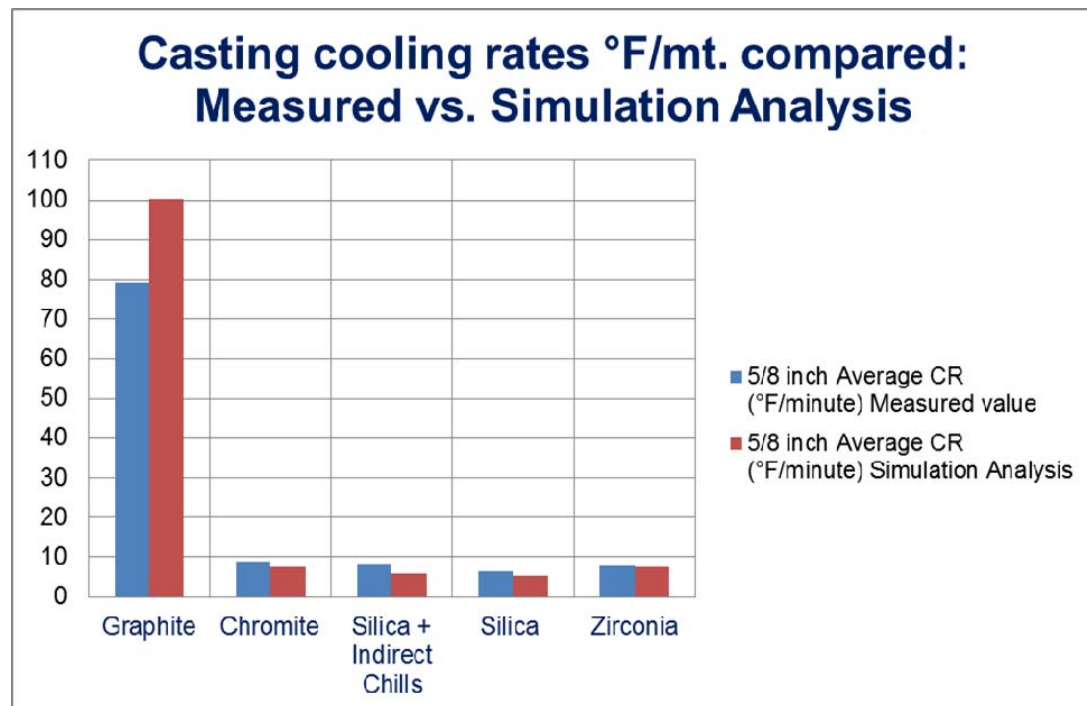


Figure 86: Casting cooling rates measured and simulated compared for different mold materials during liquidus to solidus transition temperature range

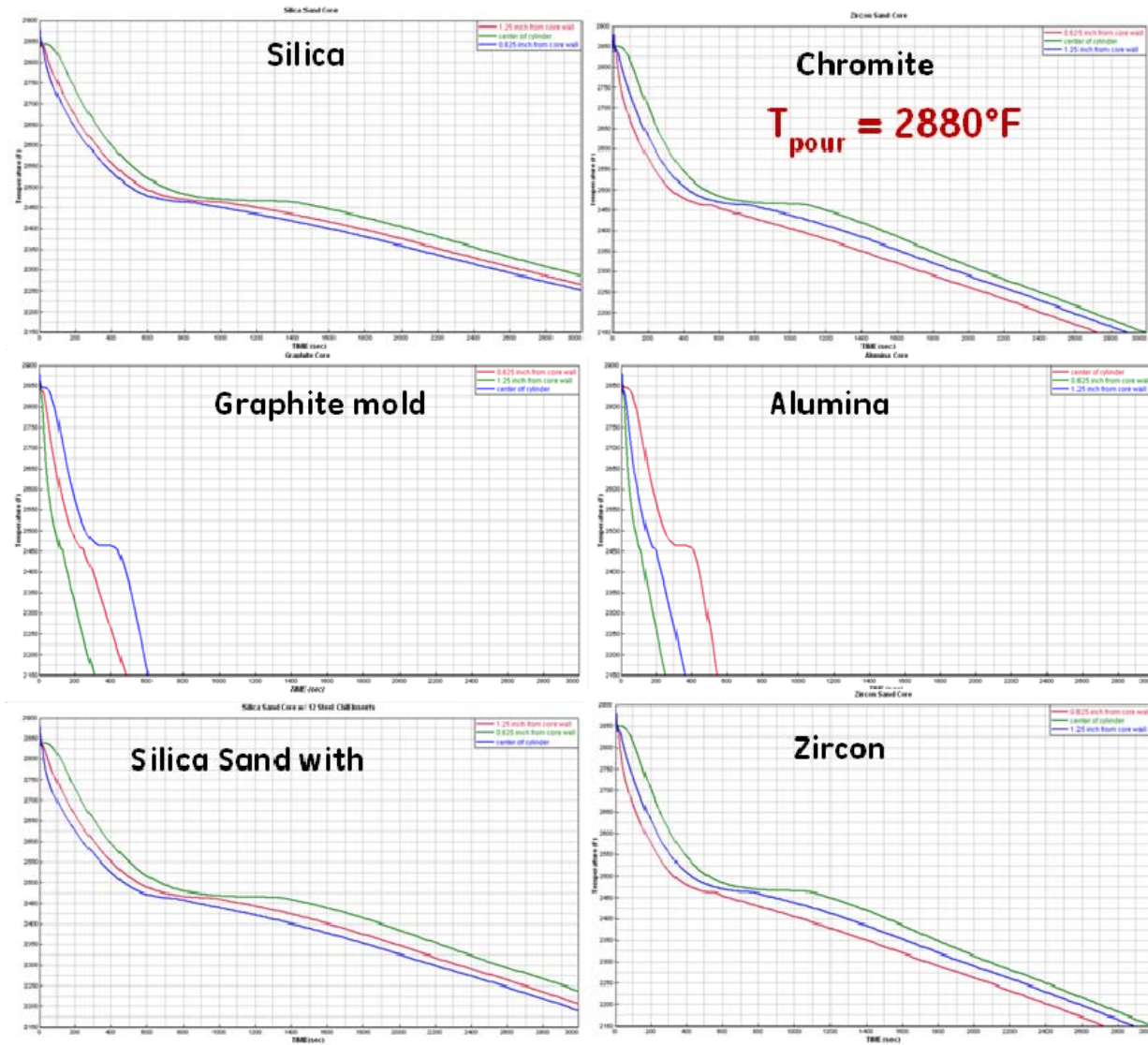


Figure 87: Casting Solidification Simulation Analysis cooling rates plot from pour to post solidification elevated temperature range for all the mold materials. Data from the 3 thermocouples T1, T2 and T3 vs. casting cooling time are plotted for different molds.

Average cooling rates at T1, T2 & T3 during Liquidus - Solidus transition temperature range

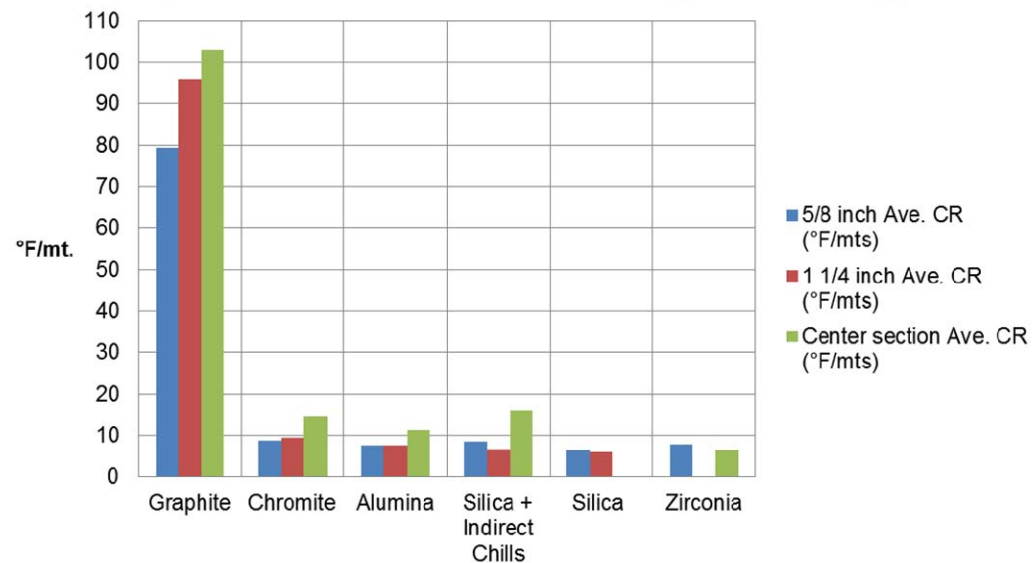


Figure 88: Haynes 282 Casting cooling rates during Liquidus to Solidus temperature range for different mold materials

Table 13: Casting cooling rates, both measured and simulated compared for different mold materials at 3 different locations within each mold

Mold material	5/8 inch Average CR (°F/minute)		1 1/4 inch Average CR (°F/minute)		Center Average CR (°F/minute)	
	Measured	Simulation	Measured	Simulation	Measured	Simulation
Graphite	79.3	100.16	95.74	62.82	102.86	41.44
Chromite	8.85	7.592	9.42	7.61	14.44	6.8
Silica + Indirect Chills	8.41	5.97	6.67	5.82	15.91	5.82
Silica	6.34	5.23	5.98	5.12	NA	5.09
Zirconia	7.73	7.46	NA	7.01	6.43	6.91

Table 14: Mold materials influence on microstructure SDAS values for Graphite, Zircon and Silica sand with indirect chills

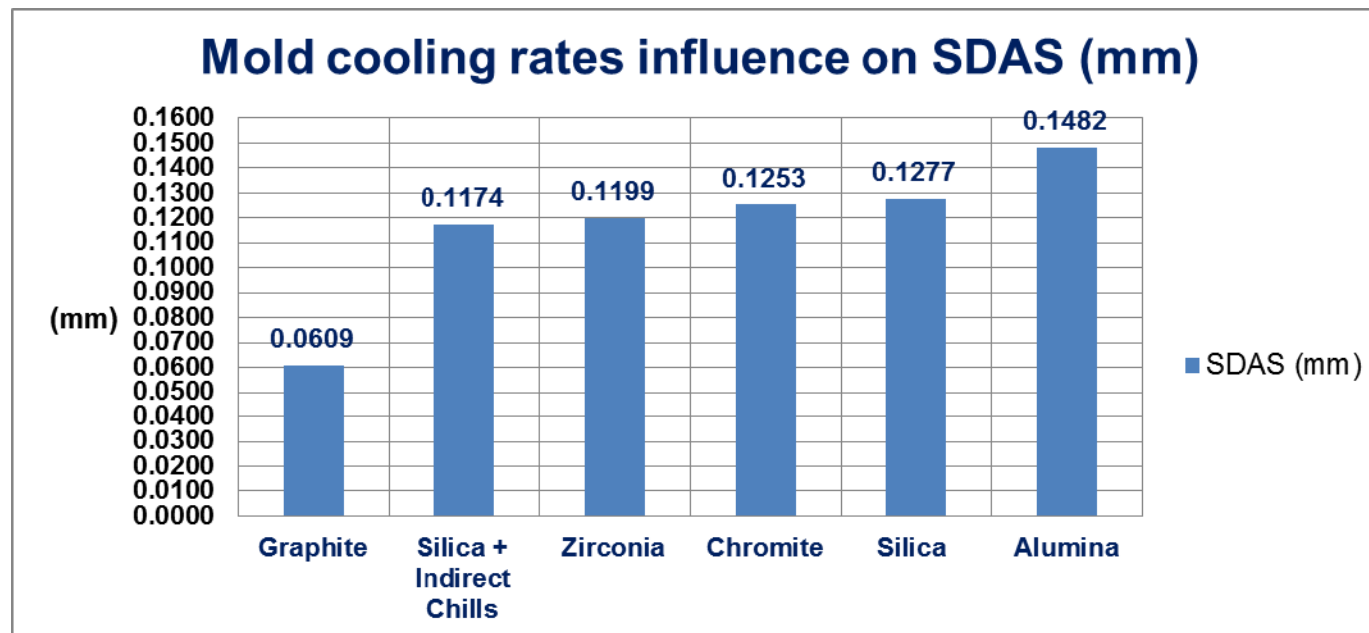
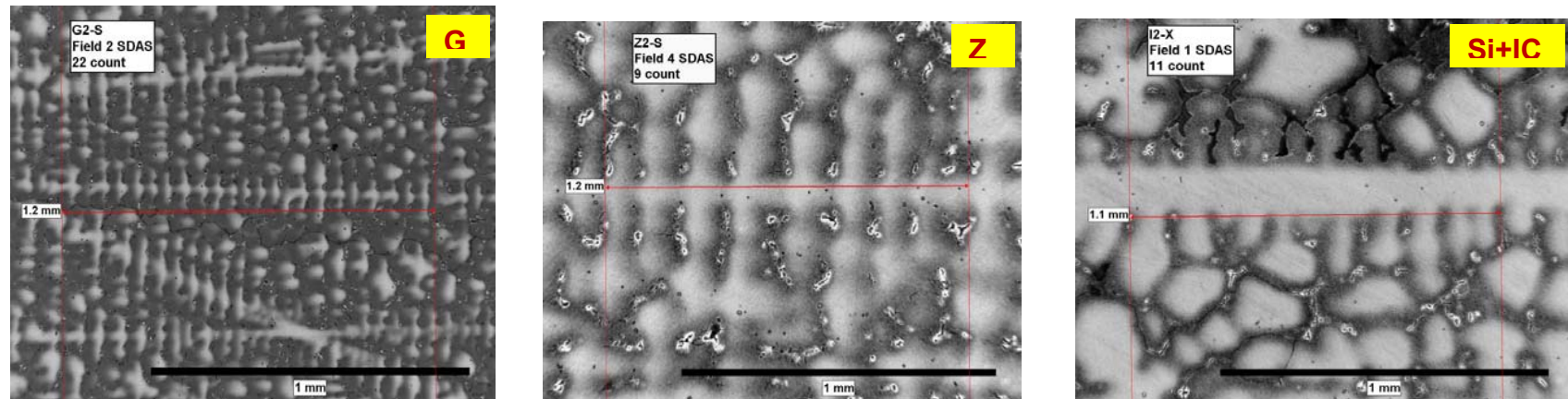


Figure 89: Mold cooling rates influence on SDAS values

Table 15: Mold materials influence on SDAS values through casting liquidus to solidus range cooling rates variation

Mold material	SDAS (mm)	SDAS Count #
Graphite	0.0609	274
Silica + Indirect Chills	0.1174	138
Zirconia	0.1199	146
Chromite	0.1253	128
Silica	0.1277	137
Alumina	0.1482	106

LARGE CASTING OF HAYNES 282

The key requisite for the success of the program was the need to demonstrate the successful scale up of the Haynes 282 for Steam Turbine Application large size castings. Hence the real need to resolve the scalability issue. GE Design engineering provided Production size prototype valve casing FEM model and drawings for this application.

As the original Valve body casting required 24,000 lbs., a partial casting was scheduled based on the available material for a pour weight of 17,000 lbs. Hence a partial valve casing was selected maintaining the actual cast dimensions, wall thicknesses inlet pipe dimensions and geometry. The gating was mimicked in such a way so that the solidification will be similar to an actual full size valve body. Engineering FEM models and supplemental requirements with applicable specifications provided to suppliers and discussed the casting quality acceptance criteria and NDT inspection requirements and key processing parameters.

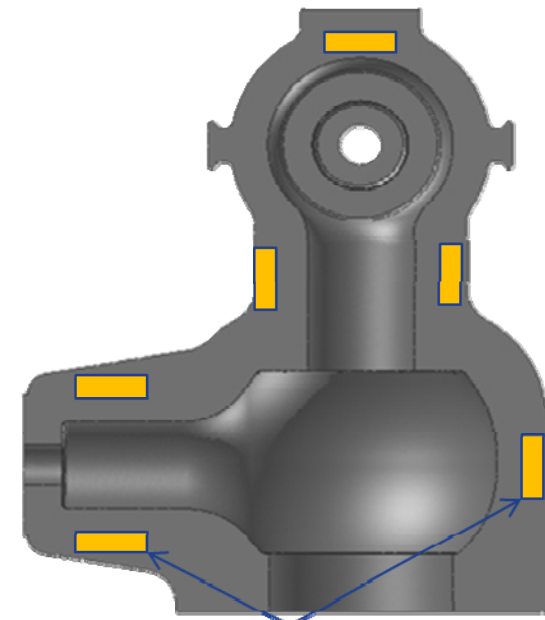
Casting methods and process quality inspection plans were reviewed and FMEA carried out. FEM based Casting solidification simulation analysis test results reviewed [Figures 93-94 and in106 for Niyama criteria] and casting methods validated prior to molding, melting and pouring.

Haynes 282 valve casing was successfully cast after casting methods were validated and the casting met NDT inspection and acceptance criteria.

Heat treated and sectioned to extract trepan samples at different locations comparing with cast on coupons test data. The H282 casting sections and cast on coupons test matrix and specimen identification is provided in Table16. Material properties requisite for design, such as tensile, creep/rupture, LCF, Fracture Toughness, Charpy V-notch chemical analysis testing were carried out. The test results will be presented in the final report.

The prototype casting features are provided in Figure 90 and pattern and cope and drag mold views are provided in Figures 91-92, with assembled mold, induction melting and pouring shown in Figures 95-97. The castings after mold shake out shown in Figure 98. The casting heat treatment Homogenizing and Aging HT cycles record are shown in Figures 99-101. The casting NDT inspection test results for 100% RT shown in Figure 102-103 and 100% surface area Liquid Penetrant Testing shown in Figure 104-105.

The casting sections cast on coupons ID and the test matrix are provided in Table 16. The order to delivery casting manufacturing schedules are provided in Figures 107 and 108. Typical time frame could be 55 weeks or better, depending on components design.



Cast-on test coupon locations

Figure 90: Steam turbine half valve casing selected for the large casting trial



Figure 91: Foundry Casting Pattern and feeder design

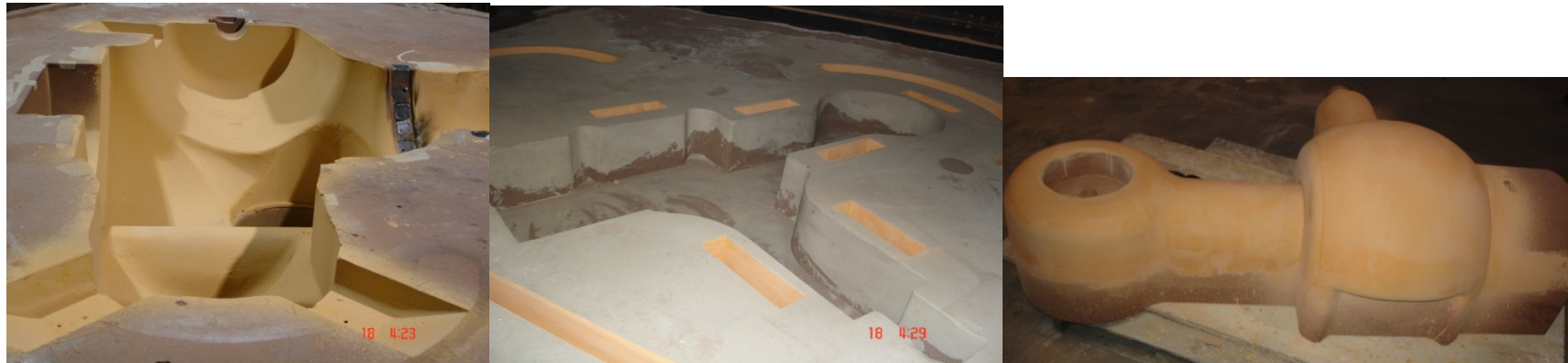


Figure 92: Picture showing Cope, drag molds and the valve body core after refractory coating and drying.

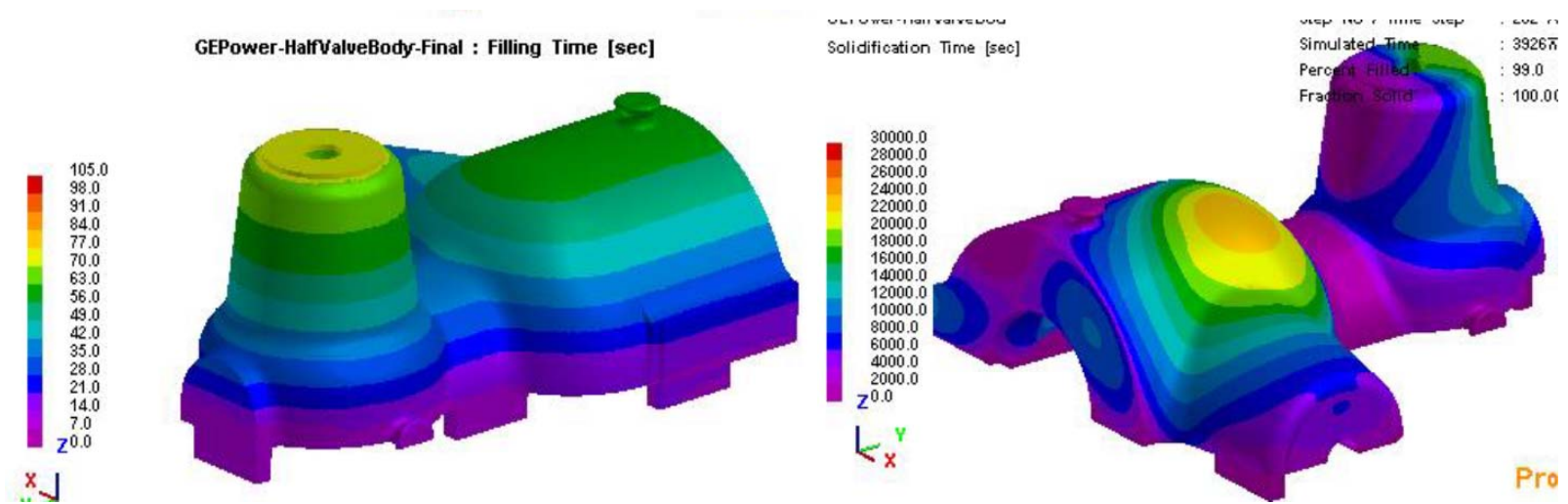


Figure 93: Solidification simulation indicates bottom to top filling (left) and temperature variation during liquidus to solidus transition temperature range (right)

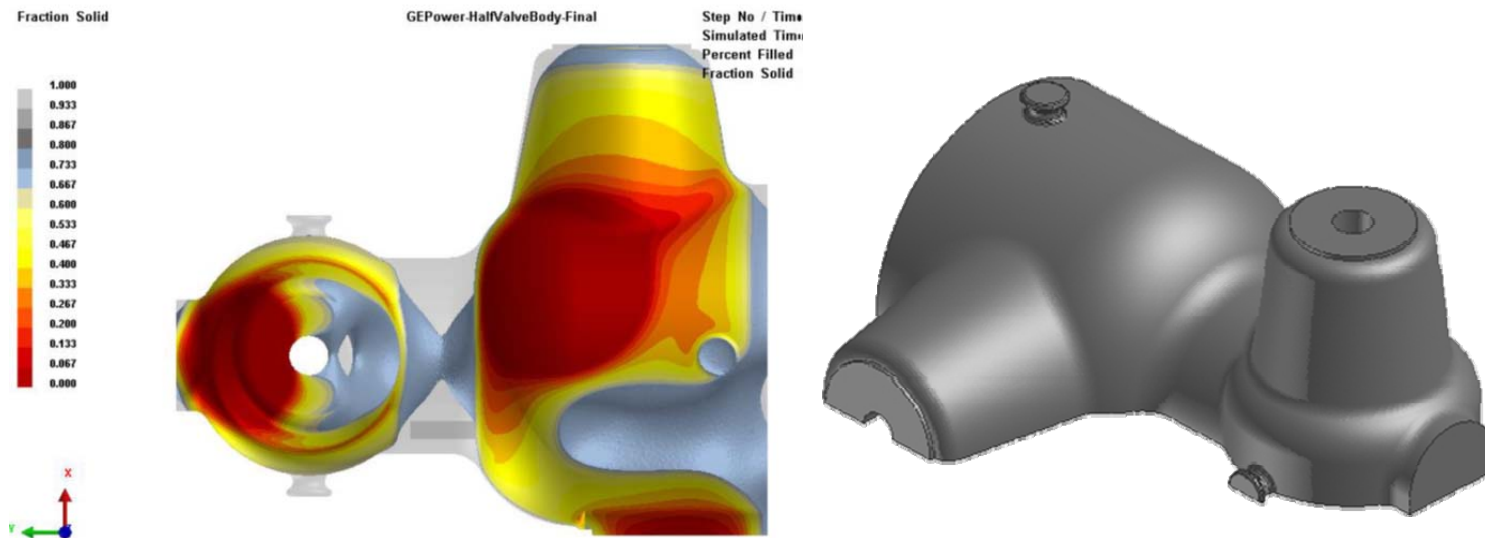


Figure 94: Solidification fraction solid cut off indicates no trail of shrinkage



Figure 95: Assembled mold, hot air dried and purged with Argon prior to pouring [Courtesy-MetalTek MO]



Figure 96: Induction melted, composition controlled with argon cover during melting and tapping melt quality controlled [Courtesy-MetalTek MO]



Figure 97: Pouring the mold after deslagging with covered ladles ensuring targeted pouring temperature and pour times



Figure 98: Casting after in mold cooling and shake out [Courtesy-MetalTek MO]

A. Homogenizing Heat Treatment Steps

- **Casting Preparation:** Coat all casting surfaces, including the cast on coupons with AO Smith CG-11 Ceram-Guard Coating or similar HT coat application.
- Part should be loaded into a room temperature furnace with Contact thermocouples attached for recording stepped Homogenization HT cycle. Along with Furnace thermocouples - HT cycle record required.

1. **Ramp furnace at a rate not exceeding 350°F/Hour**
 - Hold at 2040°F ± 25°F for 3 hours
2. **Ramp furnace to 2130°F**
 - Hold at 2130°F ± 10°F for 3 hours
3. **Ramp furnace to 2147°F.**
 - Hold at 2147°F ± 10°F for 3 hours
4. **Ramp furnace to 2174°F**
 - Hold at 2174°F ± 10°F for 8 hours
5. **Ramp to 2205°F**
 - Hold at 2205°F ± 10°F for 12 hours
6. **Ramp to 2228°F**
 - Hold at 2228°F ± 10°F for 24 hours
7. **Ramp to 2237°F**
 - Hold at 2237°F ± 10°F for 24 hours

- Forced Air Cool to RT with fans, keeping contact thermocouples attached for measuring cooling rate

B. Double Age Heat Treatment Steps

1. **Ramp furnace to 1850°F at a rate not exceeding 350°F/hour**
 - Hold at 1850°F ± 10°F for 2 Hours
2. **Forced air cool** with fans measuring cooling rate with contact thermocouples attached
3. **Ramp furnace to 1450°F**
 - Hold at 1450°F ± 10°F for 8 Hours (plus add ½ hour for through heating)

Still Air Cool to Room Temperature upon completion of the heat treatment measuring cooling rate with contact thermocouples attached

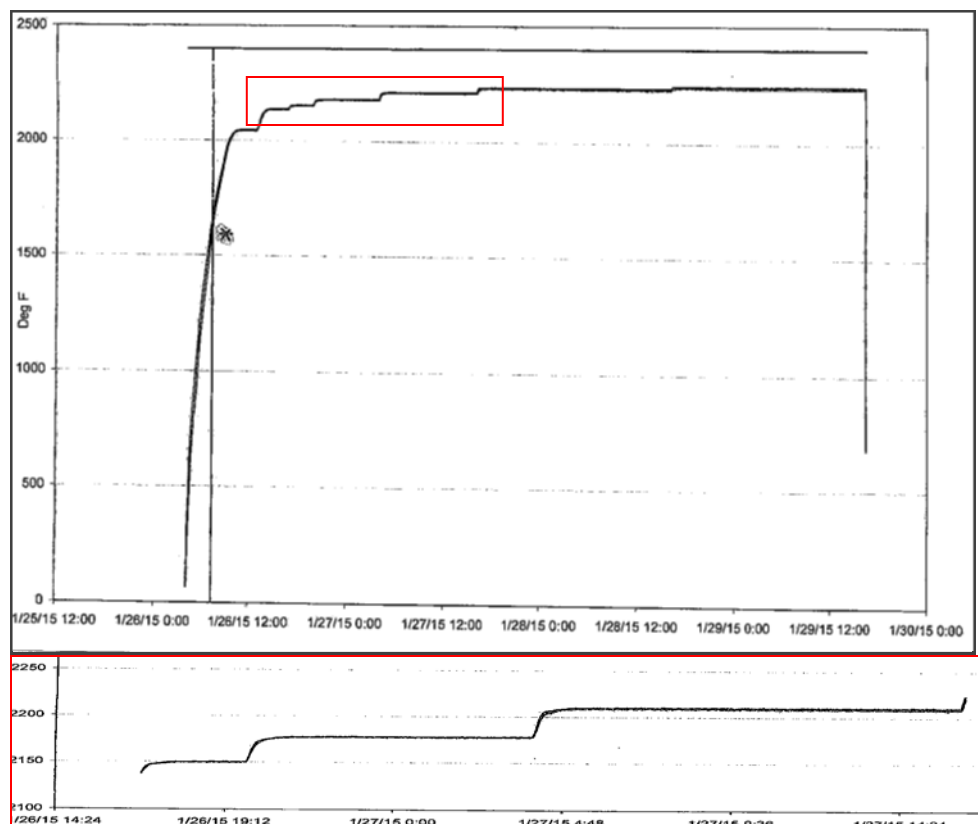


Figure 99: Homogenization HT cycle with insert HT step detailed view

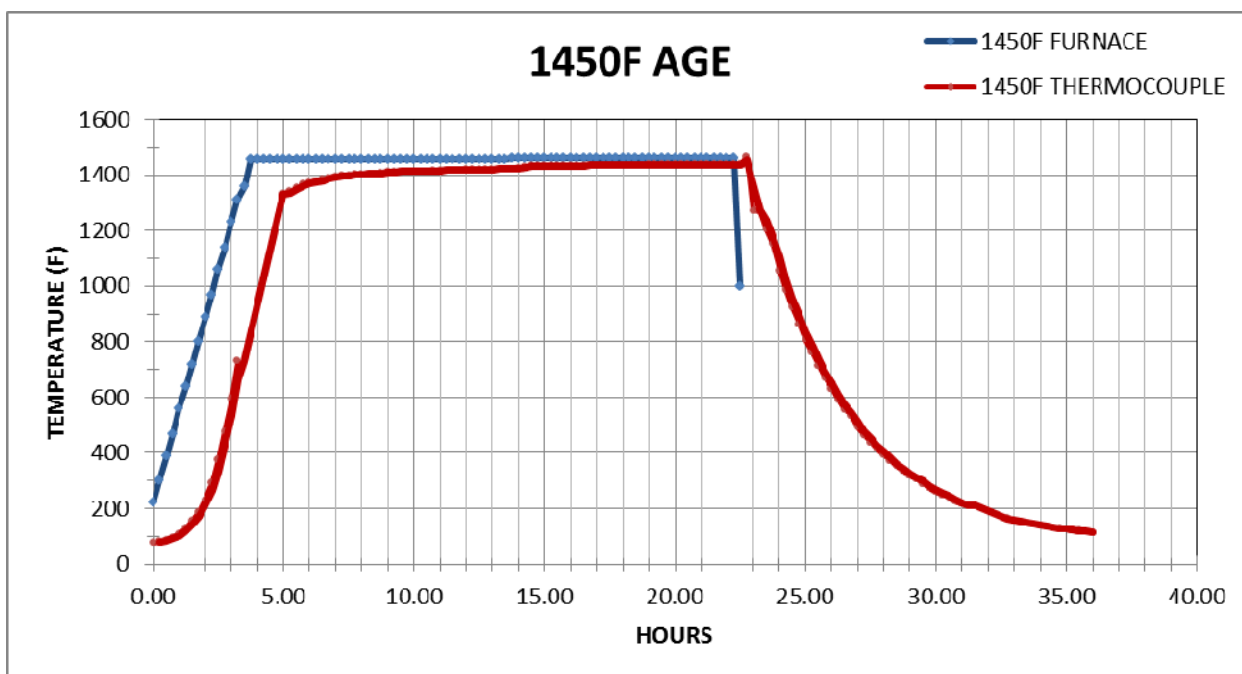
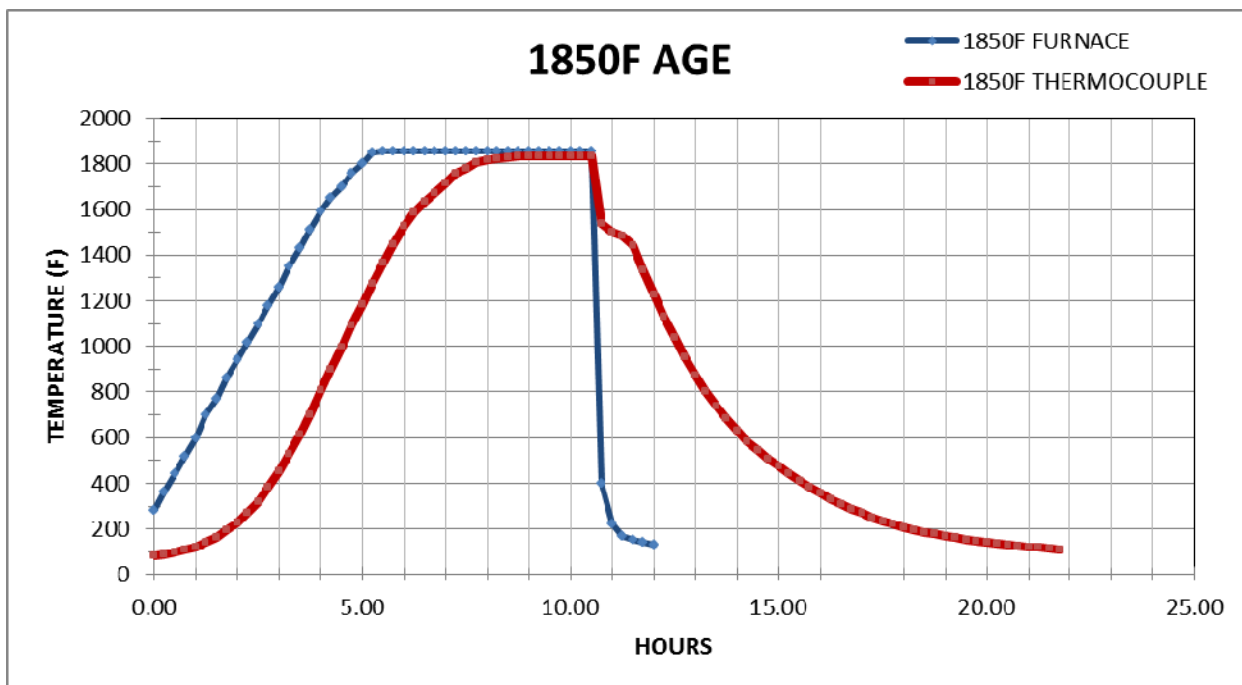


Figure 100: Two step Aging heat treat cycles thermocouple plot

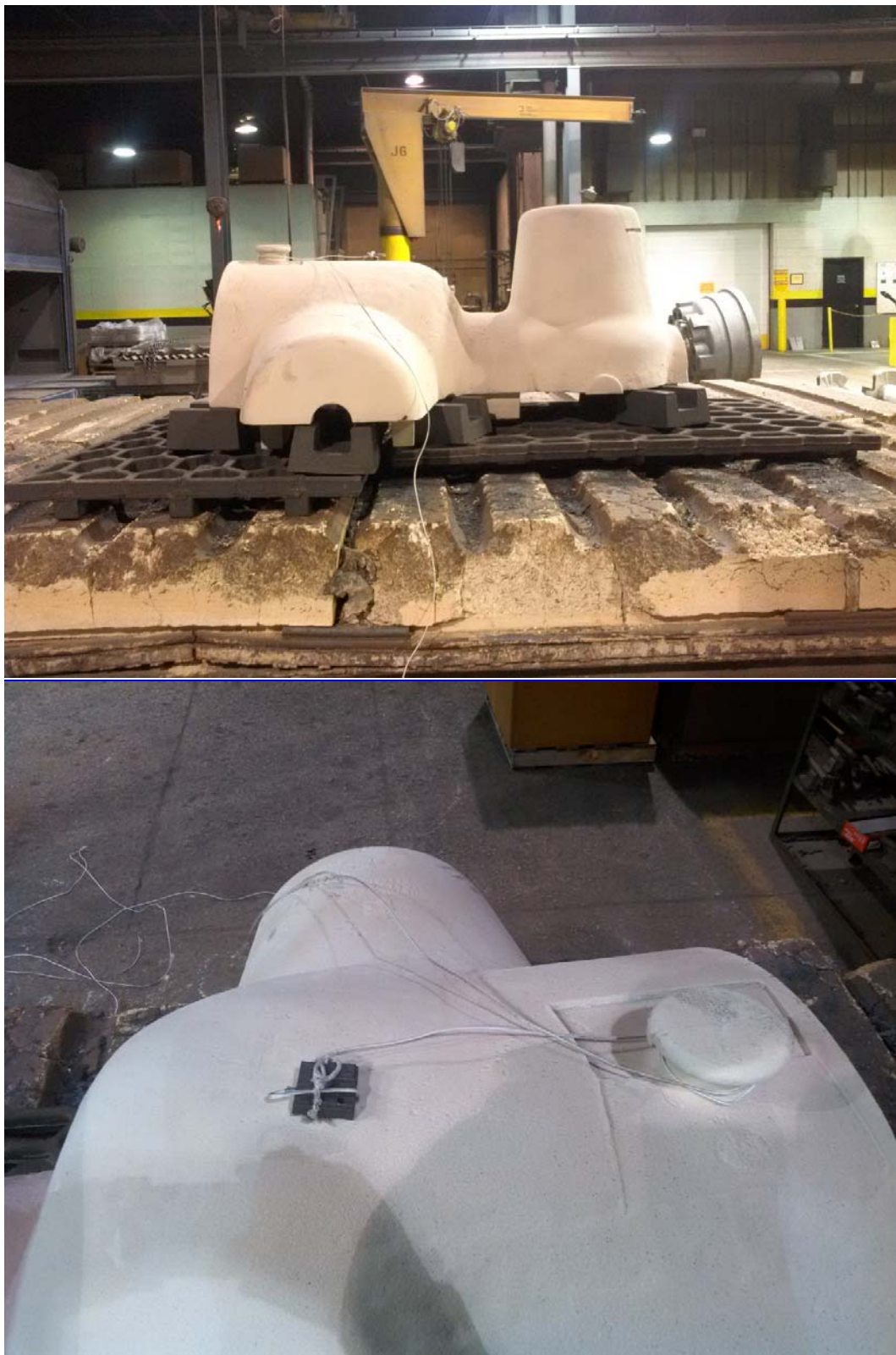


Figure 101: Thermocouples attached, coated for double Age heat treat cycle

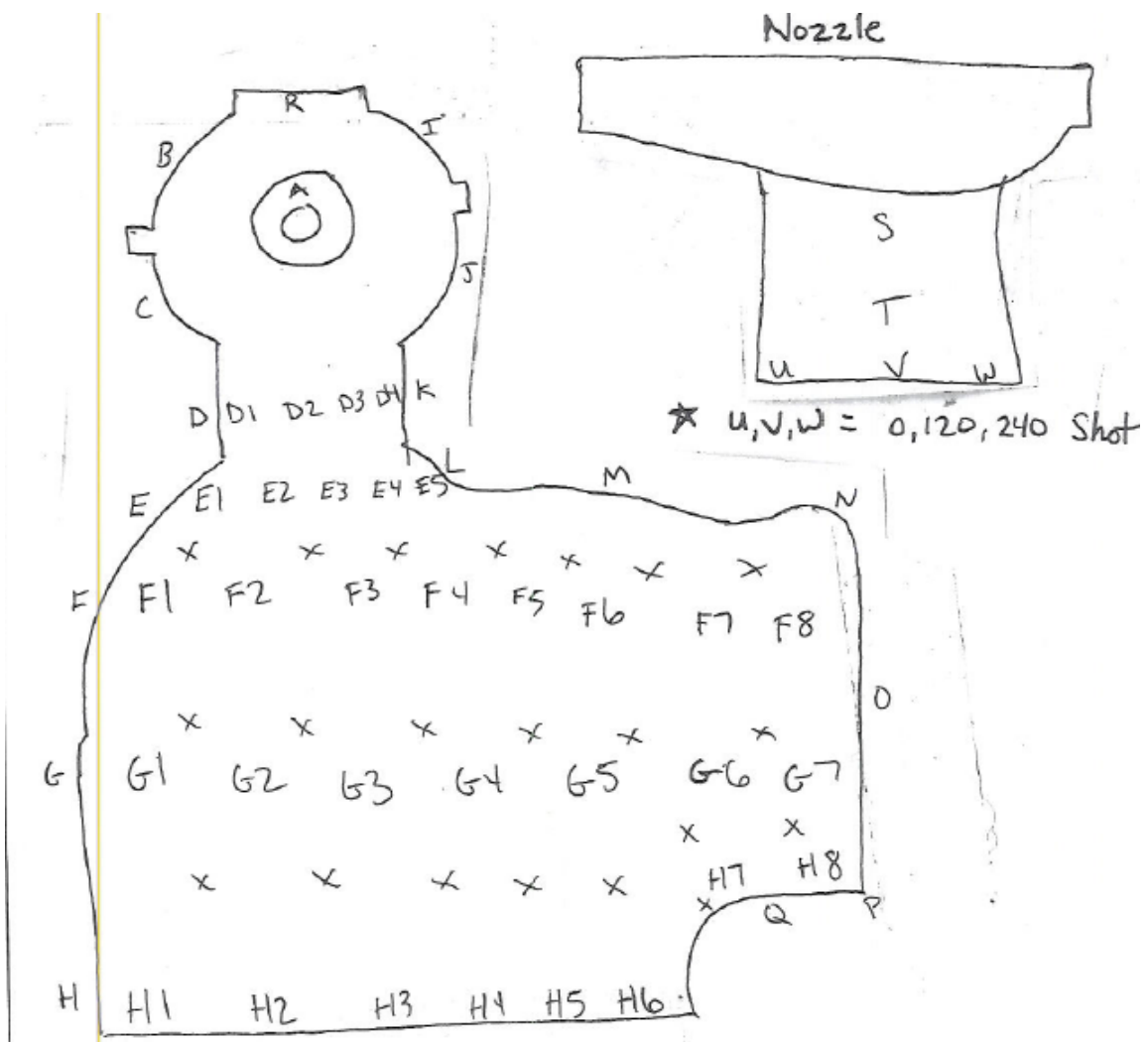


Figure 102: RT Scan sheet for the partial valve casing

PROCEDURE SPECIFICATION			ACCEPTANCE CRITERIA										SHEET 2 OF 2	
PART NUMBER	SERIAL NO.	VIEW	ACCEPTABLE		Grade to ASTM E446, E186, E280								REMARKS	
			NO APPARENT INDICATIONS	REJECTED	INCLUSION	DROSS OR SLAG	POROSITY	INCOMPLETE PENETRATION	LACK OF FUSION	GAS	CRACKS	SHRINKAGE	HOT TEARS	
106-T1024-G0001	RT-1	D1	✓	✓										
		D2	✓	✓										
		D3	✓	✓										
MS44580		D4	✓	✓										
		E1	✓	✓										
CO55060		E2	✓	✓										
		E3	✓	✓										
		E4	✓	✓										
		E5	✓	✓										
		F1			2									
		F2			2-3									
		F3	✓											
		F4	✓											
		F5	✓											
		F6	✓											
		F7	✓											
		F8	✓											
		G1									5+			
		G2									5+			
		G3	✓											
		G4	✓	✓										
		G5	✓	✓										
		G6	✓	✓										
		G7	✓											
		H1									5+			
		H2									5+			
		H3	✓											
		H4	✓											
		H5	✓											
		H6	✓											
		H7	✓											
		H8	✓											

Figure 103: RT Inspection report for the H282 valve casing



Figure 104: Haynes 282 Valve casing Liquid penetrant testing 100% surface area



Figure 105: LPT inspection pictures on 100 % Cast surface areas

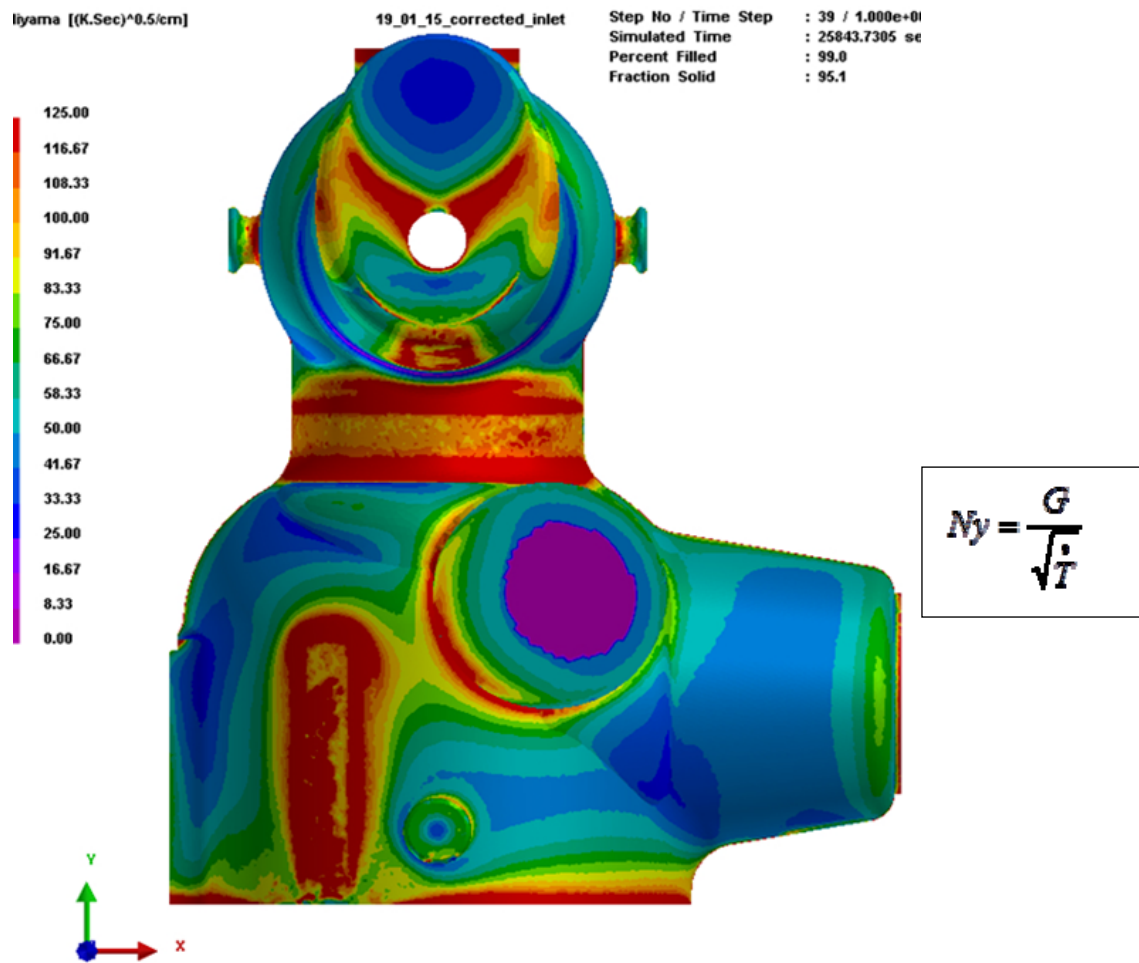


Figure 106: Niyama criteria per solidification simulation analysis. Niyama indicates potential feeding difficulty zones in the casting with lower (Ny) values. This plot is primarily used to avoid sectioning through potential zones for micro shrinkage

Table 16: H282 casting sections and cast on coupons test matrix and specimens identification

Haynes 282 casting test matrix:					Specimens Identification (ID)							
Test #	Test Type	Test condition	Step sections	Total Tests	Cast-on coupon ID (*1)		Cast Sections ID (*2)					
1	Tensile Test (UTS, 0.2% & 0.02% YS, % EL, %RA) Tensile Specimen: MPE-TNSL-001 P4 36 specimens	Temperature deg.F: RT/ 75 deg. F 500 deg. F 1000 deg.F 1250 deg.F 1400 deg.F 1500 deg F	1 Test/section in CL plane	6	CA	CC	H	D	B	C	E	K
					CA-T-75	CC-T-75	HT-75	DT-75	BT-75	CT-75		
					CA-T-500	CC-T-500	HT-500	DT-500	BT-500	CT-500		
					CA-T-1000	CC-T-1000	HT-1000	DT-1000	BT-1000	CT-1000		
					CA-T-1250	CC-T-1250	HT-1250	DT-1250	BT-1250	CT-1250		
					CA-T-1400	CC-T-1400	HT-1400	DT-1400	BT-1400	CT-1400		
					CA-T-1500	CC-T-1500	HT-1500	DT-1500	BT-1500	CT-1500		
2	Charpy V Notch Impact Impact Energy (J); % Shear, Lateral Expansion 12 Specimens	RT/ 75 deg F	2 Tests per section	6	CB-CV-1	CD-CV-1	H-CV-01	D-CV-01	B-CV-01			K-CV-01
					CB-CV-2	CD-CV-2	H-CV-02	D-CV-02	B-CV-02			K-CV-02
				A strain / TSR (%) RT/ 75 deg F	CB	CD	H	D	B	C	E	J
					1 / 1.00	4	CB-LCF-01	CD-LCF-01		D-LCF-01		E-LCF-01
					1 / 0.90	4	CB-LCF-02	CD-LCF-02		D-LCF-02		E-LCF-02
					1 / 0.80	4	CB-LCF-03	CD-LCF-03		D-LCF-03		E-LCF-03
					1 / 0.70	4	CB-LCF-04	CD-LCF-04		D-LCF-04		E-LCF-04
					1 / 0.60	4	CB-LCF-05	CD-LCF-05		D-LCF-05		E-LCF-05
					1 / 0.50	4	CB-LCF-06	CD-LCF-06		D-LCF-06		E-LCF-06
3	LCF Data Frequency: 20 cpm Waveform: Triangular A Strain 1, TSR% (1.0; 0.90; 0.80; 0.70; 0.60; 0.50) 2 temperatures: RT & 1400 deg. F. Specimen Drg. # 4013195-741 48 specimens	RT/ 75 deg F	1400 deg F	1 / 1.00	CB-LCF-07		D-LCF-07	B-LCF-07	C-LCF-07			
					1 / 0.90	4	CD-LCF-08		D-LCF-08	B-LCF-08	C-LCF-08	
					1 / 0.80	4	CD-LCF-09		D-LCF-09	B-LCF-09	C-LCF-09	
					1 / 0.70	4	CD-LCF-10		D-LCF-10	B-LCF-10	C-LCF-10	
					1 / 0.60	4	CD-LCF-11		D-LCF-11	B-LCF-11	C-LCF-11	
					1 / 0.50	4	CD-LCF-12		D-LCF-12	B-LCF-12	C-LCF-12	
			1400 deg F	1 / 1.00	CC	H		B		E		
					1450	37.5	1	H-SR-01				
					1400	45.0	1	H-SR-02				
					1300	67.5	1	H-SR-03				
					1450	35.0	1		B-SR-01			
					1400	42.5	1		B-SR-02			
4	Stress rupture Specimen per MPE-RUP 003-P3 12 specimens Creep data required	RT/ 75 deg F	1400 deg F	1 / 1.00	1300	62.5	1		B-SR-03			
					1450	40.0	1	CC-SR-01				
					1400	47.5	1	CC-SR-02				
					1300	70.0	1	CC-SR-03				
					1450	33.5	1			E-SR-01		
					1400	40.0	1			E-SR-02		
			1400 deg F	1 / 1.00	1300	58.0	1			E-SR-03		
					1450	37.5	1	CD-Kq-01	D-Kq-01	B-Kq-01		J-Kq-01
					1400	45.0	1	CD-Kq-02	D-Kq-02	B-Kq-02		J-Kq-02
					1300 deg.F			CD-Kq-03	D-Kq-03	B-Kq-03		J-Kq-03
5	Fracture Toughness Specimen per # 8024 ASTM E1820-11 Kq: J1C -16 specimens	RT/ 75 deg. F	1400 deg F	1 / 1.00	1400	42.5	1	CD-Kq-04	D-Kq-04	B-Kq-04		J-Kq-04
					1300	62.5	1					
					1450	35.0	1					
					1400	42.5	1					
					1300	62.5	1					
6	Chemical Analysis 8 Specimens	Ni,Cr,Co,Mo,Ti,Al,Fe, Mn,Si,C,B,P,S, Cu, Co,Nb, W, Zr, N(ppm), O (ppm)	Thermal Center	1 test section	CA	CD	H	D	B			K

Typical Haynes 282 large size steam turbine Casting Order to Delivery Activity Schedule

#	Description	# Weeks	1	2	3	4	5	6	7	8	9	10	12	13	14	15	16	17	18	19	20	21	22	23	24	25	26
1	Sales and commercial review	3	X	X	X																						
2	Engineering Drawings_models review	4			X	X	X	X																			
3	Pattern and core box manufacturing	6							X	X	X	X	X	X													
4	Casting process engineering review	4							X	X	X	X															
5	FEM and solidification simulation analysis	4											X	X	X	X											
6	Gating & Feeder Attachments, Ceramic tiling	2																	X	X							
7	Molding and coremaking production scheduling	6																	X	X	X	X	X	X			
8	Melting planning and schedule	3																						X	X	X	
9	Pouring, cooling and shake out	2																								X	X

Figure 107: Schedule from Purchase Order Placement to Casting Pouring ~ 26 weeks

		Weeks	27	28	29	30	31	32	33	34	35	36	37	38	39	40	41	42	43	44	45	46	47	48	49	50	51	52	53	54	55
10	Shot blast and riser cutting, gates removal	3	X	X	X																										
11	Homogenizing , solutionizing HT furnace prep	4			X	X	X	X																							
12	Grinding, Fettling	2								X	X																				
13	Aging HT Cycle, cooling	2									X	X																			
14	VT and LPT NDT inspections	2										X	X																		
15	Radiographic inspection	4												X	X	X	X														
16	Mechanical testing, Chemical analysis test certs	4											X	X	X	X															
17	Casting weld repair upgrades and Aging PWHT	4																			X	X	X	X							
18	NDT after weld repairs and casting upgrades	3																					X	X	X						
19	Casting Final Inspection and test certs	3																							X	X	X				
20	Package and delivery	2																										X	X		
		#REF!																													
Total 55-56 Weeks lead time from Order to Delivery																															

Figure 108: Schedule from Pouring to Delivery 30 weeks~

CONCLUSIONS

Activities under Task 4.0, Investigated and characterized various mechanical properties of Cast Haynes 282 and Cast Nimonic 263. The development stages involved were:

1. Small Cast Evaluation: 4 inch diam. Haynes 282 and Nimonic 263 Cylinders. This provided effects of liquidus super heat range and first baseline mechanical data on cast versions of conventional vacuum re-melted and forged Ni based super alloys.
2. Step block castings of 300 lbs. and 600 lbs. Haynes 282 from 2 foundry heats were evaluated which demonstrated the importance of proper heat treat cycles for Homogenization, and Solutionizing parameters selection and implementation.
3. Step blocks casting of Nimonic 263: Carried out casting solidification simulation analysis, NDT inspection methods evaluation, detailed test matrix for Chemical, Tensile, LCF, stress rupture, CVN impact, hardness and J1C Fracture toughness section sensitivity data and were reported.
4. Centrifugal Casting of Haynes 282, weighing 1400 lbs. with hybrid mold (half Graphite and half Chromite sand) mold assembly was cast using compressor casing production tooling. This test provided Mold cooling rates influence on centrifugally cast microstructure and mechanical properties. Graphite mold section out performs sand mold across all temperatures for 0.2% YS; %Elongation, %RA, UTS at 1400°F. Both Stress-LMP and conditional Fracture toughness plots data were in the scatter band of the wrought alloy.
5. Fundamental Studies on Cooling rates and SDAS test program. Evaluated the influence of 6 mold materials Silica, Chromite, Alumina, Silica with Indirect Chills, Zircon and Graphite on casting solidification cooling rates. Actual Casting cooling rates through Liquidus to Solidus phase transition were measured with 3 different locations based thermocouples placed in each mold. Compared with solidification simulation cooling rates and measurement of SDAS, microstructure features were reported. The test results provided engineered casting potential methods, applicable for heavy section Haynes 282 castings for optimal properties, with foundry process methods and tools.
6. Large casting of Haynes 282 Drawings and Engineering FEM models and supplemental requirements with applicable specifications were provided to suppliers for the steam turbine proto type feature valve casing casting. Molding, melting and casting pouring completed per approved Manufacturing Process Plan during 2014 Q4.
 - a. The partial valve casing was successfully cast after casting methods were validated with solidification simulation analysis and the casting met NDT inspection and acceptance criteria. Heat treated and sectioned to extract trepan samples at different locations comparing with cast on coupons test data. Material properties requisite for design, such as tensile, creep/rupture, LCF, Fracture Toughness, Charpy V-notch chemical analysis testing were carried out. The test results will be presented in the final report.

- b. The typical Haynes 282 large size Steam Turbine production casting from Order to Delivery foundry schedule with the activity break up is shown in Figures 107 and 108.

- **From Purchase Order placement to Casting pouring ~ 26 weeks.**

1. Sales and commercial review	3
2. Engineering Drawings/models review	4
3. Pattern and core box manufacturing	6
4. Casting process engineering review	4
5. FEM and solidification simulation analysis	4
6. Gating & Feeder Attachments, Ceramic tiling	2
7. Molding and coremaking production scheduling	6
8. Melting planning and schedule	3
9. Pouring, cooling and shake out	2

- **From Pouring to casting Delivery ~ 29 weeks**

10. Shot blast and riser cutting, gates removal	3
11. Homogenizing , solutionizing HT furnace prep	4
12. Grinding, Fettling	2
13. Aging HT Cycle, cooling	2
14. VT and LPT NDT inspections	2
15. Radiographic inspection	4
16. Mechanical testing, Chemical analysis test certs	4
17. Casting weld repair upgrades and Aging PWHT	4
18. NDT after weld repairs and casting upgrades	3
19. Casting Final Inspection and test certification	3
20. Package and delivery	2

Hence the Total Lead time from P.O to Casting delivery is approximately 55 weeks. The Task 4.2 and Task 4.3 activities and reporting completed.